Theoretical Studies of DNA Unzipping in Cellular Like Environment

THESIS

Submitted in partial fulfilment
of the requirements for the degree of

DOCTOR OF PHILOSOPHY

by

Neha Mathur

Under the Supervision of

Supervisor
Prof. Navin Singh

Co-Supervisor
Prof. Shibasish Chowdhury

BIRLA INSTITUTE OF TECHNOLOGY AND SCIENCE, PILANI

2024

BIRLA INSTITUTE OF TECHNOLOGY & SCIENCE PILANI – 333 031 (RAJASTHAN) INDIA

CERTIFICATE

This is to certify that the work reported in the Ph.D. thesis entitled **"Theoretical Studies of DNA Unzipping in Cellular Like Environment"**, submitted by **Neha Mathur**, ID.No. **2018PHXF0045P** at Physics Department, BITS-Pilani, Pilani Campus for the award of the degree of Doctor of Philosophy (Ph.D.), is a bonafide record of his original work carried out under my supervision. This work has not been submitted elsewhere for any other degree or diploma.

( )
Signature of Supervisor
Prof. Navin Singh
Professor
Department of Physics
BITS-Pilani, Pilani Campus
Date:

( )
Signature of Co-Supervisor
Prof. Shibasish Chowdhury
Professor
Department of Biological Sciences
BITS-Pilani, Pilani Campus
Date:

Dedicated to
My loving Late Grandfather

Acknowledgements

I would like to express my sincere gratitude to all those who were indispensable in achieving this milestone. Their steady support and guidance have been instrumental in my journey, and I sincerely appreciate their contributions. While it is impossible to adequately acknowledge everyone who has helped me along this path, I would like to express my heartfelt thanks to a select few who have played an important role in helping me along this difficult path. I would like to begin by extending my utmost appreciation to Prof. Navin Singh, my supervisor, whose exceptional guidance, support, and motivational influence have been truly inspiring. Prof. Singh's invaluable feedback and insights have consistently motivated me to enhance my abilities and strive for excellence. One of the most rewarding aspects of working with Prof. Singh has been his firm belief in my potential as a researcher and granting me the freedom to explore my interests and pursue my academic goals. His commitment to creating a quality atmosphere has played a pivotal role in keeping me focused on my research with ease. His open-door policy and willingness to invest time and effort into my progress were incredible. His guidance helped me navigate through the toughest times, providing clarity and direction when I needed it the most.

I am grateful to my co-supervisor, Prof. Shibashish Chowdhury (*Department of Biological Science*) for creating an open and collaborative environment that encourages discussion and exchanging ideas. His guidance helped me improve my research methodology and nurtured my growth as a researcher. I would like to express my deepest gratitude to my Doctoral Advisory Committee, Prof. Anshuman Dalvi and Prof. Jayendra Nath Bandyopadhyay, for their constant support, valuable insights, and critical reviews throughout the progression of my research. Their guidance and constructive suggestions during the semester presentations and the review of my draft thesis have significantly contributed to the refinement and quality of my work.

I would like to sincerely thank Prof. Rakesh Choubisa, Head of Department, and Prof. Manjuladevi V, DRC Convener, for their support. I would like to acknowledge the support from Prof. Shamik Chakraborti,

Associate Dean AGSRD and Prof. Jitendra Panwar, former Associate Dean, AGSRD. I express my indebtedness to Prof. Tapomoy Guha Sarkar and Prof. Raj Kumar Gupta for introducing me to the field of statistical mechanics and computational physics throughout my PhD coursework. Their guidance and expertise have developed my understanding of these subjects. I am truly thankful to all the faculty members of the physics department for their kind support. I extend my heartfelt thanks to the senior members of our research group, Dr. Amar Singh and Dr. Arghya Maity. Their willingness to lend a helping hand, offer constructive feedback, and share their expertise has been invaluable in navigating the challenges of doctoral studies. My most sincere thanks to Prof. Sanjay Kumar, Banaras Hindu University, for providing me with the facility of GPUs for the rigorous calculation of simulations. I am grateful to Dr. Anurag Upadhyay, IISc. Bangalore for his support and interest in my research. He has helped me with his vast knowledge and experience wherever and whenever needed, such as teaching me AMBER software and the basics of atomistic molecular dynamics simulation. Also, Mr. Rajeev Gaur, Mr. Shrikant Sharma, and Mr. Kundan (office staff from the Physics deparment) have consistently provided technical support and guidance whenever I encountered challenges or required assistance.

I humbly express my regards and deep appreciation to Prof. V. Ramgopal Rao (Vice-Chancellor BITS Pilani), Prof. Sudhirkumar Barai (Director, Pilani Campus), all Associate Deans of Pilani Campus and other office bearers of BITS Pilani, for their invaluable support, which has played a pivotal role in my doctoral journey. I express my gratitude to Prof. S. K. Verma (Dean Administration) for his down-to-earth nature, which is an inspiration for me. He demonstrates that success and humility can coexist.

I would like to thank all my seniors, with a special mention to Dr. Captain Rituraj Singh, Dr. Neelakshi Sharma, and Dr. Aditi Mondal for their support and motivation in all my endeavors. I would like to warmly thank my lab-mates Nikhil, Shubham, Charul, Mohit, Ranjan, and Renu. We have shared knowledge, ideas, and countless lighthearted moments that have made this journey memorable. I also thank the co-scholars, particularly Neha Narwal, Chandrachud, Prasoon, and

others whose names I couldn't mention due to space constraints. To my junior colleagues, Gokul and Devendra, I am truly grateful for being a vital part of my PhD experience. Your friendship, encouragement, and shared moments have made this journey truly unforgettable. I gratefully acknowledge BITS Pilani, Pilani, for providing financial support during the journey of my Ph.D. I am also deeply grateful to my hostel wardens and superintendents of Meera Bhawan, for their continued support.

Lastly, I owe a heartfelt gratitude to my parents, whose continuous encouragement and inspiration have guided me throughout my childhood and academic journey. Their love, support, and blessings have carved me into the person I am today, and I am forever grateful for their presence in my life. This thesis is a witness to our partnership, and I would like to thank my husband, Praveen, for being my support and constant source of strength. Finally, I would also like to express my respect to my late father-in-law for his invaluable support in reviewing my research papers.

Neha Mathur

Note to the reader

The intended reader of this thesis is assumed to be associated with or working in soft condensed matter physics. The reader is expected to have a basic understanding of statistical mechanics and numerical techniques, as these concepts form the foundation of the theoretical and simulation-based investigations presented. Fundamental knowledge of molecular dynamics (MD) simulations is also essential for understanding the simulation methodology employed to study the system of interest. Therefore, having a basic understanding of biology will benefit the reader in relating the findings and conclusions of the study to natural biological processes.

The thesis is written in "we" form. Sometimes this may appear strange to the reader, as the thesis is of a single author. However, to have continuity and flow in the text, I use *we* instead of *I* throughout the thesis.

Abstract

Deoxyribonucleic Acid (DNA), serves as the genetic blueprint of life and plays a crucial role in maintaining the stability and integrity of living organisms. DNA stability refers to the ability of the DNA molecule to maintain its structural integrity and resist mutation or damage. Many factors affect the stability of DNA, including chemical modifications, interactions with the environment, and proteins. It is an important biological molecule that plays a vital role in transcription, replication, translation, and gene expression. In these processes, the two strands of the DNA double helix undergo dynamic and structural changes, and the two strands either partially or entirely separate. The process is known as *denaturation* or *melting* of DNA. The strand separation is crucial to read the genetic information and DNA analysis. Both experimental and theoretical researchers have extensively studied the melting of DNA. *In vitro*, scientists attempt to use UV spectroscopy, fluorescence melting, and differential scanning calorimetry (DSC) to study biological processes. In addition to the experimental studies, various theoretical models have been developed to understand DNA melting. In **chapter 1**, the literature review explores the current understanding of DNA denaturation processes, including thermal denaturation, force-induced denaturation, and molecular dynamics simulations. It identifies knowledge gaps and suggests future research directions, emphasizing the importance of interdisciplinary approaches to advance our understanding of DNA stability and dynamics. In the **chapter 2**, we present the statistical model used to study the thesis objectives. The model incorporates key features or parameters to accurately capture the behavior and interactions of the system under study. It provides insights into the nonlinear dynamics, sequence-dependent interactions, and energy landscapes associated with DNA melting. We have used molecular dynamics simulation tools to study the understanding of the dynamic behavior and structural changes in DNA (*AMBER*). *AMBER* is a powerful tool that provides the details of the molecules by capturing the motions and interactions at the atomic level. In the **chapter 3**, we studied the force-induced unzipping of DNA in the presence of solvents. Our investigation revealed that not

only the magnitude of the applied force plays a crucial role but also the nature of the force and its application site are essential factors in the unzipping process. We explored how the applied force propagates along the DNA chain and determined the maximum length over which the force spreads when applied at different sites. In the **chapter 4**, we explore our investigations on DNA-linked gold nanoparticles (DNA-AuNPs) in the presence of solvents. In this study, we considered DNA of different lengths and attached gold nanoparticles at the end of the DNA chain while solvents were present somewhere near the molecule. We studied the melting profile of DNA-linked nanoparticles using the model discussed in Chapter 2. These hybrid systems are used in nanobiotechnology, medical, and pharmaceutical sciences. In **chapter 5**, we studied the effect of partial confinement on the melting profile of a specific B-DNA molecule that is 12 base pairs in length with sequence 5'(*CP*GP*CP*GP*AP*AP*TP*TP*CP*GP*CP*G)3'. In this part of the study, we consider different chain lengths of DNA that are confined in the cylinder of different radii. Also, we analyze the obtained results with a non-linear curve fitting program. In the **chapter 6**, we discuss the dynamics of DNA molecules in crowded solutions using *AMBER*. We have considered two different crowders (*aspartame & poly-ethylene-glycol*) to study DNA molecules' structural transformation and dynamics in a crowded environment. We have calculated the Root Mean Square Deviation (RMSD), the radial distribution of crowders, and the number of water molecules in different shells. In most studies on DNA in crowded environments, researchers take PEG as the crowders. We have also taken aspartame and compared the effect on the dynamics of DNA molecules in the presence of two kinds of crowders. Remember that the presence of aspartame molecules in the human body is a potential candidate for cancer. The last chapter of the thesis discusses the conclusion and future scope of this thesis. The structure of nucleic acids and their application in various diverse fields is discussed in Appendix A. Finally, the research work is summarized in the chapter "Conclusions and Future Work". In this chapter, we outline some conclusions and the future scope of the work.

Contents

List of Figures

List of Tables

Nomenclature

H	Hamiltonian
k_β	Boltzmann constant
κ	Single strand elasticity
ρ	Anharmonicity in stacking
b	range of anharmonicity
V_M	morse potential
D	Potential depth
a	Inverse of potential width
Z	Partition function
Z_p	Momentum part of the partition function
Z_c	Configurational part of the partition function
T_m	Melting temperature
F_c	Critical force
C_v	Specific heat
f	Free energy
S	Entropy
ϕ	Fraction of open pairs
θ	Fraction of intact pairs

MD	Molecular Dynamics
MC	Monte Carlo
PBD	Peyrard Bishop Dauxois
CFE	Constant force ensemble
CEE	Constant extension ensemble
OT	Optical tweezer
MT	Magnetic tweezer
AFM	Atomic force microscopy
SMFE	Single molecule force experiment

SMFS	Single molecule force spectroscopy
A	Adenine
C	Cytocine
G	Guanine
T	Thymine
RNA	Ribonucleic acid
mRNA	Messenger RNA
tRNA	Transfer RNA
DNA	Deoxyribonucleic Acid
ssDNA	Single stranded DNA
dsDNA	Double stranded DNA

Chapter 1

Introduction

Cells are the building blocks of all living organisms; everything from the smallest bacteria to the biggest plants and animals is made up of these cells. In the human body, millions to trillions of cells are present that contain several components like the nucleus, mitochondria, lysosomes, and cell membrane [1–4]. The nucleus is the center part of each cell and it holds important instructions that determine how the cell acts and what it looks like. The nucleus is often referred to as the "control center" of the cell. Found in eukaryotic cells, it's a distinct, membrane-bound structure that contains a nuclear envelope, nucleolus, chromatin, chromosomes, and nuclear matrix. Chromatin organizes the bulk of the deoxyribose nucleic acid (DNA), proteins (primarily histones), and some ribose nucleic acid (RNA). DNA molecule doesn't exist as a free-floating linear molecule but it is wrapped around histone proteins, forming structures known as nucleosomes. The winding of DNA around these histones allows the long DNA molecules to fit within the limited space of the nucleus and also plays a role in gene regulation. During specific times in the cell cycle, especially when the cell is preparing to divide, the chromatin further condenses to form distinct structures called chromosomes. Each chromosome represents a single, long, coiled DNA molecule and various associated proteins (Fig.1.1).

DNA primarily functions as a storage system for genetic data. Often likened to a blueprint or a recipe, it holds the essential guidelines for building various cellular elements, including proteins and RNA molecules. The segments of the DNA chain that carry this genetic information are called GENES and the rest part of the chain has structural purposes. The structural design of DNA serves specific and vital roles that ensure genetic information is preserved, accessible, and transferable from one generation to the next (*Refer to Appendix-A for introductory content*

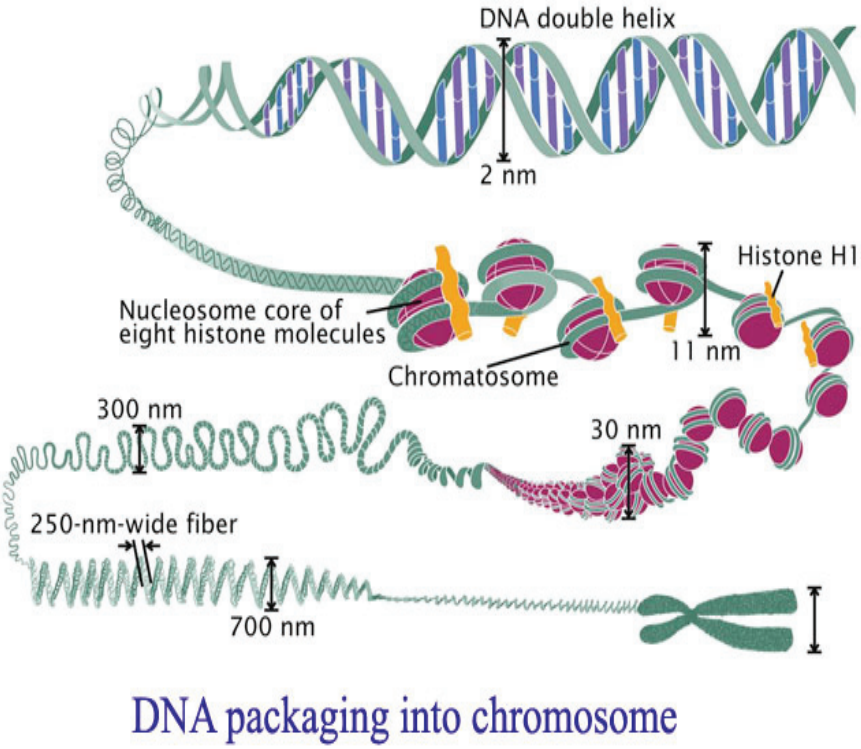

Figure 1.1: The organization of DNA within the chromosome structure. Image taken from Internet (Click Here)

6.7). The regulation of genetic information is mediated through two primary and essential processes: DNA transcription and DNA replication. Fundamental to these procedures is the unraveling of the DNA double helix. In both the processes one thing is common which is the opening of the helix, either to decipher the code (DNA transcription) or to serve as a template for daughter DNA (DNA replication). To understand these important biological processes in depth, one has to study the opening of the double helix DNA and the separation of the two strands in DNA because, without the ability of DNA to undergo melting, many of the cell's primary functions would be hindered. This separation of a double-stranded DNA to single-stranded DNA is called melting/denaturation/unzipping of DNA and it begins with the formation of bubbles and moves along the chain for complete dissociation [5–7]. In the unzipping process, few hydrogen bonds break due to increasing temperature or other denaturing agents, and small local openings or bubbles form in the DNA double helix. Hence it's worth noting that DNA melting can be influenced by various factors such as DNA sequence, salt concentration, denaturing agents, and pH of the system. In this thesis, we explore the statistical and thermodynamic characteristics of DNA denaturation under conditions that

simulate the cellular environment [7–10].

1.1 Literature review

1.1.1 Melting/Unzipping of DNA

The studies on DNA structure and its functioning were started soon after the seminal work by Watson and Crick in 1953 [11]. Since then, phenomenal work (experimental and theoretical) has been done to understand the complexity of the structure and dynamics of the DNA molecule. The thesis focuses on understanding the melting of DNA in thermal and force ensembles; I will focus on the work done in this area. In DNA, hydrogen bonds between the base pairs on opposite DNA strands are considerably weaker compared to the strong covalent bonds within the DNA molecule itself. To be specific, breaking a hydrogen bond requires only about 10^{-2} to 10^{-1} electronvolts (eV) of energy while breaking a covalent bond requires a much higher energy input, typically in the range of 5 to 10 eV [12, 13]. Consequently, during the temperature-induced separation of DNA strands, the primary structure of the DNA molecule remains largely unaffected and this process is fully reversible.

When a solution containing DNA is heated, the hydrogen bonds between the complementary strands break which creates bubble(s) in the sequence. Once the bubble is formed, it may grow and hence break the other base pairs. This process is similar to the nucleation and propagation of bubbles in crystal structures. The temperature at which half of the base pairs are open in a DNA chain is known as the melting temperature, (T_m) [14]. The (T_m) of a DNA molecule depends on several factors such as the length of the molecule, specific base pair sequence, number of mismatches or defects in the sequence, etc. The solution conditions like buffers, pH, salt concentration, hydrophobicity, or even surfactants may also affect the melting transition.

Several experiments and theoretical models were designed/proposed to understand the complex behavior of DNA melting. The most commonly used experimental method to study DNA unzipping is UV Absorbance, Fluorescence, Circular Dichroism, Differential Scanning Calorimetry, and Fluorescence Resonance Energy Transfer [15–18]. Understanding the melting process helps us design applications such as DNA sequencing, polymerase chain reaction, gene therapy, and encapsulations. In Fig.1.2, we have shown the thermal melting profile of DNA in which we

can see that as temperature increases DNA molecule melts and the two strands separate. Also as DNA becomes single-stranded its absorbance increases.

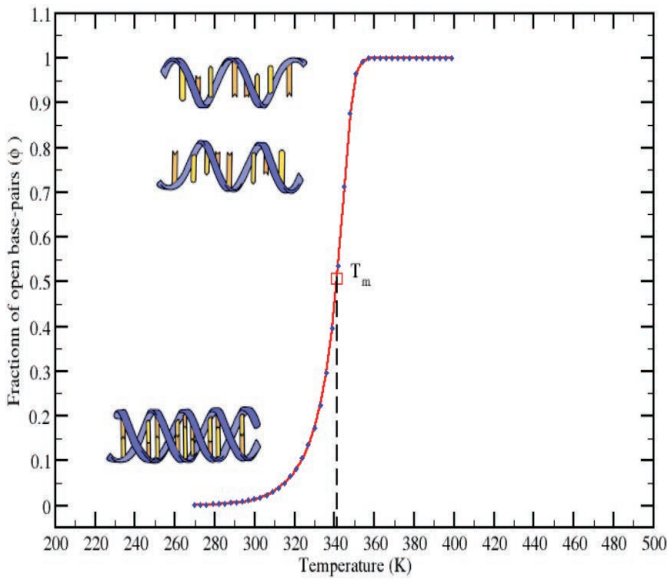

Figure 1.2: Melting curve of DNA and increase in fraction of open base pairs with temperature for a homogeneous DNA.

In 1996, Thomas *et al.* studied thermal denaturation by differential scanning calorimetry (DSC) and Raman Spectroscopy [19]. Their study shows several energetic and structural changes that accompany the melting of the B-form of DNA. In another study through Raman spectroscopy, they studied the thermal denaturation of DNA in the presence of ions like Sr^{+2}, Br^{+2}, Mg^{+2}, Ca^{+2}, Mn^{+2} and many more. In one of the interesting studies, Theodorakopoulos *et al.*, using neutron scattering and the Peyrard-Bishop-Dauxois (PBD) model, studied the thermal denaturation of DNA. They calculated the *Bragg peak* as a function of temperature [20]. Owen *et al.*, through the experiments, showed the dependence of the melting temperature on GC content and concentration of Na^{+} ions in solution [21]. The analysis of experimental findings supports the hypothesis that the change in T_m with salt concentration is due to changes in the screened interactions between the negatively charged phosphate groups. Stellwagen and colleagues conducted a study to explore the effect of monovalent cation size on the thermal stability of DNA hairpin structures [22]. Their discoveries demonstrate that larger-sized cations lead to a reduction in the DNA melting temperature. This decrease can be attributed to the reduced effectiveness of larger cations in shielding the charged phosphate residues in duplex DNA. One plausible explanation for this observation

is that the larger cations cannot approach the DNA backbone as closely as their smaller counterparts. Despite numerous efforts, a definitive conclusion regarding the helix-coil transition in an ionic environment remains elusive.

In addition, scientists put forward various statistical models and empirical relations to understand DNA denaturation. Gibbs proposed the first model (zipper model) to study DNA melting. Poland and Scheraga proposed a simple model to study DNA denaturation in 1966, later modified by Fisher in 1970 [23, 24]. In this model, the DNA molecule comprises an alternating sequence of bound and denatured states. The bound state is energetically favored over unbound states, while the loop segment or open states are entropically favored. The model explained the phase transition in the DNA by determining the critical exponent c of the underlying loop. The model displays a continuous phase transition in both two and three dimensions. Another approach was taken by Prohofsky *et al.* to study DNA melting using the lattice dynamic theory based on the modified self-consistent phonon approach. In 1989, Peyrard and Bishop proposed a statistical model that describes DNA as a one-dimensional chain with nearest neighboring potentials representing stacking energy. The hydrogen bonds between the base pairs are represented by morse potential [25, 26]. Deng *et al.* studied the stochastic dynamics and local denaturation of the thermalized PBD DNA model by using the stochastic averaging method for quasi-Hamiltonian systems. They calculated the stationary probability density function of the average energy and the mean square of the base-pair separation is obtained by solving the reduced Fokker-Planck equation [27]. Buyukdagli *et al.* [28] studied the finite size effect on DNA melting. Krueger *et al.* studied the base pair opening probabilities by calculating the partition function using the unified nearest neighbor parameters [29]. They proposed that the open base pair proceeds through the formation of a highly constrained small loop or a ring. An entropic penalty parameter, ring factor, was included for the unfavorable positioning of the unbound base. The values for this factor were estimated from the comparison of theoretical probabilities with the probabilities measured by NMR experiments. Y. Lui developed a thermodynamic model to predict DNA melting in ionic solutions [30]. The predicted melting temperatures and melting curves, through their model, capture the general feature of DNA melting and are in good match with the available simulation and experimental results. They found that T_m increases with increasing ionic concentration, particularly at low and much less at high ionic concentrations. Singh *et al.* investigated the role of salt concentration on the thermal and mechanical unzipping behavior of heterogeneous dsDNA

Table 1.1: Range of forces with respect to their techniques

Technique	Force range
Atomic force microscopy (AFM)	10 to 10^4 pN
Optical tweezers (OT)	10^{-1} to 100 pN
Magnetic tweezers (MT)	10^{-2} to 100 pN
Bio-membrane force-probe	10^{-2} to 1000 pN

molecules [31–33]. Among various theoretical model studies, Molecular Dynamics Simulation provides insights into the behavior of individual atoms and molecules with the help of computer algorithms. Also, Monte Carlo Simulations provide valuable results for the kinetics and thermodynamics of DNA melting.

In living organisms, the DNA strands are open due to force applied by proteins/enzymes on selected locations along the molecule [2, 3, 34–36]. Experimental techniques like optical and magnetic tweezers and atomic force microscopes have now made it possible to probe the force elongation characteristics of the double-stranded DNA (dsDNA) molecule [37–40]. In Table 1.1, we have mentioned several developed techniques to manipulate single molecules, each with its unique force range and application. Atomic Force Microscopy (AFM) utilizes a cantilever with a sharp tip to interact with the molecules. It's capable of applying and measuring forces in the range of 10 to 10^4 pN [41]. This technique is not only used for manipulating molecules but also for imaging surfaces at an atomic scale making it a versatile tool in nanotechnology and molecular biology. Following AFM, Optical Tweezers (OT) employ a highly focused laser beam to trap and move small, dielectric particles. They are particularly noted for their ability to manipulate objects in the force range of 10^{-1} to 100 pN [42]. In Magnetic Tweezers (MT), researchers apply magnetic fields to manipulate magnetic beads attached to molecules. They can exert forces between 10^{-2} to 100 pN and it is especially beneficial for their ability to apply torsional stress to study supercoiling in DNA and the mechanical properties of protein complexes [43]. Lastly, the Bio-membrane Force Probe is another technique that is particularly adept at measuring the interactions between individual biomolecules and their receptors with forces that are typically in the 10^{-2} to 1000 pN range [44]. In 1992, Smith *et al.* conducted an experiment where single DNA molecules were attached at one end to a glass surface and at the other end to a magnetic bead. They observed the equilibrium positions of the

beads under known forces in an optical microscope and analyzed extension versus force curves at different salt concentrations [45]. Four years later, the same group demonstrated force-measuring laser tweezers to stretch single molecules of double-stranded DNA (dsDNA). They found that under longitudinal stress of about 65 piconewtons (pN), the dsDNA molecules undergo a highly cooperative transition into a stable form that was 70% longer than the regular B-form dsDNA [46]. In 1992 Cluzel *et al.* measured the force-displacement response of a single duplex DNA molecule and observed that the force plateaued at around 70 pN when the DNA was stretched about 1.7 times its contour length. They termed this state "S-DNA" and found that the addition of an intercalator suppressed this transition [47]. Later in 2002, Tinoco and Bustanamete suggested that in addition to temperature and pressure, the force could be used as an extra variable to affect chemical reactions. They put forward an approach in which a molecule is linked to either the atomic force microscope cantilever's tip or a bead within a laser light trap [48]. This force-induced DNA melting is a directional process, where the DNA unwinds through the formation of bubbles or loops [9, 34]. There are two ways by which force can be applied to DNA. Either it is pulled in a direction perpendicular to the helical axis, or it is pulled along the helical axis of DNA [8, 49]. The study of Mosayebi *et al.* argues that duplex rupture is an activated process, where the strands separate in a finite time, depending on the duplex length and applied force. Their findings have important implications for a new force-sensing nanodevice that operates between shearing and unzipping modes, showing a sigmoidal dependence on the fraction of the duplex under shearing at a fixed time scale and duplex length. They have shown a pictorial representation of all possible methods through which the DNA is unzipped (as shown in Fig.1.3) [50].

Further, Nath *et al.* conducted simulations to analyze the force-extension curves of DNA unzipping and rupture. The main focus of their investigation was to understand the process of DNA separation, both in the presence and absence of interstrand crosslinks (ICLs). Their research revealed important insights with implications for drug design. They suggested that there is potential to develop drugs that are less toxic by specifically targeting the interactions of DNA with ICLs. These findings could pave the way for the development of more effective and targeted therapies in the future [51]. Privalov *et al.* conducted an interesting investigation into the dissociation of DNA strands, displaying a cooperative process characterized by substantial heat absorption and a notable increase in heat capacity. Their study highlighted the stabilizing effect of CG base pairs, attributed

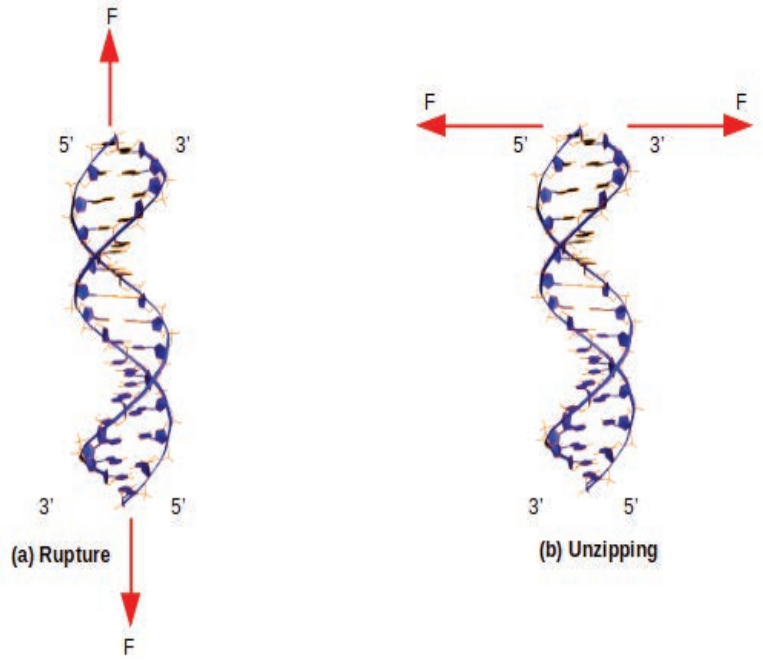

Figure 1.3: The figure displays the rupture (a) and unzipping (b) processes in DNA molecules. The classification is based on whether the DNA is pulled along the axis or pulled in the directions perpendicular to the helical axis.

to their relatively smaller entropic contribution compared to AT pairs. Notably, AT pairs demonstrated higher enthalpic and entropic contributions due to the presence of water molecules fixed in the minor groove of DNA [52]. In addition, the study of DNA melting in force ensemble also reveals that the amount of force varies with the chain length. A detailed study on different chain lengths from 12 to $1,00,000$ was studied by Danilowicz *et al.* In their study, they have explained that for short molecules, the melting force is independent of the ends, and shear force as a function of length is described by de Gennes's theory [53]. Kumar and Giri investigated the behavior of a stiff polymer chain subjected to an external force and studied its complete state diagram [54]. They discovered the existence of a folded-like state in a stiff homopolymer and concluded that as the temperature decreases the stiffness parameter (b) of the chain increases.

Bhattacharjee performed one of the first theoretical works based on the lattice model in which he discussed the opening of the Y-fork, which is the initial step of DNA replication, and how it is influenced by an external force applied at one end [55]. Later on, Hamiltonian-based studies were conducted to study the force unzipping of DNA [54, 56–58]. The simulation study of Upadhyay *et al.*, investigated the stability of the hairpins and the effects of closing the base pair that

seals the loop. They used unzipping force histograms to compare the stability of hairpins with A4 and T4 loops. Their study highlights the complexity of DNA hairpin stability and suggests that single-molecule experiments are needed to further explore and resolve these stability issues [59]. A recent study by Everaers *et al.* explains the single-molecule stretching experiments of flexible molecules in a force ensemble. In their research, they derived the elongation-force and force-elongation relationships of long polymers [60]. The Langevin Dynamics Simulation study of Kumar *et al.* shows the effect of a shear force applied along the direction of the helix and rupture mechanism. Their study in constant force ensemble also describes that de Gennes's length remains independent of the applied force and regimes of extension in the covalent bond along the chain [61]. Guttmann *et al* studied the unfolding of bioploymers in constant force and constant distance ensembles. They have shown that in the constant force ensemble, the force-extension curve shows multiple plateau regions, which are the intermediate states. Similarly, in constant distance ensemble, these states provide a unified response to pulling and compressing forces [62].

One of the interesting studies of the unwinding of DNA by Free energy simulations was performed by Liebl *et al.* with the help of AMBER14 [63]. Employing a torque on the ends of DNA oligonucleotides during the simulation shows the local unwind of DNA beyond an elastic regime. Also, the local melting with complete dissociation of base pairs and flipping of nucleotides was observed in the AT-rich region, while the GC-rich region showed stacking changes. Utilizing theoretical models, our study investigates the deformation of DNA molecules under mechanical stretching, as discussed by Zoli *et al.* [64]. They explored the mechanical behavior of DNA using a coarse-grained Hamiltonian model which focuses on radial and angular fluctuations of base pairs. Their approach enables the determination of the macroscopic elastic response by analyzing the effective potential of the Hamiltonian. Another Hamiltonian model was studied by Singh and Singh, which suggests that genome sequence plays a specific role in the melting of DNA and how the force-extension curve directly explores the free energy landscape of force profile [65]. In 2023, Rudra *et al.* performed a scientific study that focuses on the force-induced melting of a DNA hairpin on a face-centered cubic lattice. Their findings were consistent with the predictions of the Gaussian network model and Langevin dynamics simulations [66].

Researchers have conducted substantial studies in the field of DNA melting. However, attempting to encompass all of this research within a single thesis is not

feasible. Consequently, my thesis will focus exclusively on examining studies that directly align with my research objectives.

1.1.2 DNA in the presence of solvents

Force-induced melting, also known as mechanical unfolding, refers to separating the two strands of DNA by applying mechanical forces. In the presence of solvents, this melting phenomenon leads to exciting and vital implications in various fields. When a biopolymer is subjected to an external force in the presence of solvents, it can disrupt the regular lattice arrangement and melting temperature of the system. Experimental techniques such as single-molecule force spectroscopy (SMFS) and optical tweezers are commonly used to apply mechanical force and monitor the unzipping dynamics of DNA in the presence of solvents. The viscous drag of solvent, hydration, and presence of ions/salt in the surroundings can perturb the force-induced unzipping of DNA. Important to note that when a substance dissolves in another substance, the chemical potential of the system decreases. It is because of the increased entropy of the system due to the mixed solution. This increase favors the dissolution process unless strong, energetic interactions exist between the substances that oppose it. Orwoll *et al.* calculate the interaction parameter χ to describe the thermodynamic properties of polymer solutions, which provides a quantitative measure of the interactions between the polymer and the solvent [67]. The theoretical frameworks based on statistical mechanics, such as the Kirkwood-Buff and liquid state theories, provide a statistical description of solvent properties. These theories establish a connection between the microscopic structure and the macroscopic characteristics of a mixture. They enable the computation of different thermodynamic properties, including excess enthalpy, excess entropy, and excess volume [68]. Another interesting theoretical model is the "Solvent Accessible Surface Area (SASA)" model, which estimates the surface area of a molecule or a biomolecule that is accessible to a solvent. This model is based on the concept of a solvent probe, which is an imaginary spherical particle representing a solvent molecule. The model calculates the surface area of a molecule by rolling the solvent probe over the molecular surface and measuring the area covered by the probe without intersecting the molecule itself [69]. The study of Mohanta *et al.* extended the self-avoiding walk (SAW) model to investigate the behavior of double-stranded DNA (dsDNA) in the presence of an attractive surface [70]. They observed that the melting process of the DNA was primarily influenced by entropy, which could be significantly reduced when an external force was applied. They con-

sidered three cases: weakly attractive, moderately attractive, and highly attractive surfaces. In 2014, Arcella and colleagues conducted a molecular simulation to examine how DNA behaves in low-polarity solvents [71]. Their study emphasizes the significance of neutralizing DNA charges to facilitate efficient transfer to apolar solvents. A recent study by Majumdar used the "pruned and enriched Rosenbluth" computational method to analyze the melting phase diagram of double-stranded DNA in a poor solvent. They found that as the quality of the solvent changed from good to poor, there was a non-monotonic change in the melting temperature. His study also revealed that the critical exponent continuously varied along the melting curve, and the nature of the melting transition is non-universal [72]. Menhaj *et al.* investigated the thermal stability of DNA-bound AuNPs in the presence of other molecules and solvents [73]. They consider water molecules and seven types of ionic liquids as a solvent in the surrounding DNA. They analyzed the presence of cations of ionic liquids (ILs) and observed DNA stability at low concentrations. Several experimental techniques like spectroscopy (e.g., infrared, nuclear magnetic resonance) and calorimetry are used to study the interactions between solvents and polymers. These experiments help us to determine the solubility, swelling behavior, and compatibility of solvents with different types of polymers [74, 75]. In addition, diffusion coefficient measurements using techniques like pulsed-field gradient nuclear magnetic resonance (PFG-NMR) allow for investigating solvent diffusion rates and transport properties. These studies provide insights into solvent mixtures, investigating the behavior of binary or ternary solvent systems and diffusion mechanisms of solvents.

1.1.3 DNA-Linked Gold Nanoparticles

The formation of a system involving DNA and gold nanoparticles typically involves a controlled and precise process in a laboratory setting. Once the gold nanoparticles are formed, they are coated or functionalized with molecules that can interact with DNA. The formed DNA-gold nanoparticle complexes are characterized using various techniques such as spectroscopy, electron microscopy, and gel electrophoresis. This step ensures the successful formation of the complex and allows for optimization of the binding conditions. Adding gold nanoparticles to DNA forms a complex system with unique optical and electronic properties [76–78]. These conjugates are useful in studying biosensing, bioimaging, and drug delivery. Generally, in this technique, the ssDNA molecule is attached to the surface of gold nanoparticles. For example, it may be used in drug delivery by attaching thera-

peutic molecules to the system or employed in biosensors by de- signing specific DNA sequences for target detection. In contrast, silver nanoparticles (AgNPs) are smaller than gold and are known for their antibacterial or antiviral properties [79, 80]. It is also viewed that DNA linked with silver nanoparticles changes DNA's stability and structure, leading to potential toxicity issues. In opposition to this, gold nanoparticles (AuNPs) enhance the strength and stability of the system, which further increases the melting temperature of DNA. These conjugate systems have important applications in various fields like biotechnology, medicine, and nanotechnology, where they have been used to synthesize novel electronic materials (nanowires, nanoscale transistors, etc....). The size of both the AgNPs and AuNPs is primarily controlled during the synthesis process. For AuNPs, the size can be finely tuned with relatively high stability over a wide range of sizes but AgNPs, however, might exhibit less control and stability, especially at smaller sizes, due to their tendency to react with components in the environment. Therefore the stability of AuNP-DNA complexes and the influence of nanoparticle size on this stability are primarily determined by the interaction between the gold surface and the DNA strands. This interaction is significantly affected by the surface-to-volume ratio of the nanoparticles: smaller AuNPs possess a larger surface area relative to their volume, potentially leading to more robust interactions with DNA molecules.

Several experimental and theoretical researchers have worked on this interesting problem of the DNA-AuNPs system. Mirkin pioneered the assembly of DNA nanoparticles in 1996, marking the inception of this field of research [81]. They studied the assembly of colloidal gold nanoparticles by attaching the $13nm$ gold particles to the non-complementary DNA strands. In their research, TEM (transmission electron microscopy) images of aggregated DNA showed the sequence of DNA-linked Au nanoparticles. In a recent study by Xiaoyi *et al.*, DNA is not only considered a genetic material but also shows biocompatibility, correct base pairing, and an excellent ligand for AuNPs [82]. They describe various methods for preparing DNA-AuNPS in which they have explored the salt-aging method (developed by Mirkin *et al.*), vacuum centrifugation method (developed by Brust *et al.*), modification method assisted by dATP (developed by Hsing *et al.*) and freezing method (developed by Liu *et al.*) [83–85]. All these presentations demonstrated that there are versatile and precise tools for genetic information associated with AuNPs proving promising tools for fluorescence, electrochemical biosensors, bioimaging, and photothermal therapy. Miyoshi *et al.* showed the melting curves

of the DNA-AuNPS system at different concentrations of molecular solvents [86]. It concluded that, as compared to free DNA, AuNPs allow a sharp change in melting temperature. After analyzing DNA-AuNPs conjugates, Zhang *et al.* opened up new avenues for this study and explained the synthetic routes and state-of-the-art applications through the combination of nucleic acids and synthetic polymers [87]. They explained that various biomolecules like proteins, nucleic acids, and lipids are present inside the cell. The presence of all molecules occupies $20-40$ % of the cell volume. To understand the stability of DNA-functionalized AuNPs, they varied PEG's concentration and molecular weight. Their analysis showed that DNA-AuNPs are very stable in a buffer solution where no PEG (Crowder) is present, while citrate-capped AuNPs are stable in a PEG medium [88]. In addition, PEG undergoes a phase transition at high salt concentration and temperature, but the DNA-AuNPs remain unaffected, indicating a solid indication of this conjugate.

In 2023, Dutta explained the interaction between DNA bases (A, T, G, and C) and a gold surface. The research also calculates the relative affinity ranking of these four DNA bases when interacting with the gold surface [89]. Their study has explained the sharp melting of conjugates caused by the simultaneous cooperation of all DNA strands and tighter binding to cDNA in which the equilibrium binding constant (k_{eq}) for DNA-AuNPs is three-fold greater than non-modified DNA. Huaping*et al.* studied AuNPs attached DNA using a protein corona [90]. Their study explains that using AuNPs in the biological environment leads to the adsorption of proteins onto its surface, forming protein corona. Further, this protein corona can attach DNA to the nanoparticles. The protein corona helps to control DNA degradation and enhance its stability. In the 2019 study of Kokkinos, electrochemical DNA biosensors attached with nanoparticles are also a promising technology and give the advantage of detecting the small sequence of DNA [91]. Different gold, silver, and magnetic nanoparticles have been used in environmental monitoring, medical diagnosis, and food safety. From the application point of view, these DNA-AuNPS are feasible to calculate the sequence of nucleic acids, identification of heavy metal ions, therapy in the living systems, delivery of specific genes into the cells, and many more [92, 93]. The interesting study of Busson *et al.* showed the optical and topological Characterization of AuNP dimers linked by a single DNA strand. They demonstrated symmetric and asymmetric AuNP dimers with scattering cross-sections and plasmon coupling. Their statistical analysis of the optical and morphology of dimers is analyzed by darkfield and cryoelectron microscopies, which are in conjunction with Mie theory calculations and suggest

that electrostatic interactions cause the stretching of particle dimers in water [94].

1.1.4 DNA in confined geometry

DNA in confined geometry refers to studying DNA when placed and confined in small spaces or environments. Inside the cell, DNA is confined in a limited space or a highly dense medium [9, 95, 96]. This confinement restricts the free movement of DNA molecules due to which it can adopt different conformations and structures [97–99]. The packaging or confinement of DNA shows compression, stretching, bending, twisting, and sliding of base pairs which further affect the mechanical properties, stability, and reactivity of the system. This research helps us understand how DNA interacts with other molecules in the cell and how it behaves when confined in a nanochannel to calculate physical and chemical properties [100]. Sometimes due to genetic changes, a segment of one nucleic acid molecule breaks off and attaches to the other part. The movement of nucleic acids, termed "translocation", is a genetic process that has implications in the realm of human genetics. The study of polymer translocation through natural or artificial channels is interesting in nanotechnology, genetic engineering, and biotechnology. Various biomolecules like protein, RNA, and DNA pass through the nuclear pores [101]. In DNA sequencing, genetic material passes through biological or solid-state pores. The translocation of DNA uses solid-state pores and nanopore technology. Nanopore technology uses a protein nanopore which is also known as a biological channel, and its diameter is a few nanometers [102–105]. The passing of DNA through nanopores changes the electrical resistance, which is further analyzed and measured to study genome sequencing. Solid-state nanopores are artificial and manufactured with the use of silicon and graphene [106–110]. When DNA translocates to this type of nanopores, it causes a change in electric current. Therefore translocation of DNA through both the nanopores offers high resolution and the ability to understand the nanofluidic system [111–114].

In the 1990s, Akeson and his colleagues considered α-hemolysin channel to detect and characterize single DNA or RNA molecules as they pass through the pore driven by an applied electric field. The main finding of their study revealed that as DNA or RNA translocates through the nanopore, the individual nucleotides in the polynucleotide must pass through the pore sequentially. This is because the pore's restricted diameter can only accommodate one DNA or RNA strand at a time [115]. In addition, Derrington *et al.* consider the crystal structure of MspA (Mycobacterium smegmatis porin A) as a nanopore (as shown in Fig.1.4).

This nanopore comprised amino acids and calculated the residual current when DNA passes through the pore. [116]. In recent years, the study of nanopore

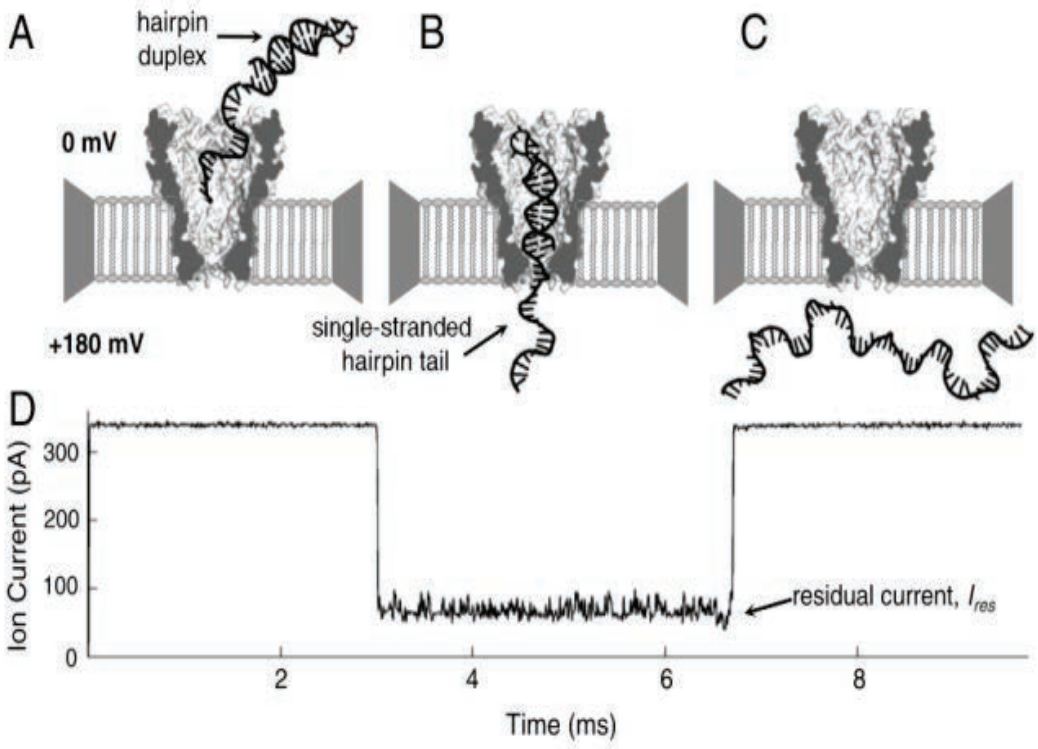

Figure 1.4: Translocation of DNA through the nanopore MspA. (A) The positive voltage attracts the negatively charged hairpin into the pore. (B) The DNA threads through the pore until the hairpin prevents translocation. (C) Complete translocation through the protein nanopore. (D) The corresponding residual current and time plot for all three cases. The image is taken from I. M. Derrington *et al.*, PNAS **107**, 16060 (2010).

translocation has given promising results in sequencing, genomic mapping, and barcoded target detection [117]. The basic science behind the study utilizes the hypothesis that the passing of nucleotides through the nanopores generate an ionic current, and recording this current gives remarkable result about the sequence of DNA. The key point of these studies is to calculate the scaling components of the translocation time with the chain length of DNA and the electronic signature of translocating different bases [118]. Studying nanopores is essential to read out the genetic information because pores are sensitive to changes in the environment like salt concentration, pH, and chemical environment [119]. These parameters affect the stability of nanopores and manipulate their functions. Hence, all these nanopore instabilities can be removed with the development of Solid-State nanopores. The data obtained through the solid-state nanopores are high-speed and significant, in which typical velocities of nucleotides are 10-1000ns per base

across the pores. Sometimes short DNA chains or protein data are less identified due to the high velocities. This undetected data prevents the accurate study of cancer disease, analysis of miRNA segments, and many more. Multiple techniques have been introduced that slow down the translocation processes. Among various approaches, some important properties like the viscosity of the electrolytes, use of optical/magnetic tweezers, rectification in surface charge density, and manufacturing of nanopores with dielectric material (Al_2O_3, HfO_2) resolve these issues and reduce the translocation speed. Yuan *et al.* recently discussed the potential of monolayer 2D materials, such as graphene, MoS_2, WS_2, and h-BN, for nanopore devices in DNA sequencing. Their study explained that these 2-D materials are fragile, with thicknesses comparable to the spacing between DNA nucleotides, making them suitable for nanopore-based DNA sequencing. The author also suggests that a helium ion beam may be a key technology to address these fabrication challenges [120]. Another recent study on DNA translocation was performed by Yao *et al.* in which they explained the effect of molecular crowding on the translocation process [121]. They focused on the translocation of single-stranded DNA (ssDNA) under conditions of molecular crowding (specifically PEG (polyethylene glycol)) using nanopore single-molecule techniques. They observed that a crowding agent significantly improves the ssDNA translocation's event frequency and dwell time through the nanopore. Further analysis of these groups extended their work to study the behavior of other biomolecules, such as RNA, enzymes, proteins, and other interactions in macromolecular crowding conditions at the single-molecule level, which has broader implications for understanding biological processes in complex cellular environments. The theoretical study of Klaus Schulten and Peter described a sensitive method called "Continuous Fluorescence Microphotolysis" for studying translational diffusion in the plasma membrane of single living cells and related systems [122]. In addition to these studies, computer simulation methods also address the structural and dynamic properties of DNA translocation. Recently Zhao *et al.* performed the simulation of DNA with GROMACS. They explained the appearance of MoS_2 nanopores for which the force field parameters are present in their study and also used the CHARMM27 force field required for DNA simulation [123]. In this first and interesting study, they have calculated the I-V characteristics of MoS_2, the electrostatic potential of nanopores under external biasing, the interaction of ssDNA with MoS_2 surface, and translocation traces of individual nucleotide at different voltages. Hence this field of research has gained much interest in various applications such as DNA nanotechnology, drug delivery,

gene therapy, and DNA sequencing [124]. *In vivo*, the confinement of DNA within the nucleus serves as a protective mechanism against damage from radiation and harmful molecules. After considering all these, researchers have developed techniques such as micro-nanofabrication, microfluidics, and imaging methods to study the DNA in confined geometries.

Several theoretical and experimental methods have been developed to study DNA behavior in confined geometries. Kratky and Porod developed the well-known wormlike chain model (WLC) in 1949. The model assumes that the polymer behaves like a semi-flexible rod, and it can be bent and twisted after applying external forces [125]. The critical parameters of this model are the length and diameter of the DNA molecule, as well as the shape and size of the confinement. Another ancient method is the self-avoiding walk model, which assumes DNA is a random coil and cannot intersect itself. These statistical methods also explain the change in entropy and enthalpy of the system. The study conducted by Giri *et al.* focused on understanding the conformational properties of the DNA chain and how the base pair interactions and the nature of the pore (cone-shaped versus flat) influence the equilibrium properties of the attached DNA chain at varying distances from the pore's edge. Their findings demonstrated that the confinement arising from the cone-shaped channel leads to interesting properties with potential applications in understanding biological processes such as transcription and translocation [126]. One of the famous studies by Reisner *et al.* explained the statics and dynamics of DNA molecules confined in the nanochannels [127]. They have calculated extensions and relaxation time for DNA molecules stretched in nanochannels for which widths vary between 30 to 400nm. Also, calculating the critical width of the nanochannel determines the degree of confinement. The extension in width is consistent with the power law $D^{-0.85}$, which differs from the de Gennes theory $D^{2/3}$. To clarify the concept of the persistence length of DNA molecules in nanochannels, Peter Cifra *et al.* study the influence of confinement on the persistence length of dsDNA under a high ionic strength environment [128]. They have done coarse-grained Monte Carlo simulation to compute the dimensional properties of DNA, and the methodology was based on the Bead-spring Model of dsDNA. This model explains the bond stretching potential, bead interaction potential, and bending energy of the DNA chain for which an effective bond is represented by the FENE (finitely extensible nonlinear elastic) potential. Recently Maity *et al.* worked on the problem of DNA confinement with a statistical method [129, 130]. They have calculated the stability and melting of DNA duplex with cylindrical and conical

confinement. Their results also show how the effect of confinement changes with the linear size of the molecule and the 3-D opening of the complete DNA chain. Another aspect of confinement is enclosing DNA molecules within the protective structure, such as liposomes or nanoparticles. This DNA encapsulation is used to protect from degradation, facilitating DNA delivery into cells and controlling the release of DNA at a desired location [131]. Recently Chauhan and Kumar investigated the combined impact of conical geometry and polymer interactions on polymer translocation. Their results revealed that conical channels exhibit asymmetric free-energy barriers and wells, leading to faster translocation with slightly repulsive or zero pore interactions [132]. The study of Mohanta *et al.*, explained the impact of solvent gradients within a finite-width strip on the transfer of ds-DNA from one side of the strip to the other. They used a realistic lattice model of the polymer and observed that the solvent gradient plays a crucial role in driving the dsDNA from the lower layer (high temperature) to the upper layer (low temperature). The study of the equilibrium properties of a linear polymer chain with finite length confined within an infinite wedge formed by two perfectly reflecting hard walls meeting at a variable apex angle (α) was performed by Kumar *et al.* in 2020. They discussed the nonmonotonic behavior and its potential significance in understanding cellular processes occurring in nanoconfined geometries.

1.1.5 DNA in crowded solution

Crowding refers to the high concentration of macromolecules in a cellular environment, which results in a reduced volume in which other molecules can move and interact. This crowded environment can profoundly influence the behavior, interactions, and functions of biomolecules, making them different from those in dilute solutions [1, 4, 133]. Living cells contain a diverse array of biomolecules, such as nucleic acids, proteins, lipids, and metabolites, which collectively occupy a significant portion (20-40%) of the cellular space. This indicates that the volume excluded by these biomolecules and chemical interactions are critical for determining the structure and stability of DNA molecules. For example, an *E. coli* cell is only about $2\mu m$ long, $0.5\mu m$ in diameter, and the cell volume is $0.6 - 0.7\mu m^3$. However, *E. coli* can have as many as $4,288$ different proteins, and about 1000 are produced at levels high enough to be easily detected. It is understood that the crowding particles decrease the entropy of the folded or unfolded state as well and hence stabilize the ordered structure. The effects of molecular crowding on the mechanical stability of protein molecules studied by Yuan *et al.* [134]. It was

found that the mechanical stability of ubiquitin molecules was enhanced by molecular crowding. However, there is a lack of reports on the mechanical stabilities of DNA molecules under macromolecularly crowded conditions, which prevents the interpretation of the biological relevance of these molecule structures.
In experiments and simulations, researchers used various solutes such as polyethylene glycols (PEGs), dextrans, and Ficoll 70 in aqueous solution to mimic the cellular environments [135–137]. The prime reason for their use is that they are inert with nucleotides and they are available in different molecular weights. Osmolytes are also used to study the base pair stability in the crowded solution. Harve *et al.*, found a variation of 0.5-2.5 K in the increase of melting temperature of 20 oligomers DNA in a crowded solution. These studies suggest that the effect of crowding on the melting and stability of nucleic acids is an interesting area for research [138]. The molecular crowding of double-stranded DNA has been interestingly studied experimentally by Naoki Sugimoto's group. In their previous work, they considered different PEGs with molecular weights of 200, 4000, and 8000 and calculated the UV absorption and temperature of DNA duplexes with the help of Fluorescence spectrophotometers. They explained the significance of the molecular crowding conditions in the cytoplasm and nucleus. The studies helped to understand the structure, stability, and function of nucleic acid, which is helpful in biotechnology and nanotechnology. The presence of crowding also changes the physical and chemical properties of DNA molecules. Khimji *et al.* investigated the stability of DNA duplexes in polyanionic solutions [139]. Conversely, the condensation of expanded DNA into a compact structure is also affected by cations, lipids, and crowding agents. The fluorescence spectroscopy showed that DNA condensation by PEG is more flexible than binding agents such as polyethyleneimine. Using the nearest neighbor model (NN model), Ghosh *et al.* studied the duplex stability in diverse molecular crowding conditions [140]. Their study helps to determine the behavior of DNA in live cells and calculate the thermodynamic parameters (ΔH, ΔG and ΔS) and melting temperature (ΔT_m) for different chain lengths in the presence of $PEG200$. Miyoshi *et al.* studied the effects of loop length on the conformation, thermodynamics stability, and the hydration of DNA Guanine-rich quadruplexes[1] under molecular crowding conditions have been investigated [141]. The effects of molecular crowding with PEP-Na (ploy ethylene sodium phosphate) on the thermodynamics of DNA duplexes, triplexes, and G-quadruplexes were systematically

[1] G-rich strand of human telomeric DNA can fold into a four-stranded structure, that is called as G-quadruplex

studied [142]. The thermodynamic analysis demonstrated that PEP-Na significantly stabilized the DNA structures. Goodrich *et al.* [143] also investigated the effect of polymeric solutes on the thermal denaturation behavior of DNA-Gold nanoparticle assemblies.

Shang *et al.* conducted a theoretical study to examine the effect of molecular crowding on DNA unwinding. Their thermodynamic model explains that each nucleotide pair in dsDNA and each nucleotide in ssDNA are represented by two types of Lennard-Jones fragments and water molecules are modeled as spherical particles [30]. In this system, they considered crowders of different sizes, chain lengths, and interaction strengths which give predicted changes in entropy, Gibbs energy, and enthalpy. This study also shows that the melting of DNA in a crowded environment is affected by entropic and enthalpy. Singh *et al.* studied the effect of molecular crowding and confinement by protein in the cell on the unfolding mechanism of DNA. They described the stretching of polymers in molecular crowding conditions with the help of the self-attracting self-avoiding walks (SASAWs) model [144]. Other statistical models also explain the melting of DNA in the crowded solution. The well-known Peyrard-Bishop-Dauxious model is a Hamiltonian-based model that explains many parameters like free energy, specific heat, and average separation of base pairs in the presence of crowders. Singh and Singh showed that crowders prevent the propagation of bubbles created by thermal fluctuations. The different density profiles of the opening also show how crowders block the base pair's movement and hamper the DNA opening mechanism. In a study by Brackley *et al.* [145], the effect of molecular crowding agents on protein-DNA detection was reported using coarse-grained Brownian Dynamics (BD) simulations. They studied the presence of crowders in the cytosol and along the DNA molecule. Their findings suggest that an accurate interpretation of the crowded cellular environment is essential for a better understanding of protein-DNA targeting. The theoretical method of Sanbo and Zhou [146, 147] is rich enough to enable conformational sampling to model crowding effects. It covers the challenges posed by large protein oligomers and by complex mixtures of crowders. In this model, instead of calculating the free energy differences between two end states in the absence and presence of crowders. Using molecular dynamics simulations and a theoretical approach, Kim *et al.* showed that a flexible chain molecule could be compacted by crowding particles with variable sizes in a (cell-like) cylindrical space [148]. Taylor *et al.* studied the reduction in configurational entropy due to crowding agents. They used the Wang–Landau simulation algorithm to construct the density of

states for this chain in a crowded environment and study the folding of the chain from the coil to a collapsed-globule state [149]. These studies show that denaturation and folding processes in crowded environments are affected by entropic and enthalpic factors. However, understanding DNA melting or denaturation in a crowded solution still needs to be completed.

1.2 Existing research gap

Although significant progress has been made in elucidating the fundamental mechanisms and factors involved in this process, many areas of DNA denaturation require further investigation. Scientists have explored the problem through experimental, theoretical, and simulation approaches. However, we must explore the effect of various factors on DNA melting, such as sequence, epigenetic modifications, and the presence of proteins or other biomolecules. The structure and dynamics of biopolymers, especially DNA, are complicated. Despite significant work to understand the dynamics of the molecule similar to the *in vivo* conditions, we are far from the actual system. This thesis aims to fill the theoretical research gap with the existing experimental investigations. A few of the research gaps addressed in this thesis are listed here.

- Understanding how DNA molecules adapt and undergo conformational changes when confined within small spaces is crucial for various applications, including DNA sequencing, gene delivery, and DNA-based nanotechnology. The influence of partial confinement of DNA in cylinder geometry of different sizes explains the entropic changes in the system. Further, the correlation between the melting conditions and the size of the cylinder may enhance our understanding of the molecule confined in a shell and be a helpful process for gene therapy.

  One of the significant research gaps lies in understanding the influence of confinement on conformational changes in the DNA molecule.

- DNA-functionalized gold nanoparticles (AuNPs) have been widely used to assemble materials, biosensors, and drug delivery. The practical application of DNA-linked gold nanoparticles (AuNPs) heavily relies on the thermal stability of these complexes. For instance, in PCR, the amplification of specific DNA sequences requires repeated heating and cooling cycles. For better accuracy, the DNA-linked AuNPs should be thermally stable. Our

understanding of these bio-interfaces still needs more attention to address issues related to the development of engineering hybrid materials.

- DNA has enormous power in storing hereditary information. The stored information is beneficial for people working in the area of nanotechnology and molecular computing. The solvent present in the solution containing DNA plays a crucial role in the functioning of DNA. The solvents present in the solution can perturb the hydrogen bonds and electrostatic interactions within the DNA molecule, potentially affecting its stability and energy required for unzipping. Scientists have already studied how different solvents affect the shape of DNA, but there is still more to learn. We need additional research to fully understand how various solvents influence DNA molecules.

- DNA in the presence of crowders relates to the understanding of how crowding agents impact DNA structure, dynamics, and function within complex biological environments. The understanding of DNA unzipping in the presence of "aspartame" and Polyethylene-glycol 200 ($PEG-200$) molecules shows how they are settled down in the grooves of DNA and change their conformations. The variation in the number of crowders in the surrounding DNA influences the overall shape and flexibility of DNA molecules that can provide insights into DNA packaging, protein-DNA interactions, and chromatin organization within the crowded cellular environment. Most of the work in DNA in the presence of crowder is done by taking the PEG molecules. How molecules like aspartame alter the activities of molecule still need proper attention.

We expect future research on the above-discussed issues will elucidate the response of DNA molecules in the confinement of different geometries, in DNA linked with a Gold-nanoparticles complex system, force-induced unzipping in the presence of solvent molecules, and the presence of different crowders.

1.3 Objectives of the present work

The present work aims to accomplish the following objectives:

1. To understand the role of solvent molecules on DNA Melting.

2. To study the structural transitions in DNA linked with Gold nanoparticles (AuNPs).

3. To study the effect of partial confinement on melting transition in DNA.

4. To study the effect of molecular crowders on DNA molecules.

To accomplish the objectives mentioned above, we use the Peyrard-Bishop Dauxois model (PBD) and molecular dynamics tool ($AMBER$). The advantage of the Peyrard-Bishop-Dauxois model lies in its computational efficiency and ability to capture DNA melting behavior. The model helps us to understand the thermodynamic stability that enables us to understand the DNA dynamics and the biological processes of transcription and replication studies. In addition, simulations provide a high level of atomistic detail and allow researchers to observe the behavior and interactions of individual atoms and molecules over time. Chapter 2 of this thesis provides a comprehensive and detailed discussion of two key aspects: the Peyrard-Bishop-Dauxois (PBD) model and the Molecular Dynamics (MD) method to study DNA in a crowded and confined environment.

Chapter 2

Nonlinear Hamiltonian Model of DNA

The Peyrard-Bishop-Dauxois (PBD) model was developed through a collaborative effort by many researchers and has had a significant impact on the field of DNA mechanics. In 1989, Peyrard and Bishop proposed a theoretical model that describes DNA as a nonlinear oscillator network. Their focus is on capturing the local dynamics and thermal fluctuations of DNA, particularly its denaturation or melting behavior [25, 26]. Later, Dauxois and Michel Peyrard extended this model in 1993 by incorporating long-range interactions between base pairs [150, 151]. The model has proven useful in studying many aspects of DNA mechanics. It has been used to investigate force-induced DNA unzipping and to analyze DNA unzipping under different cellular conditions. In addition, the model allows the analysis of numerous thermodynamic and statistical properties of the system. As such, it has many applications as an important theoretical framework in the study of DNA mechanics and has made an important contribution to the field [152–154].

- **Understanding of DNA melting:** The model describes how dsDNA molecules melt or unzip in a complex and dense cellular environment [9]. It also explains how DNA behaves when exposed to heat or other denaturing conditions. The unfolding of DNA is important in many biological functions such as replication and transcription etc. Therefore all these processes contribute to understanding the genetic code of life [155].

- **Analysis of DNA stability :** The model helps to understand how DNA maintains its structure and stability under various conditions, such as pH, the presence of salts or solvents, and other biomolecules. Also, DNA inter-

acts with enzymes, and changing its conformation from a double-stranded structure to a single-stranded structure is always an interesting part of the study. All this knowledge can be fruitful to prevent DNA breaking or DNA damage and mutations.

- **DNA mechanical property :** PBD model has been used to study the different properties of DNA such as bond stretching, bending, twisting, opening and base pair displacement, and many more [156–158].

- **Predicting DNA dynamics :** The information about the movement and vibration of molecules provides information about the dynamics of DNA. When this biomolecule is present in any thermal bath, its constituents such as bases, sugar rings, and phosphate atom moves constantly. This movement of a group of atoms changes its dynamics continuously [159, 160].

Overall, the PBD model contributes to the understanding of many physical, mechanical, and biological properties. From the statistical point of view, this model calculates the total energy of the system which further gives entropy, specific heat, and free energy of the system [161, 162]. This model also resembles the ising model because both mathematical models are based on the nearest neighbor interactions. The ising model explains the behavior of interacting spin in a lattice while the PBD model represents the behavior of coupled nonlinear oscillators which represent a base pair in the DNA molecule.

2.1 Fundamental presumptions of the model :

The basic assumption of this model is to understand the phenomenon of thermal and mechanical denaturation of dsDNA helix and it is effectively described by the 1-D representation. The Peyrard-Bishop-Dauxois (PBD) model makes some assumptions about the physical properties of DNA but ignores the 3-D motion of base pairs. Some basic features are:

- **One-dimensional model :** This model treats DNA as a linear chain of beads, where each bead represents a base pair of mass m and the nearest neighbor interaction is presented by W. This interaction captures the elastic properties of DNA.

- **Interaction between base pairs :** Two opposite strands of DNA are joined through the hydrogen bonds. This hydrogen bonding is represented by the morse potential which indicates not only the attraction between two base pairs but also the repulsion between the phosphate groups of opposite strands.

- **Arrengement of atoms in DNA :** This DNA model ignores the twisting, winding, and knotting in DNA, and all the base pairs lie in the same plane. Later the model is modified for the helicoidal geometry [163]. Also, initially, the model was restricted to the homogeneous DNA chain in which the same type of base pairs are present. After modifications, the stability of the heterogeneous chain was also observed [164].

- **Thermal fluctuation on base pairs :** This model is based on the fact that base pairs obtain thermal energy from the system and fluctuate around the equilibrium position. This fluctuation with thermal energy leads to the dissociation of bonds and DNA unzipping.

- **Nonlinear Oscillator :** The non-linearity in the model arises from the anharmonic potential that captures the fact that bond stretching and bending in the dsDNA is not perfectly linear. This nonlinearity is crucial to represent the base pair opening and studying various phenomena related to its structure and dynamics [156].

2.2 Hamiltonian Mechanics

The DNA molecule has a double-stranded structure, with the two strands running opposite each other. These two strands are coiled on the same axis and joined with nitrogenous bases. If the sequence of one strand is known, the sequence of bases of another strand can be assumed [165]. In this model, the helical structure of DNA is assumed to be a straight ladder (Figure 2.1(a)) and it is a fundamental and iconic representation of DNA's three-dimensional shape. In the ladder structure of DNA, base pairs have two degrees of freedom, and the bases of two strands are connected by hydrogen bonds. The behavior of hydrogen bonds is represented by the morse potential and it describes the interactions between non-adjacent nucleotides along the DNA chain. Similarly, the interaction between the adjacent bases on a helix is represented by the stacking interaction which acts as a harmonic potential [166]. Therefore the combination of hydrogen bonding between complementary base pairs

and the stacking interaction between adjacent bases allows the DNA double helix to maintain its stable and compact structure, effectively storing and transmitting genetic information.

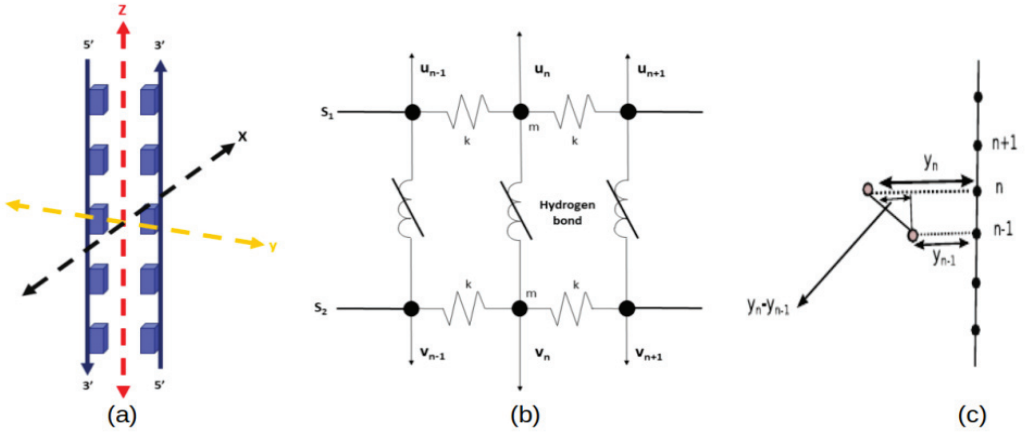

Figure 2.1: (a)The pictorial representation of the simplified ladder structure of DNA. (b) The ladder structure of DNA shows the motions of bases and pairs. (c) displacements of nucleotides from the equilibrium positions.

For the chain of n^{th} base pair, if u_n represents the displacement of bases on one strand and v_n represents the displacement of bases on another strand then the Hamiltonian of the system can be written as :

$$H = \sum_n \left[\frac{1}{2} m\{\dot{u}_n^2 + \dot{v}_n^2\} + \frac{1}{2} k \left(u_n - u_{n+1}\right)^2 + \frac{1}{2} k \left(v_n - v_{n+1}\right)^2 + V(u_n, v_n) \right], \tag{2.1}$$

where, m = mass of the nucleotide; k = elasticity of the DNA strand. In this one-dimensional model, base pairs can move towards or away from each other. Mathematically this *in-phase* and *out-of-phase* motion of base pairs are given as:

$$x_n = \frac{u_n + v_n}{\sqrt{2}} \quad ; \quad y_n = \frac{u_n - v_n}{\sqrt{2}} \tag{2.2}$$

In terms of these two types of motion, hamiltonian can be re-written as:

$$H = \sum_n \left[\{\frac{1}{2} m\dot{x}_n^2 + \frac{k}{2} \left(x_n - x_{n+1}\right)^2\} + \{\frac{1}{2} m\dot{y}_n^2 + \frac{k}{2} \left(y_n - y_{n+1}\right)^2\} + V(y_n) \} \right], \tag{2.3}$$

We know that with the help of this model, we can explain the base pair separation or melting of DNA. Hence *out-of-phase* motion is solely responsible for the

hydrogen bond stretching. In the interest of our study hamiltonian is described by the scalar variable y_n exclusively while the x_n term can be ignored. After this modification, the Hamiltonian takes the following form:

$$H = \sum_{n=1}^{N} \left[\frac{p_n^2}{2m} + V(y_n) \right] + \sum_{n=1}^{N-1} \left[W(y_n, y_{n+1}) \right], \tag{2.4}$$

where

$$V(y_n) = D(e^{-ay_n} - 1)^2 \quad \& \quad W(y_n, y_{n+1}) = \frac{k}{2}(y_n - y_{n+1})^2 \tag{2.5}$$

In the above equation, $V(y_n)$ denotes the morse potential, $W(y_n, y_{n+1})$ is the stacking interaction term while D denotes depth of the potential and a = inverse width of the potential well. Both potentials play a crucial role in the unzipping process and explain the DNA dynamics.

Morse Potential: This potential represents the variation in potential energy as a function of internuclear distance and it describes the behavior of diatomic molecules, where two atoms are bonded together. At the equilibrium distance,

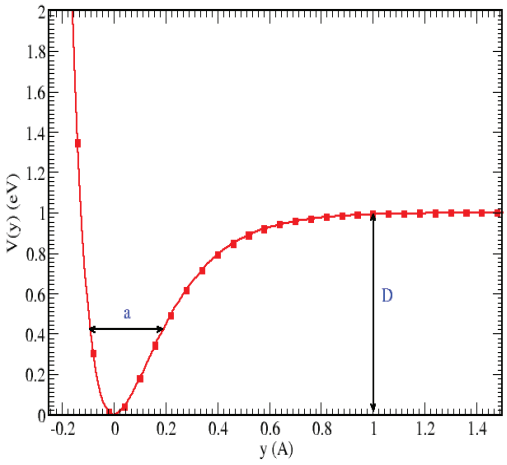

Figure 2.2: The on-site potential for the base pair interaction of the strands of DNA where D is the depth of the potential and a is width of the potential.

the two atoms are present in the most stable condition and potential energy gives the lowest value. As the atoms move away from this distance, the potential energy increases, and after some extent it gets saturated. This saturation shows the

confirmed dissociation of the base pair. In the mathematical equation of $V(y_n)$, the parameter D controls the well's depth, representing the maximum potential energy at the equilibrium distance (Fig. 2.2). Similarly, the parameter a is associated with the width and curvature of the potential well. By adjusting the values of D and a, the potential can be tailored to match both experimental and theoretical data.

Stacking potential: The stacking potential refers to the attractive interaction between adjacent nucleotide bases within the double helix. This term plays a significant role in stabilizing the 3D structure of DNA [167]. This interaction comes from the flat aromatic rings of bases and these bases can stack on top of each other. Vander Waals forces and π-π interactions in the aromatic rings of bases are mainly responsible for this type of interaction. Hence the strength of this potential depends on the sequence of bases and their chemical environment [168].

Researchers have extended their studies to calculate several intra and inter-base pair parameters of helical DNA. We know that the double helix structure of DNA is stabilized by both intra-base pair hydrogen bonds (which hold the two strands of DNA together) and inter-base pair stacking interactions. The prefix "intra-" refers to something that occurs inside a particular group or interactions that happen within a single base pair, such as the hydrogen bonds between adenine (A) and thymine (T) while The prefix "inter-" refers to something that occurs between different groups or the interactions that happen between adjacent base pairs. In fig. 2.3, We have shown the schematic picture of different base pair orientations. Among various stacking possibilities of bases, this model uses the stretching of base pairs. In this potential, interactions can be approximated as a harmonic potential in which potential energy is proportional to the square of the displacement. Also, the inclusion of anharmonicity in harmonic potential gives an accurate description of the dynamics of DNA like denaturation, thermal fluctuations, and DNA breathing. Hence after adding the anharmonic term the equation of stacking energy can be written as:

$$W(y_n, y_{n+1}) = \frac{k}{2}(y_n - y_{n+1})^2[1 + \rho e^{-b(y_n + y_{n+1})}], \tag{2.6}$$

where k is known as the force constant and is related to the stiffness of a single strand. The second term defines the anharmonicity and the parameters ρ and b define the range of anharmonicity. Thus, the complete Hamiltonian of the system

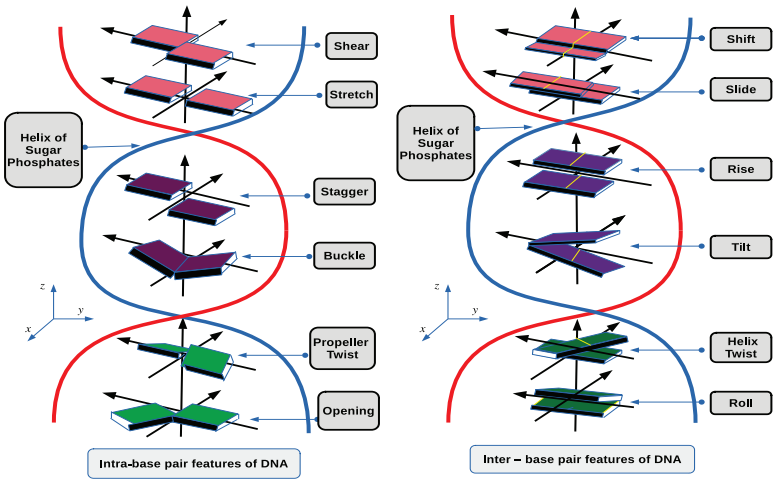

Figure 2.3: The schematic of intra and inter-base pair orientations in the DNA molecule.

is,

$$H = \sum_{n=1}^{N} \left[\frac{p_n^2}{2m} + D(e^{-ay_n} - 1)^2 \right] + \sum_{n=1}^{N-1} \left[\frac{k}{2}(y_n - y_{n+1})^2 [1 + \rho e^{-b(y_n + y_{n+1})}] \right], \quad (2.7)$$

The above equation contain five parameters ρ, k, b, a and D and to make the model accurate and meaningful, we carefully selected these specific parameters. Among all the parameters ρ, b, α primarily influence the sharpness of the transition but they are not overly sensitive in the melting study. Specifically, they modify the landscape of the potential well without significantly altering the qualitative behavior of the melting transition. Hence, their exact values are less critical to the overall physical behavior we are investigating. On the other hand, the parameters κ and D are important and in which the parameter κ is intimately related to the stacking interaction, which is a key factor in the stability of the DNA double helix. Meanwhile, D represents the depth of the potential barrier and thus directly impacts the energy scale of the melting transition.

2.3 Enumeration of the Partition Function

Partition function is a fundamental quantity and the calculation of this quantity provide insights into various aspects of physical system which includes thermodynamic properties of the system, equilibrium states, statistical behavior of quantum systems and it also helps bridge the gap between microscopic interactions and

macroscopic observables. After using the above Hamiltonian Eq.2.7, the partition function can be determined as,

$$Z = \int \prod_{n=1}^{N} \{dy_n dp_n \exp(-\beta H)\} = Z_p Z_c, \tag{2.8}$$

where Z_p = momentum part of the partition function, Z_c = configurational part of the partition function, N = number of base pairs in the chain and $\beta = \frac{1}{k_B T}$. The momentum part of the partition function can be calculated by the Gaussian integral method and this gives kinetic-energy factor for the chain of N particles.

$$Z_p = (2\pi m k_B T)^{N/2}, \tag{2.9}$$

Where m = reduced mass of the base pair and k_B is Boltzmann constant. The solution of the configurational partition function, Z_c, is define as:

$$Z_c = \int_{-\infty}^{\infty} \left[\prod_{n=1}^{N-1} dy_n \exp\{-\beta [W(y_n, y_{n+1}) + V(y_n)]\} \right] \times dy_N V(y_N), \tag{2.10}$$

Here y_n is the displacement of the n^{th} base pair from equilibrium. Here the configurational part of the partition function has coupled terms, so the calculations are a little tricky. To solve the equation for Z_c one can define a Kernel $K(x, y)$ as [169],

$$K(y_n, y_{n+1}) = \exp[-\beta H(y_n, y_{n+1})], \tag{2.11}$$

If the DNA chain is homogeneous then, we have $K(x, y) = K(y, x)$. Thus, the partition can be written as,

$$Z_c = \int_{-\infty}^{\infty} \prod_{n=1}^{N} dy_n K(y_n, y_{n+1}), \tag{2.12}$$

The equation for partition function can be solved by introducing the integral equation

$$\int dy K(x, y)\phi(y) = \lambda\phi(x), \tag{2.13}$$

because of symmetry and the fact that $K(x, y) > 0$, if one assumes

$$\|K(x, y)\| = \left[\int_{-\infty}^{\infty} \int_{-\infty}^{\infty} \{K(x, y)\}^2 \right]^{1/2} < \infty,$$

the integral equation contains a positive Hilbert Schmidt-type kernel and will be having positive eigenvalues and orthonormal eigenfunctions. If the eigenvalues are denoted by λ_i and eigenfunctions as ϕ_i, the orthonormality condition demands that,

$$\int dx\phi_n(x)\phi_m(x) = \delta_{nm} \qquad \text{and} \qquad \sum_{n=1}^{\infty} \phi_n(x)\phi_n(y) = \delta(x-y), \quad (2.14)$$

In terms of these orthonormal eigenfunctions, the kernel $K(x, y)$ can be expanded as [170]

$$K(x, y) = \sum_n \lambda_n \phi_n(x)\phi_n(y), \quad (2.15)$$

Substituting the expression of $K(x, y)$ in terms into Eq.2.12 and applying the orthonormality conditions (Eq.2.14), the configurational partition function will be,

$$Z_c = \sum_{n=1}^{\infty} \lambda_n^N, \quad (2.16)$$

The above expression is valid for the periodic boundary condition. For the open boundary conditions, we have,

$$Z_c = \sum_n \left(\int dy \phi_n(y) \exp\left\{ -\beta \frac{V(y)}{2} \right\} \right)^2 \lambda_n^{N-1}, \quad (2.17)$$

To find the eigenvalues and corresponding eigenstates, we have to diagonalize the matrices that appear in Eq.2.11. Important to note that, the kernal which we defined in the TI (Transfer Integral method) is positive Hilbert Schmidt-type and it works only when the onsite potential are unbounded. However, PBD model uses morse potential which is bound (by D value) and therefore, the Kernel K(x, y) is not Hilbert-Schmidt type, but it is singular. Considering the heterogeneity in the sequence of a DNA chain makes the calculations of the partition function more complex. In this scenario, each site along the DNA chain may not be of the same nature as its neighboring sites. To address this issue, different approaches have been proposed by various research groups. Zhang *et al.* proposed an extended transfer matrix approach (ETMA) where the different kernels can be expanded in terms of the same or different bases [169]. Another approach, proposed by Cule, introduces heterogeneity through quench disorder. For a chain with open boundaries the configurational part of the partition function can be evaluated numerically with the help of the matrix multiplication method [162, 171, 172]. The

important part of the integration of the configurational space is the selection of proper cut-offs for the integral appearing in Eq.2.10. A larger cut-off implies that the probability of the molecule being completely denatured increases for the finite chain. This probability becomes 1 in the limit of infinite cut-off. This is related to the fact that the integral of Eq.2.10 is divergent in nature. To address this issue and avoid the divergent nature of the partition function in numerical computations, T. S. Van Erp *et al.* introduced a double-stranded ensemble [161]. In this ensemble, certain constraints are applied to the DNA chain, which prevents it from exploring infinitely large configurations and effectively regularizes the integral. By utilizing this approach, they were able to establish that an upper cut-off can be $\approx$ 144 Å and a lower cut-off of -0.4Å was appropriate for a specific set of model parameters at a temperature of $300K$. We are using the matrix multiplication method to calculate the partition function by defining different kernels corresponding to the sequence of the chain. The integration in the Eq.2.10 can be written as:

$$Z_c = \int_{-\infty}^{\infty} \exp\left(-\beta \frac{V(y_1)}{2}\right) dy_1 \prod_{n=1}^{N-1} dy_n \exp\left[-\frac{\beta}{2}\{V(y_n) + V(y_{n+1}) + 2W(y_n, y_{n+1})\}\right] \exp\left(-\beta \frac{V(y_N)}{2}\right) dy_N, \tag{2.18}$$

The accuracy of these approaches is limited first by discretization errors in the integrations and by the need to numerically evaluate integrals over an infinite domain. This can be partially lifted by a finite-size scaling analysis, which involves a properly controlled approach to infinity. Integration methods, such as the Gauss-Legendre quadrature (discussed in Chapter 6.7) [173] which select appropriate abscissa for the evaluation of the function according to the number of points involved in the calculation, are useful to integrate over a large domain with a reasonable number of points [174]. We choose the order of the Gauss-Legendre node to be equal to the number of the points used to discretize the integration (this will be the dimension of the matrix that appeared in the Eq.2.11). In our calculations, we found that to get a precise value of melting temperature (T_m) one has to choose the large grid points. The dimension of 900×900 was found to be suitable for this analysis.

After a discretization of the coordinate variables and the introduction of a proper cutoff on the values of the y_n, the task is reduced to discretize the space to evaluate the integral numerically.

The calculated partition functions, Z_p (Eq.2.9) and Z_c (Eq.2.10) can be used to calculate the other thermodynamic quantities of interest by evaluating the Helmholtz free energy of the system. The free energy per base pair is,

$$f(T) = -\frac{1}{2}k_B T \ln\left(2\pi m k_B T\right) - \frac{k_B T}{N}\ln Z_c, \tag{2.19}$$

The other thermodynamic quantities like entropy S, specific heat C_v are evaluated using the following relations,

$$S(T) = -\frac{\partial f}{\partial T}, \tag{2.20}$$

and

$$C_v(T) = -T\frac{\partial^2 f}{\partial T^2}, \tag{2.21}$$

2.4 Calculation of fraction of open base pairs (ϕ)

Theoretically, the fraction of open pairs, ϕ can be calculated by using the partition functions and it is given by $\phi = 1 - \theta$, where the average fraction of bonded base pairs, $\theta(= 1 - \phi)$ is defined as [162, 175]:

$$\theta = \theta_{\text{ext}}\theta_{\text{int}}, \tag{2.22}$$

θ_{ext} represents the average proportion of strands forming duplexes, whereas θ_{int} denotes the average proportion of unbroken bonds within duplexes. To calculate θ_{int}, we need to distinguish between configurations describing a double strand on one hand and dissociated single strands on the other. The n^{th} bond is considered broken if the value of y_n exceeds a cutoff value y_0. Thus, we can define θ_{int} as follows:

$$\theta_{\text{int}} = \frac{1}{N}\sum_{n=1}^{N}\langle\vartheta(y_0 - y_n)\rangle, \tag{2.23}$$

Here, $\vartheta(y)$ represents the Heaviside step function, and the canonical average $\langle . \rangle$ is computed by considering only the configurations with double strands. Upon analyzing the $\langle y \rangle$ values with temperature, we observe a significant rise at approximately $2.0; \text{Å}$. Therefore, we can select $y_0 = 2.0; \text{Å}$ as the threshold value, indicating when a bond can be considered broken.

To calculate θ_{ext}, we follow the formulation proposed by Campa and Giansanti [162, 176]. The equilibrium dissociation of the duplex C_2 into single strands C_1 can be described as $C_2 \rightleftharpoons 2C_1$. In the case of long chains, the dissociation equilibrium

can be ignored as θ_{int} and consequently θ approach zero while θ_{ext} remains close to 1. This means that even if most bonds are disrupted and the DNA is denatured, the two strands may not fully separate due to a few remaining bonds preventing their complete separation. Only at significantly higher temperatures ($T >> T_m$, where T_m is the melting temperature), an absolute separation occurs. Hence, for long chains, we only need to compute θ_{int} since the double strand effectively behaves as a single molecule during the transition. On the other hand, in the case of short chains, the process of breaking individual bonds and strand dissociation takes place within a narrow temperature range. In this scenario, we need to calculate both θ_{int} and θ_{ext}. To determine θ_{ext}, we adopt the following approach.

$$\theta_{\text{ext}} = 1 + \delta - \sqrt{\delta^2 + 2\delta}, \tag{2.24}$$

where

$$\delta = \frac{Z(s_1)Z(s_2)}{2N_0 Z(ds)}, \tag{2.25}$$

here $Z(s_1)$, $Z(s_2)$ and $Z(ds)$ are the configurational isothermal isobaric partition functions of systems consisting of molecular species single strand s_1, single strand s_2 and the double-strand configuration dsDNA respectively. If $2N_0 = 2N_{AB} + N_A + N_B$ and $N_A = N_B$, θ_{ext} is defined as,

$$\theta_{\text{ext}} = \frac{N_{AB}}{N_0}, \tag{2.26}$$

The internal and external parts of the partition function are,

$$\frac{Z(s_1)Z(s_2)}{2N_0 Z(ds)} = \frac{Z_{int}(s_1)Z_{int}(s_2)}{a_{av} Z_{int}(ds)}, \frac{a_{av} Z_{ext}(s_1)Z_{ext}(s_2)}{2N_0 Z_{ext}(ds)} \tag{2.27}$$

where $a_{av.} = \sqrt{a_{AT} a_{GC}}$. In analogy to what has been proposed for the ising model based on the partition function of rigid molecules, one makes the following choice [162]

$$\frac{a_{av.} Z_{ext}(s_1)Z_{ext}(s_2)}{2N_0 Z_{ext}(ds)} = \frac{n^*}{n_0} N^{-p\theta_{\text{int}}+q}, \tag{2.28}$$

and then,

$$\delta = \frac{1}{a_{av}} \frac{Z_{int}(s_1)Z_{int}(s_2)}{Z_{int}(ds)} \frac{n^*}{n_0} N^{-p\theta_{\text{int}}+q}, \tag{2.29}$$

where n^* is a chosen reference concentration as $1\mu M$ while n_0 is the single strand concentration we have chosen as 3.1 μM. The parameters p and q are obtained through fitting the experimental data [162, 175], with values of $p = 29.49$ and

$q = 27.69$. Using Eq. 2.29, we calculate θ_{ext} and consequently the fraction of open pairs, denoted as ϕ, as a function of temperature. In the current work, we keep the concentration constant, but it would be intriguing to explore how the dynamics of the molecules change with varying salt concentration values.

2.5 Computational Methods

Molecular dynamics (MD) simulation is a computational technique used to study the behavior of atoms and molecules over time [177, 178]. It is a powerful tool to understand the behavior and interactions of atoms and molecules in atomic-level molecular systems. In MD simulations, the positions and velocities of atoms or particles are numerically integrated using classical mechanics equations of motion. These equations describe how the particles interact with each other through interatomic forces, such as the Coulombic forces and Lennard-Jones forces. By repeatedly updating the positions and velocities of the particles, the simulation can predict the movement and behavior of the system over time [179]. It acts as a bridge between theory and experiments. It provides a lot of information that is difficult to measure. Since its beginning, molecular dynamics simulation has become a crucial tool in many scientific fields such as chemistry, biology, physics, and materials science.

Further, simulation plays an important role in the study of DNA melting where we can explore interactions between nucleotides, the basic building blocks of DNA, and incorporate factors such as temperature, solvent conditions, and DNA sequence variations [180, 181]. Thus, after combining MD simulations with experimental data, researchers can validate and refine theoretical models of DNA melting to gain a better understanding of biological processes. The principles of statistical mechanics used in molecular dynamics (MD) simulation are based on concepts from statistical physics. These principles help us understand and explain how complex systems behave. In MD simulation, statistical mechanics has been used in various ways, including working with different ensembles, utilizing the Boltzmann distribution, considering ergodicity, and using ensemble averages to estimate thermodynamic properties [182, 183].

Many simulation tools are available for different types of simulations in different scientific fields. Some of the most common simulation tools are GROMACS (Groningen Machine for Chemical Simulations) [184], AMBER (Assisted Model Building with Energy Refinement [185], CHARMM (Chemistry at Harvard Molec-

ular Mechanics) [186], NAMD (Nanoscale Molecular Dynamics) [187] and LAMMPS (Large-scale Atomic/Molecular Massively Parallel Simulator) [188]. In this chapter, we used the AMBER package. This software is mainly designed for performing MD simulations and provides a range of force fields that describe the interactions of atoms in a molecular system. Such simulations tool have parameters and methodologies, such as the integration algorithms (such as the Verlet algorithm) to solve Newton's equations of motion, and the use of techniques such as Particle Mesh Ewald (PME) to control long-range electrostatic interactions [189].

2.6 Force Field Formulation

The force field equation is a mathematical representation of the potential energy of atoms or particles in a system. It explains the details of inter and intra-molecular interactions involved between the constituent of biomolecules. The parameter of the force field is usually calculated experimentally or from first principle quantum mechanical calculations [190, 191]. The force field equations used in AMBER are based on different functional models and parameterization methods. AMBER uses a variety of force fields, such as AMBER94, AMBER99, and AMBER ff14SB, each with its equation forms. The force field for a system consisting of N particles can be written as the sum of the following energy terms:

$$V(r) = V_{bond} + V_{angle} + V_{torsion} + V_{vdw} + V_{elec} \tag{2.30}$$

Where $V(r)$ denotes the total energy which is the function of position r of N particles. V_{bond}, V_{angle}, and $V_{torsion}$ are the bond stretching, the angle bending, and the torsional energy terms, respectively. V_{vdw} (Van der Waals) and V_{elec} (electrostatic energy) are non-bonded energy terms such as Lennard-jones and Coulomb potential and calculated between all pairs (i and j). The energy terms V_{bond}, V_{angle}, and $V_{torsion}$ are bonded interactions that sum over the sets of all bonds, angles, and dihedral angles respectively. So the typical form of force field looks like this,

$$V = \sum_{bonds} k_b(b - b_0)^2 + \sum_{angles} k_\theta(\theta - \theta_0)^2 + \sum_{torsion} \frac{V_n}{2}[1 + cos(n\phi + \delta)] + \sum_{LJ} 4\epsilon_{ij}\left(\frac{A_{ij}}{r_{ij}^{12}} - \frac{B_{ij}}{r_{ij}^{6}}\right) + \sum_{elec} \frac{q_i q_j}{r_{ij}}, \tag{2.31}$$

In the first term of potential energy, k_b represents the spring (harmonic) force constant, b is the bond length between atoms and b_0 is the equilibrium bond length. Similarly, the bond-angle bending between three consecutively bonded atoms (i, j, k) forms an angle that can be modeled by a simple harmonic potential function. Also, k_θ represents the angle-bending force constant and θ is the actual bond angle between the three consecutive bonded atoms (i, j, k) and θ_0 is the equilibrium bond angle. In the torsion term, V_n refers to the barrier height, and

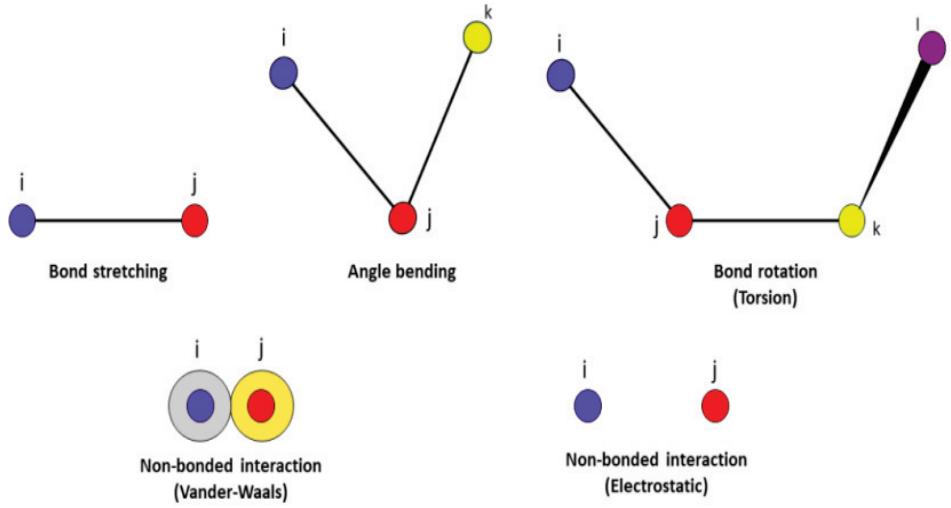

Figure 2.4: The schematics shown for various parameters present in typical force field equation.

ϕ is the torsion angle for the quadruple of atoms i -j -k -l. n is the multiplicity that gives the number of minima in the cosine function and δ (the phase factor) determines which dihedral angle values correspond to these minima. V_n ,n, δ are set for each type of atom quadruplets. The van der Waals interactions between non-bonded atoms are usually represented by a Lennard-Jones potential function where A_{ij} is the repulsive term coefficient, B_{ij} is the attractive term coefficient and r_{ij} is the distance between the two atoms i and j. In addition, nucleic acids are considered as difficult to simulate because of the negative backbone charge and the polyelectrolyte's behavior. In simulations, particular attention should be paid to the atomic charges. The electrostatic interactions are often described by a simple coulomb function; where q_i and q_j correspond to the atomic charges of interacting atoms i and j, respectively and r_{ij} corresponds to the distance between the two atoms (Fig.2.4).

2.6.1 Simulating Atomic Behavior through Classical Approaches

There are several types of molecular dynamics (MD) simulations, each designed to study different aspects of molecular systems. This includes Classical, Quantum, Coarse-grained, and Hybrid simulations. Each method has its advantages and applications, and the choice depends on the specific research question, system size, and desired level of accuracy or computational efficiency. Among them, classical MD simulations are widely used to study the behavior of atoms and molecules at the atomic scale [192, 193]. In this MD, the atoms are treated as classical particles whose motion is governed by the principles of classical mechanics. To perform a classical MD simulation, the equations of motion (typically Newton's second law of motion) are numerically integrated over time. The positions, velocities, and accelerations of the atoms are updated at each time step based on the forces exerted on them by neighboring atoms. The simulation is done by repeatedly calculating the forces and updating the atom positions. The time evolution of a molecular system is determined by solving the following Newton's equation of motion for all atoms.

$$F_i = m_i a_i = m_i \frac{d^2 r_i}{dt^2} = F_i = -\frac{\partial V}{\partial r_i}, \tag{2.32}$$

Where F_i is the force experienced by the i^{th} particle of mass m_i due to the potential energy V of the system and a_i is the acceleration. As mentioned above, potential energy is a complex function and the equation of motion has no analytic solution, so these equations have to be solved numerically. They are derived from the Taylor expansion. The expansion for the position(r), velocity(v) and acceleration(a) of the particles at some instant of time t are:

$$\mathbf{r}(t+\delta t) = \mathbf{r}(t) + \mathbf{v}(t)\delta t + \frac{1}{2}\mathbf{a}(t)\delta t^2 + ...,$$

$$\mathbf{r}(t-\delta t) = \mathbf{r}(t) - \mathbf{v}(t)\delta t + \frac{1}{2}\mathbf{a}(t)\delta t^2 - .....,$$

$$\mathbf{r}(t+\delta t) = 2\mathbf{r}(t) + \mathbf{r}(t-\delta t) + \mathbf{a}(t)\delta t^2 + ...,$$

$$\mathbf{v}(t) = \frac{1}{2\Delta t}[\mathbf{r}(t+\delta t) - \mathbf{r}(t-\delta t)],$$

where δt is the time step used in the simulation. Many algorithms/numerical schemes exist for integrating Newton's equations of motion.

The molecular dynamics (MD) simulation process consists of several steps. First, the system is prepared by specifying the initial positions and velocities of atoms based on the desired initial conditions. Then the equations of motion are integrated using methods such as the Verlet or Leapfrog algorithm. Careful consideration is taken in choosing an appropriate integration step size (time step) to balance accuracy and computational efficiency. At each time step, the forces on the atoms are calculated based on the positions and interactions defined by the force field potential. This force calculation includes contributions from bonded and non-bonded interactions. By controlling the temperature of the system during the simulation, it is possible to perform simulations in different groups such as canonical (NVT) or isothermal and isobaric ensemble (NPT) [194]. By following these steps carefully, various properties and characteristics of the system can be calculated and analyzed. This includes energy profiles, structural changes, diffusion coefficients, and thermodynamic quantities that can be inferred from the simulation trajectories. MD simulations provide information about the dynamic behavior, stability, and interactions of molecules under different conditions.

2.6.2 Constraints of Molecular Dynamics (MD) Simulation

MD simulation provides researchers with valuable information about the dynamics, thermodynamics, and properties of molecules at the atomic scale. However, as with all computational methods, it has certain limitations that must be taken into account. These simulations use force fields to describe atom interactions. Although AMBER force fields are widely used and well parameterized, they are only approximate and may have limited precision. In AMBER simulations, solvent effects are often represented using simplified models or boundary conditions [195]. While these approximations are computationally efficient, they may not fully capture the complexity of solvent interactions or reproduce experimental solvent properties. In addition, MD simulation tools are limited to relatively short time scales due to computational limitations. Simulating processes that occur over a long period, such as large conformational changes or rare events, may require significant computational resources or specialized techniques.

Chapter 3

Force-induced unzipping of DNA in the presence of solvent molecules

3.1 Introduction

In this chapter, utilizing a statistical model, we study the solvent-dependent melting behavior, identifying key factors that influence the stability of DNA melting in the presence of solvent molecules. It is well known that in a cell, during the transcription or replication process, many enzymes or proteins are attached to the DNA molecule and separate it [4, 196–199]. This separation helps to read the genetic code of DNA and protein synthesis. *In vivo* some specific enzymes bind to DNA and exert a force of the piconewton order [52] to separate it. Several experimental techniques, *e.g.* atomic force microscopy and magnetic tweezers, are popular techniques used to unzip the DNA [40–42, 44, 200]. However, theoretical studies of unzipping DNA by applying force are still an exciting part of the research [9, 201]. The force-induced melting is also known as directional melting because either we can apply force perpendicular to the helix or parallel to the helix. In perpendicular applied force, both the strands of DNA melt, while parallel force is known as the rupture mechanism [202, 203]. This DNA unzipping in force ensemble is also a process mimicked by motor proteins that unwind the double helix and shows the transition from dsDNA to ssDNA which is highly cooperative and sustains up to several base pairs (bps). For this study, organic solvents like methanol and formamide induce the strand separation process while the solvents like glycerol or room-temperature ionic liquids maintain the duplex structure. Hence the

mechanical response of DNA molecules in the presence of solvent molecules to the applied forces allows us to investigate molecular free energy landscapes.
In the present work, We first investigate the melting profile of short homogeneous DNA molecules in the presence of solvent molecules in a force ensemble. This research focuses on investigating the unzipping of DNA when pulled from various locations along the chain when solvents of equal strengths are present at these different locations. In the other part of the study, we have done the calculation in a thermal ensemble and show the melting profile of short heterogeneous DNA chains which are surrounded by the solvents of the same and variable strength.

3.2 Modified Hamiltonian

How the force affects the opening of DNA surrounded by solvent(s) is an exciting way to look into the physics of a complex mechanism. In most unzipping experiments, a dsDNA transforms into two single strands by pulling them from an end [155, 204, 205] and also they have the potential to identify specific locations where proteins and enzymes bind to the DNA [206]. Theoretical investigations of DNA-solvent interactions reveal that the presence of these molecules significantly influences molecular transport, reaction rates, and chemical equilibrium within the system. To study the effect of molecular solvents on the melting of DNA molecules in the force and thermal ensemble, we use the well-known Peyrard-Bishop-Dauxois model. The model is quasi-one-dimensional and expresses the dynamics of the molecule through the stretching of the hydrogen bonds [25, 168]. For this study, how to realize the solvents in the model is an interesting task. To study the interaction of DNA-solvents complex system, we modify the potential depth as $D = \gamma * D_0$, where γ is the multiplicity factor which signifies the barrier's strength, $\gamma = 1$ means there is no solvent in the surrounding (see Fig. 3.1a). The selection of this parameter depends on the strength of the solvent particle. We also assume that the presence of a solvent particle near a base pair hinders the motion of that base pair and creates an additional barrier for its breaking [207]. As a consequence, the base pair requires more energy to break. To account for this effect, we have increased the value of D_0 in the morse potential for the pair surrounded by a solvent particle. Following the modification of the morse potential, the modified form of the Hamiltonian for mechanically pulling DNA in a constant

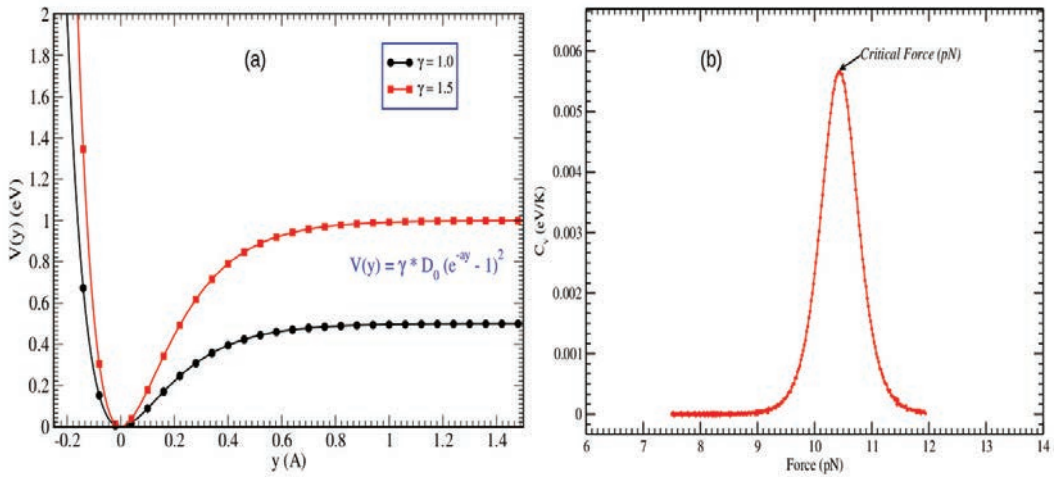

Figure 3.1: (a) The realization in the model. We modify the depth of the potential for the base pair surrounded by a molecular solvent as $D = \gamma * D_0$, where γ is a scaling factor. (b) The change in the specific heat with the applied force at T = 300 K. The critical force of the chain depends on the temperature of the system.

force ensemble (CFE) is expressed as [65, 208].

$$H_f = \sum_n \left[\frac{p_n^2}{2m} + W(y_n, y_{n+1}) + V(y_n) \right] - F \cdot y_n, \tag{3.1}$$

where F is the applied force at the n^{th} base pair in the chain and y_n is the displacement of the bases from the equilibrium.

3.3 Melting of DNA in force ensemble

Initially, we consider a homogeneous chain of 25 base pairs and three solvents of the same strength 1.5. As an approximation, we have considered a value of $1.5 * D_0$ for the base pair that is surrounded by a solvent particle. Any value greater than ($\gamma > 1$) is sufficient to represent the presence of a solvent. One can choose any value of $\gamma > 1$; however, the physical interpretation of the results will remain the same. One may observe minor changes in the microscopic details of the transition. We then apply a force on different locations in a direction perpendicular to the helical axis (see fig. 3.2). In the force ensemble study, we have adjusted the model parameters as follows: $D = 0.07$ eV, $a = 4.2$ Å^{-1}, $\rho = 2.0$, $\kappa = 0.03$ eV/Å^2, $b = 0.35$ Å^{-1}.

At first, we place three solvents of strength 1.5 in the middle section of the 25

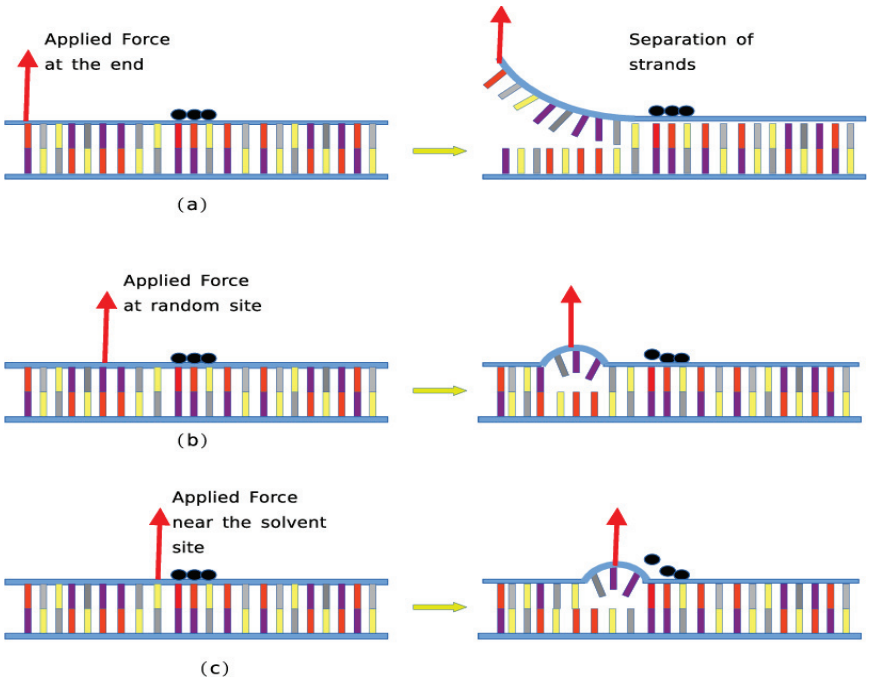

Figure 3.2: The DNA is pulled from a point perpendicular to the helical axis. The DNA is pulled from various positions along the chain where the solvent molecules are absent.

base pair chain. We then pull the chain from one of the ends and sequentially move toward the other ends of the chain. The force is applied on a pair along the chain at a temperature of 300 K. At the critical force, we observe a kink in the free energy which gives rise to the peak in the specific heat at constant force as shown in Fig (3.1b). Our calculations show that we need higher force when the chain is pulled from the location that is farthest from the location of solvent molecules (please see fig. 3.3a). When the chain is pulled from one of the ends with the solvents located on 11, 12, 13 sites, F_c is 8.71 pN. The critical force reduces as we move toward the location where the solvent molecules are present. The F_c is minimum (8.68 pN) when the chain is pulled from a site adjacent to the solvent location. Since the chain is homogeneous, there is symmetry in the value of F_c on both sides of solvent molecules. The interesting part of the study is the reduction in the value of F_c when the chain is pulled from the farthest location to the nearest location from the solvent molecule ($\Delta F_c = 0.03$ pN).

In the second case, we placed the solvent in equidistant places in the middle of the chain and their locations are now 10, 15, & 20. Instead of a single minimum, we obtain something more interesting (see fig. 3.3b). We have the minimum value of F_c in the nearest locations, and there is an increase in F_c when we move to the

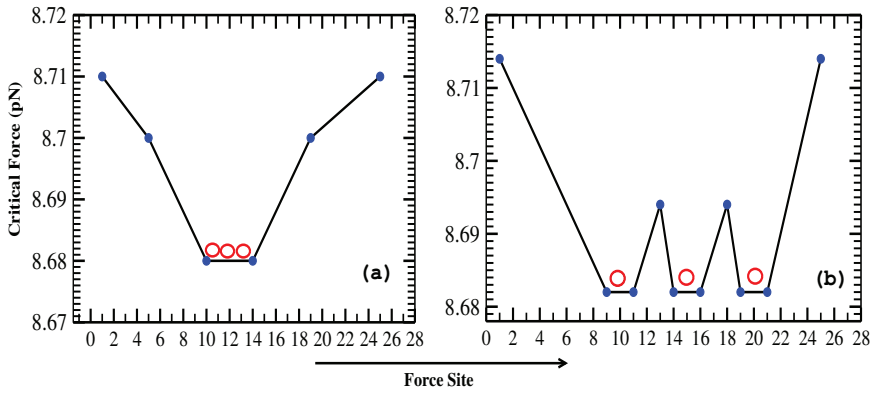

Figure 3.3: The critical force necessary to unzip the DNA chain in the presence of solvent molecules in two different scenarios: (a) when the solvent molecules are present in the middle section of the chain, and (b) when the solvent molecules are located at equidistant positions along the chain. The DNA is pulled from various positions along the chain where the solvent molecules are absent, as illustrated in Fig. 3.2.

next nearest point. While the F_c is highest when the chain is pulled from the ends (8.715 pN), it has a minimum value of 8.681 pN with a slight increase of 8.695 pN to the next nearest point. One can argue that the change in the value is tiny. To recheck our results, we place a single solvent of strength three times that of a single solvent molecule in the middle of the chain. This means we have a single solvent molecule of strength 4.5. The outcome is shown in the following Fig. 3.4. The trend in the F_c, moving from one of the ends towards the other, is the same. However, the value of the critical force is increased now. When the chain is pulled from the farthest point (one of the ends), the F_c is 10.46 pN, while it reduces to 10.43 pN when pulled from the nearest point. In this case, the solvent is located at 12^{th} site. We repeat the calculations for the chain of 50 base pairs to check the finite size effect. The transition is very similar for the 50 base pairs chain, as shown in Fig. 3.4b. In last, again to check how the solvent affects the critical force, we place the solvent at one of the ends of the 25 and 50 base pair chain and apply the force at different sites. To our surprise, the trend in the critical force is showing a similar pattern as we have observed in Fig. 3.3 & 3.4. Again, the critical force is minimal when the chain is pulled from the nearest point from the solvent. However, there is a difference from what we observed earlier. After ≈ 15 base pairs, the critical force saturates. While the minimum force for the 25 base pair chain is 10.42 pN, the maximum force is 10.48 pN. The minimum value for a 50 base pair chain is 18.28 pN, while the maximum is 18.33 pN, as shown in Fig. 3.5(a) & (b). The critical force's maximum change (ΔF_c) is 0.06 pN in these cases.

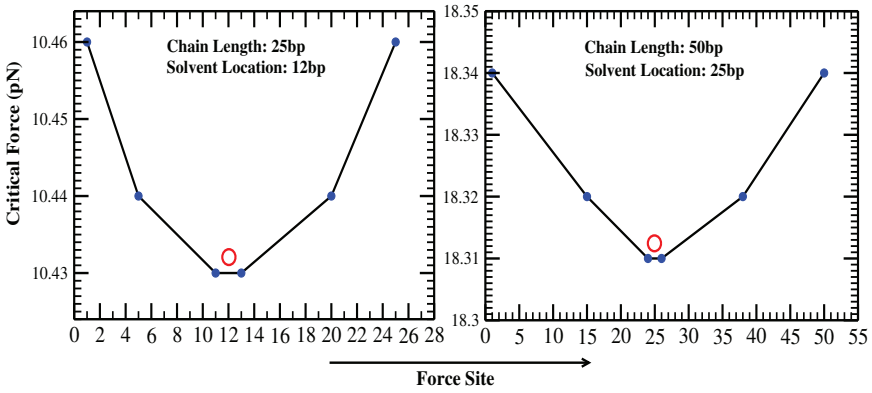

Figure 3.4: The critical force required to unzip the chain is when the solvent molecule is somewhere in the middle of the chain. (a) For a chain of 25 base pairs, (b) for a chain of 50 base pairs. The temperature of the system is 300 K. The red circle represents the location of the solvent molecule.

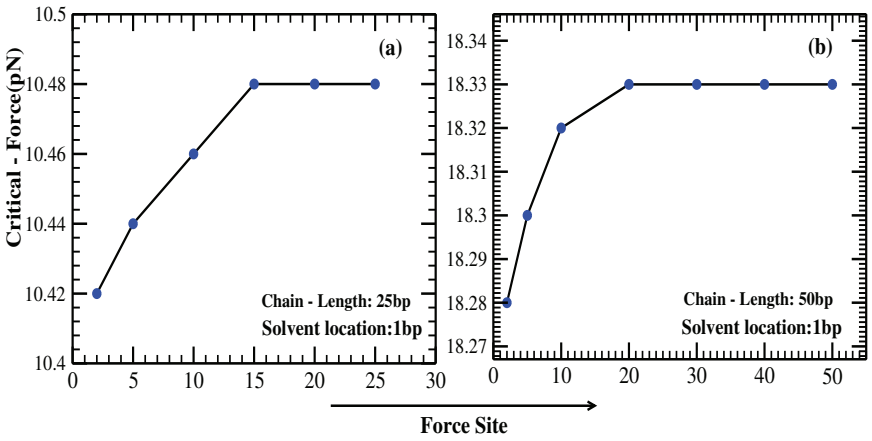

Figure 3.5: The critical force required to unzip the chain when the solvent molecule is at one of the ends. (a) For a chain of 25 base pairs, (b) for a chain of 50 base pairs. The temperature of the system is 300 K.

3.4 Melting of DNA in thermal ensemble

To understand the opening process in the thermal ensemble, we calculate the fraction of open pairs (θ) with the change in the temperature of the chains using the method discussed by Campa and Giansanti (discussed in Chapter 2) [162].

3.4.1 Melting of short heterogeneous chains

We study the melting of short heterogeneous DNA molecules with solvent molecules of equal strength and variable strengths. First, we discuss the effect of solvent molecules of equal strength on the melting of two heterogeneous sequences: (chain-A) $5'-G,G,C,A,G,T,T,C-3'$ and (chain-B) $5'-G,G,T,T,C,A,G,C-3'$. We

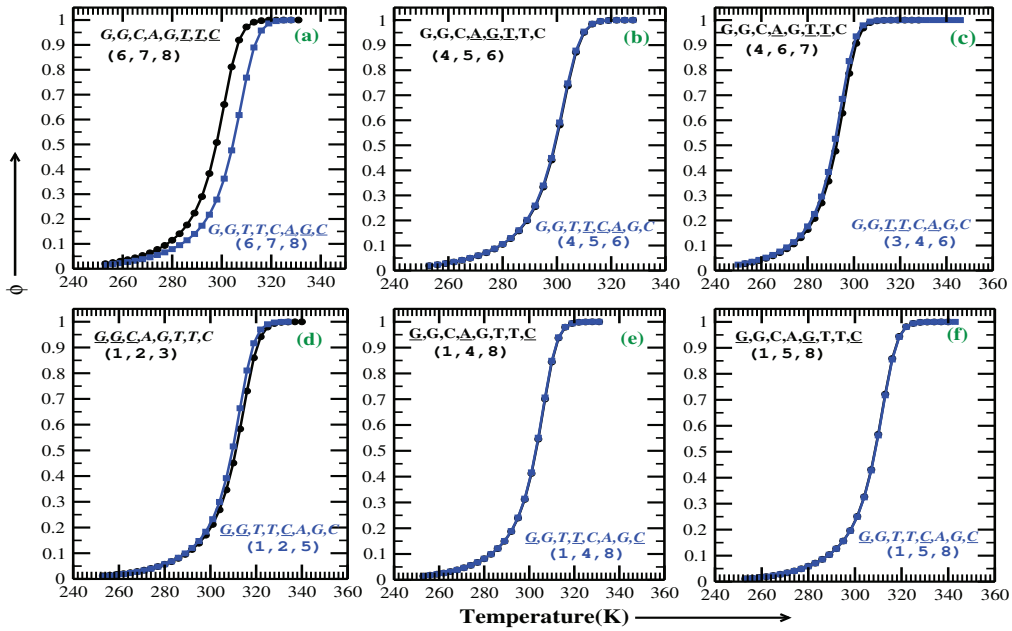

Figure 3.6: Change in the fraction of open base pairs with temperature for chain-A and chain-B. Chain-A $(5'-G,G,C,A,G,T,T,C-3')$ is represented by a black line, while the chain-B $(5'-G,G,T,T,C,A,G,C-3')$ is represented by a blue line. The underlined letters are the sites where the three solvents are present. (a): At the ends of the chain. (b): In the middle of the chain. (c): On the AT sites only. (d): On the GC sites only. (e): Two are at the ends while the third is at 4^{th} site. (f): Two are at the ends while the third is at 5^{th} site.

place the solvent molecules in specific locations. The choice depends on the location of the A or G base. We consider solvents strength as $\gamma = 1.5$. Since we are considering a heterogeneous chain, the set of parameters differs from what we have taken in the previous section. The parameters are: $D_{\rm AT} = 0.0395$ eV, $D_{\rm GC} = 0.059$ eV, $a_{\rm AT} = 4.2$ Å^{-1}, $a_{\rm GC} = 6.3$ Å^{-1}, $\rho = 2.0$, $\kappa = 0.03$ eV/Å^2, $b = 0.35$ Å^{-1}. Let us discuss the results shown in Fig. 3.6(a-f) one by one. An underline in the figures shows the sites where the solvents are present. In Fig. 3.6a, the solvents are present at $6^{\rm th}, 7^{\rm th}, 8^{\rm th}$ sites. In this case, the distribution of solvents is such that the chain is bound to open from the other end where no solvent molecule is present. If we closely look at the composition of the two chains, although both the chains have 5 GC and 3 AT pairs, the sequence is different. Both chains have a GC pair at the ends. However, there is a difference in the $2^{\rm nd}$ last pair. We observe that chain A melts at a lower temperature than chain B. The melting temperature T_m for chain-A is $\sim$ 299 K, while the T_m of chain-B is $\sim$ 301 K. There is a difference of 2K in melting temperatures of two chains because of the

change in base pair at 7^{th} location. We then place the solvent molecules in the middle section at 4, 5, 6 locations (fig. 3.6b). To our surprise, there is no change in the T_m for both chains for this location. In both chains, these locations have a AGA kind of sequence. This means that the T_m is very sensitive to the location of solvents. Despite the change in the sequence at 7^{th} site, the T_m is the same. In fig. 3.6c, we place the solvent molecules near AT pairs. Again, we find no change in the value of T_m for both chains. In fig. 3.6d, we place solvent molecules near GC pairs. Since the number of GC pairs is five and we have chosen only three solvent molecules, we place them at 1, 2, 3 (chain-A) and at 1, 2, 5 (chain-B) as in chain-B on 3^{rd} and 4^{th} locations AT pairs are present. Again, we find a very slight change in the value of T_m for both chains. Similarly, in Fig. 3.6e and 3.6f, when we place the solvent molecules such that they restrict the movement of end and mid pairs, there is no change in the T_m for both the chains; however, the T_m in fig. 3.6f is slightly larger than Fig. 3.6e because in Fig. 3.6f all the GC pairs are restricted due to the presence of solvent molecules. The results are susceptible to the location of the solvents.

3.4.2 Melting of a short homogeneous DNA molecule

To insight more into the melting process, we calculate the probabilities of opening a pair of DNA molecules. The probability of opening of the n^{th} pair, in a sequence is defined as

$$P_n = \frac{1}{Z_c} \int_{y_0}^{\infty} dy_n \exp\left[-\beta H(y_n, y_{n+1})\right] Z_k, \tag{3.2}$$

where

$$Z_k = \frac{1}{h} \int_{-\infty}^{\infty} \prod_{k=1, k\neq n}^{N} dy_k \exp\left[-\beta H(y_k, y_{k+1})\right],$$

and Z_c is the configurational part of the partition function. For y_0, we have taken a value of 2.0 Å[162] and keep the rest of the model parameters the same. Since the melting of DNA molecules offers more avenues to explore, we now take a homogeneous DNA molecule of 12 base pairs. We place the solvent molecules of the same strengths (1.5) in different locations along the chain and calculate each pair's opening probability. We, here, discuss the findings for the four possibilities: (a) the two solvents at the two ends (1^{st} and 12^{th} sites) while the third in the middle (6^{th} site) chain, (b) two solvents in one half of the chain (1^{st} and 2^{nd} sites), while third one at the other end of the chain (12^{th}), (c) all the three solvents in the middle section of the chain at (5^{th}, 6^{th}, 7^{th}) sites, (d) all the three solvents in one

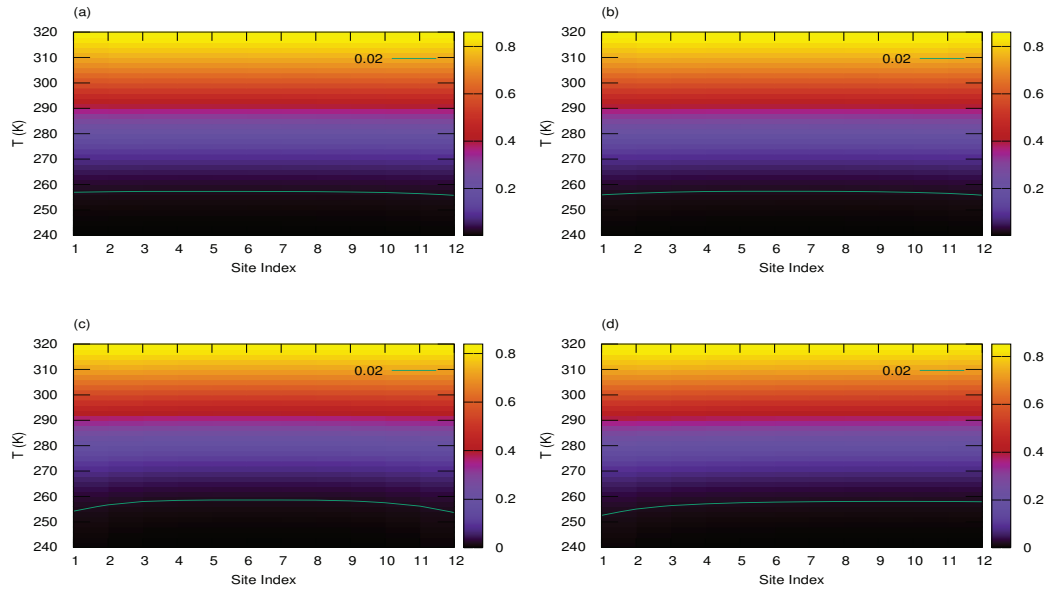

Figure 3.7: The probability profile of the 12 base pair homogeneous chain for four arbitrary locations of solvents of the same strength. (a) The solvents are present at 1, 6, 12. (b) The solvents are present on 1, 2, 12 sites. (c) The solvents are present on 5, 6, 7 sites. (d) The solvents are on 10, 11, 12 sites.

half of the chain at (10^{th}, 11^{th}, 12^{th}) sites. We are using the method discussed in Chapter 2, and we calculate the melting temperature of the chain for each case. For case (a) is 288.8 K, case (b) is 288.3, case (c) is 290.5 K, while case (d) is 290.0 K. Except for the case when the solvents are distributed at the center, there is no significant change in the melting temperature of the chain. From fig. 3.7, we observe certain interesting patterns at the onset of the opening of the chain. When the solvents are present at the ends of the chain, there is little impact of the third solvents on the opening profile of the chain (see fig. 3.7a-b). When the solvents are present in the middle section of the chain, not only is there an increase in the melting temperature of the chain, but there is a change in the onset of the opening of the chain (see fig. 3.7c). We observe a similar trend for case (d), where the chain opens from the other end while the melting temperature of the chain is almost the same as in case (c). The reason for the difference in the chain's opening is the suppression of the end or loop entropy of the chain. While in cases (a) & (b), the end entropy is suppressed, for cases (c) & (d), the end entropy dominates the opening process.

To get a deeper understanding of the solvent's strength and its location on the stability of the DNA molecule, we study the case when the solvents of variable strengths are distributed near the 12 base pair chain. We take $\gamma = 1.5,\ 2.0,\ 2.5$. This investigation aims to compare the opening profile of the same molecule with

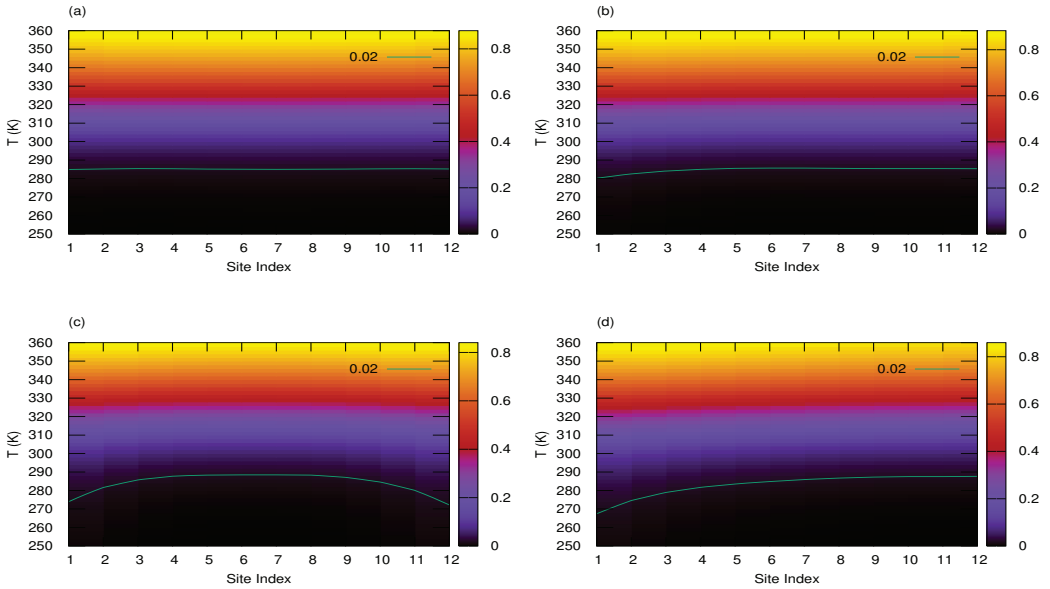

Figure 3.8: The probability profile of the 12 base pair homogeneous chain for four random distributions of solvents of variable strength. (a) The solvents are present at 1, 6, 12. (b) The solvents are present at 1, 2, 12. (c) The solvents are present at 5, 6, 7. (d) The solvents are present at 10, 11, 12.

the same locations of solvents with variable strengths. We consider the same four cases as considered earlier. For the chain having solvents at 1^{st}, 6^{th}, & 12^{th} locations, the value of γ is 1.5 for 1^{st} site, 2.0 for 2^{nd} site, & 2.5 for 3^{rd} site. Note that the case of solvents at 1, 6 & 12 is not the same as 6, 1 & 12 or any other distribution as the value of γ we take in order as 1.0, 1.5 & 2.5. To our surprise, there is a substantial shift in the melting temperature of the molecule in each case. The melting temperature of the chain for case (a) is 325.2 K, for case (b), is 322.3 K, for case (c), is $328.5K$, while for case (d) is 325.2 K. The values of melting temperatures for different cases are shown in Table 3.1.

3.5 Summary

We have studied the effect of solvents on the melting profile of homogeneous and heterogeneous DNA molecules in force and thermal ensembles. In the first part

Table 3.1: Complete table of melting temperature for the chains investigated in sec. 3.4.2

Base pair	Location of solvents	$T_m(K)$ for solvents of	
		same strength	Different strength
		(1.5,1.5,1.5)	(1.5,2.0,2.5)
12	1,2,12	288.3	322.3
	1,6,12	288.8	325.2
	5,6,7	290.5	328.5
	10,11,12	290.0	325.2

of the studies, we have taken a homogeneous DNA of 25 and 50 base pairs and calculated the unzipping of DNA in the presence of solvent molecules in the constant force ensemble. Here we have studied the effect of the location of solvent molecules on the critical force required to unzip the chain. We have considered two cases. In the first case, we placed the solvent at the central location and pulled the chain from various sites. In the second case, we placed the solvent molecules at one of the ends (1^{st}) and pulled the chain from various sites. Interestingly, when the solvent is present at the end, and we pull the chain from a location nearer to the restricted location, we need a slightly higher force to unzip the chain. There is a saturation in the value of critical force as we move toward the other end of the chain. When the solvent molecules are placed at the center of the chain, we found a higher amount of force to unzip the chain than the chain pulled from a site near the restricted site. In all these cases, we need more force to unzip the chain. It is because of the reduction in the end entropy of the chain. When we pull the chain from any site that is away from the solvent location, the entropy of the chain reduces. Hence we need a slightly higher force to unzip the chain. When the chain is pulled from a location near a restricted site, the thermal fluctuations at the other end boost the opening process.

In the next part of our studies, we have taken a short heterogeneous DNA molecule of 8 base pairs. We placed the solvent molecules in different locations as per the chain's sequence and found the chain's melting profile. Next, we studied the effect of the location of solvents on the melting profile of short homogeneous DNA molecules. We have found that while there is a little difference in the melting temperature of the chain for different distributions of solvents, the onset of the opening

is different for the case when the solvents are present in the middle section of the chain with other distributions. However, the melting temperature of the chain in case (b) is much higher than in case (a). In the present studies, we attempt to understand the solvent molecules' effect on the DNA molecule's stability.

It is interesting to note that the pathways of DNA melting in force ensemble and thermal ensemble are entirely different. A pulling force overcomes the stable hydrogen bonding and stacking interactions in a force ensemble. Here the bond breaking is sequential from the point of applied force. In a thermal ensemble, the bond breaks due to the thermal fluctuations attributed to the energy of k_BT/N. The open pair increases the entropy of the system, which acts as a driving force for the nearest hydrogen bond to break. While there is a change in enthalpy and entropy during DNA melting, force-induced melting is primarily due to a change in enthalpy, in contrast, temperature-induced melting is an entropy-driven transition.

Our studies provide a better understanding of the melting and unzipping of ds-DNA in the presence of solvent molecules. This study can be a valuable guideline for predicting DNA thermodynamic quantities and designing DNA nanostructures. How the time scale of the presence of a solvent at a particular location along the chain affects the melting of the DNA molecule will be part of our future studies.

Chapter 4

Melting of dsDNA attached with AuNPs

4.1 Introduction

DNA-linked gold nanoparticles (DNA-AuNPs) are fascinating nanomaterials that combine the unique functions of DNA with the optical and electronic properties of gold nanoparticles (AuNPs). These hybrid systems have found applications in nanobiotechnology, medical sciences, and pharmaceutical research. [209, 210]. Recently, there has been a growing interest in investigating how DNA-AuNPs behave in the presence of molecular solvents. We know that the human body contains millions of cells, each with complex structures, including membranes, DNA, and ribosomes [148, 211]. These cells are filled with diverse biomolecules of varying shapes and sizes, influencing molecular transport, reaction rates, and chemical equilibrium [86, 212–214]. Understanding the behavior of DNA molecules in such dense environments is crucial to understanding the fundamental cellular activities, as well as advancements in DNA nanotechnology, medicine, and pharmaceutical sciences. In the 1990s, researchers synthesized DNA-linked gold nanoparticles and observed that the thermal melting transitions of these materials differed from free DNA in solution [81]. The melting curves of DNA-AuNP aggregates exhibited sharper transitions. Similar behaviors were also noticed in DNA-linked polymers and molecules [215–220]. Additionally, the presence of molecular solvents in the solution was found to modify the opening of DNA, which has implications for DNA sequencing, drug delivery systems, and nanoscale devices. Researchers have explored how these molecules affect DNA condensation, cell surfaces, and cellular interiors [139, 221, 222]. The influence of molecular solvents on DNA and

RNA polymerase reactions has been investigated by Menhaj and other researchers [73, 89, 223]. Furthermore, the effect of attaching gold nanoparticles on the melting profile of double and single-stranded DNA has been studied using various spectroscopic techniques [224, 225].
In this research, we explore the thermal melting of DNA-linked gold nanoparticles (DNA-AuNPs). The first part of our study centers on examining the melting profile of short heterogeneous DNA-linked AuNPs in the presence of solvent in the solution. Furthermore, we explore how the position of the gold nanoparticle attachment on the DNA molecule influences the melting behavior. By systematically shifting the location of the AuNP along the DNA chain, we observed that near the ends of the DNA, the melting temperature is sensitive to the AuNP's position. Also, we found that in the middle section of the DNA chain, there exists a region where the melting temperature remains constant.

4.2 Modified Model Hamiltonian

Several groups have studied the influence of gold nanoparticles and oligonucleotides on the thermal melting behavior of dsDNA [216, 226–228]. These studies have utilized experimental and simulation approaches to incorporate polymers like polyethylene glycol (PEG) and dextran to mimic cellular conditions realistically [229]. The experimental results have highlighted that DNA is soluble in specific solvents such as ethanol, dimethyl sulfoxide, and acetonitrile, where the presence of hydrophobic groups reduces the stability of DNA duplexes. In our current research, we focus on studying the melting of DNA-linked gold nanoparticles, both at the ends and surrounded by the same and different molecular solvents. The presence of heavy gold nanoparticles at the ends of DNA reduces the contribution of end entropy.
To understand the melting behavior under such conditions, we employ the Peyrard-Bishop-Dauxois (PBD) model, discussed in Chapter. 2. This model can describe various DNA conformations, including the double helix, single-stranded DNA, and denatured DNA. It allows us to explore critical DNA properties such as stability, melting behavior, and response to external forces like stretching and twisting. As a result, we gain knowledge of the dynamics of essential cellular processes, including DNA replication, transcription, and recombination. Though the PBD model underestimates the entropy associated with different DNA conformations, it still provides valuable calculations for various thermodynamic and statistical quantities of interest, such as partition function, free energy, specific heat, and the fraction

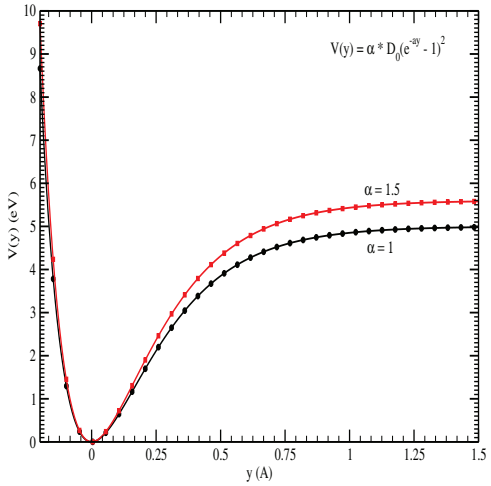

Figure 4.1: The modification to the morse potential to account for the influence of a solvent molecule. we adjust the potential depth for the base pair when surrounded by a solvent molecule by scaling it with a factor α ($D = \alpha * D_0$).

of open base pairs. With the help of this model, we understand the interactions between DNA and DNA nanoparticles. In this study, we modify the depth of the morse-potential which represents the hydrogen bonding between base pairs. We know that molecular solvents present in the surrounding acts as a barrier, and restrict the movement of base pairs. Hence an additional amount of energy is required to move the solvents. This shows that, wherever the solvent is present, the height of the potential barrier is higher than those where there is no solvent present in the surrounding of a pair. We modify the height of the barrier by $D = \alpha * D_0$, where The choice of α depends on the strength of the solvent particle or AuNP. If we compare the molecular weights of a gold nanoparticle with a pair, the gold nanoparticles are roughly 0.8 times heavier than the molecular weight of a base. The other solvent molecules have relatively lighter molecular weights but create a barrier to the movement of the base pair.

4.3 Melting of short heterogeneous DNA

First, we consider $5' - A, T, C, C, T, T, A, T, C, A, A, T, A, T, T - 3'$ sequence studied by Lee *et al.* [226]. To explore the complex interactions between DNA-AuNPs and molecular solvents, we specifically examine the chain's end base pairs, which are associated with heavy nanoparticles. We analyze two different scenarios: (a) The chain with three solvents of equal strength, and (b) The chain with three solvents

of varying strengths. For the base pairs surrounded by a solvent particle, we set the modified potential depth as $1.5D_0$, while for the AuNP, it is adjusted to $4.5D_0$. We consider various values of α ranging from $1.5 - 2.5$ for the sites where solvents are present, and we observe how these values affect the DNA melting curves. We

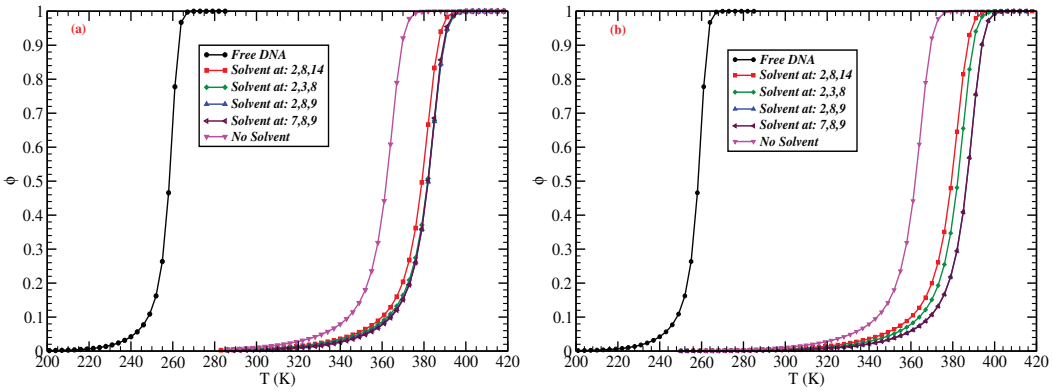

Figure 4.2: Figure shows the fraction of open base pairs as a function of temperature in DNA sequence $(A, T, C, C, T, T, A, T, C, A, A, T, A, T, T)$ as a function of temperature. (a) Three solvents of the same strength are present at different locations along the DNA chain. (b) Three solvents of different strengths are located at different positions. Here distinct colors show the specific situation of the system. In each case, AuNPs are present at the ends of the DNA chain, except for the case of free DNA.

investigate the effects of our modifications in the two mentioned cases and present the results through plots in Fig. 4.2(a-b). For the case of free DNA, the melting temperature (T_m) is found to be 258.4 K, while for DNA-linked gold nanoparticles, it increases to 362.4 K. These changes occur in the absence of any solvent. Next, we examine the impact of three solvent molecules with the same strength (a) and variable strength (b). In case (a), all three solvent molecules have a strength of 1.5, whereas in case (b), their strengths are $1.0, 1.5, 2.0$. Fig. 4.2(a), reveals that placing solvent molecules at positions (2,3,8), (2,8,9), or (7,8,9) leads to only a nominal change in T_m. Please refer to the table-4.1 for more details. However, to our surprise, when solvent molecules are placed at positions (2,8,14), T_m is significantly reduced to (379.4 K). These results show the significance of solvent molecules in the thermal melting process. When solvent molecules are situated at positions (2,3,8) or (2,8,9), two solvent molecules are in adjacent locations, while the third is farther away. Conversely, when solvent molecules are at positions (7,8,9), all three are concentrated in the middle section of the chain. The plot indicates that the chain is more stable when solvent molecules are concentrated

Solvent's location	Equal strength	Variable strength
2,8,14	379.4K	379.4K
2,3,8	381.6K	382.9K
2,8,9	382.1K	386.4K
7,8,9	381.8K	387.0K

Table 4.1: Comparison table of melting temperature (T_m) for different scenarios of solvent presence in the solution. The T_m of free DNA is 258.4 K. In the absence of any solvent, the T_m is 362.4 K.

in a specific location. This is applicable for solvents of the same strength, as adjacent solvents increase the system's stability, restricting the opening of base pairs. However, the same argument does not apply when solvents of different strengths are present in the chain. In this scenario, the chain becomes most stable when solvent molecules are located in the middle section, *i.e.*, at positions (2,8,9) or (7,8,9) (refer table-4.1) [230].

4.4 Influence of a nanoparticle on the opening profile of DNA

We investigate how the melting profile of a homogeneous DNA chain with 12 base pairs is affected when a single gold nanoparticle (AuNP) is attached at different locations along the chain. The goal is to understand how the thermal stability of the molecule changes upon attaching the AuNP. Starting with an AuNP attached at one end, the melting temperature (T_m) is approximately ~ 344 K. As we move the AuNP towards the other end, the T_m gradually increases, reaching a maximum value of around ~ 347 K at a specific position. Surprisingly, in the middle section of the chain, there is a region where the T_m remains constant, spanning about one-third of the chain length. To validate this finding, we repeat the study with longer DNA chains of 18 & 24, and we observe a similar trend in the T_m values for these longer chains. However, the overall T_m decreases as the chain length increases (see Fig. 4.3). Important to note that, for all three chain lengths, the melting temperature is influenced by the location of the AuNP near the ends. Additionally, we observe an interesting effect of heavy nanoparticles on short DNA sequences. While the shortest chain is the least stable in the absence of any solvent molecule, it becomes more stable in the presence of a solvent (see table 4.2). This observation

can be explained by considering the effect of heavy nanoparticles on short DNA chains. In polymer chains, the increase in loop and end entropies leads to chain opening. When a heavier molecule surrounds a base pair, it reduces the entropy of the chain. This effect is more pronounced when the solvent particle is situated in the middle of the chain. Due to the shorter chain's narrower temperature range for bond breaking and chain separation, the effect is more significant, resulting in a higher melting temperature when solvent molecules are present compared to longer chains.

Chain length	No AuNP	AuNP attached
12	260 K	344-347 K
18	278 K	339-342 K
24	288 K	336-338 K

Table 4.2: The melting temperature of three DNA chains in the presence and absence of gold nanoparticles (AuNPs). In each case, the single AuNP is attached at various positions along the chain, ranging from one end to the other.

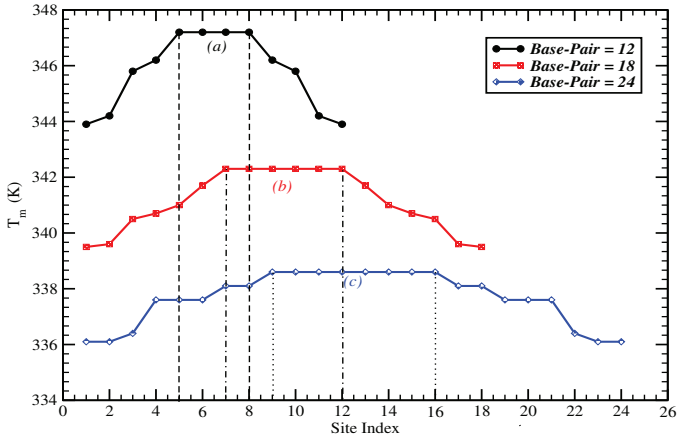

Figure 4.3: The change in the melting temperature of three DNA chains containing 12, 18, and 24 base pairs, respectively, when a single gold nanoparticle is attached at various positions along each chain, ranging from one end to the other end. This plateau region constitutes approximately 1/3 of the total pairs in each chain.

4.5 Individual separation of base pair due to the presence of AuNP

To gain insights into the influence of a heavy nanoparticle on the opening of individual base pairs in the DNA chain, we fix the AuNP to the 33^{rd} base pair in the middle of a homogeneous DNA chain comprising 50 base pairs. In our analysis, we assume a scaling factor of $\alpha = 4.5$ for this specific location of the nanoparticle. Using a one-dimensional Peyrard-Bishop-Dauxois (PBD) model, we limit the movement of a base pair to the y direction. Our choice of the 33^{rd} site is arbitrary, as the results would remain consistent with any other restricted location. To assess the separation of individual base pairs, we calculate the change in the average displacement, $\langle y_j \rangle$, over a range of temperatures between $280 - 350$ K. This average separation $\langle y_j \rangle$ provides valuable data on how individual base pairs respond and open in the presence of the AuNP.It is defined as,

$$\langle y_j \rangle = \frac{1}{Z} \int \prod_{j=1}^{N} dy_j y_j \exp(-\beta H_c) \tag{4.1}$$

In Figures 4.4(a-f) present the outcomes at six distinct temperatures. The figures display how individual base pairs respond and open in the vicinity of the AuNP. At the 33^{rd} location of the DNA chain, where the heavy nanoparticle is presented, the movement of the base pair will be significantly restricted. As a consequence, the value of $\langle y_{33} \rangle$ remains almost zero within the temperature range of $280 - 306$ K. By monitoring the average displacement, $\langle y_j \rangle$, on either side of the restricted site, we observe a striking pattern. Except for fluctuations at the chain's ends, there is saturation in $\langle y_j \rangle$. The entire figure forms a necklace-like pattern at 280 K, where the saturation region extends up to 20 base pairs on the left section (L) of the chain and up to 6 base pairs on the right section (R). The asymmetrical placement of the nanoparticle in the chain results in the absence of symmetry in the opening pattern on either side of the restricted site. As the temperature rises to 300 K, $\langle y_{33} \rangle$ remains close to zero, but the saturation regions on either side of the chain begin to shrink. The saturation length decreases to 8 base pairs in the left section and completely vanishes in the right section. With further increase in temperature, the saturation regions disappear entirely and the necklace-like pattern is converted into a bird-like pattern (depicted in Fig. 4.4(f)).
To obtain more about the opening process, we examine the correlation between the

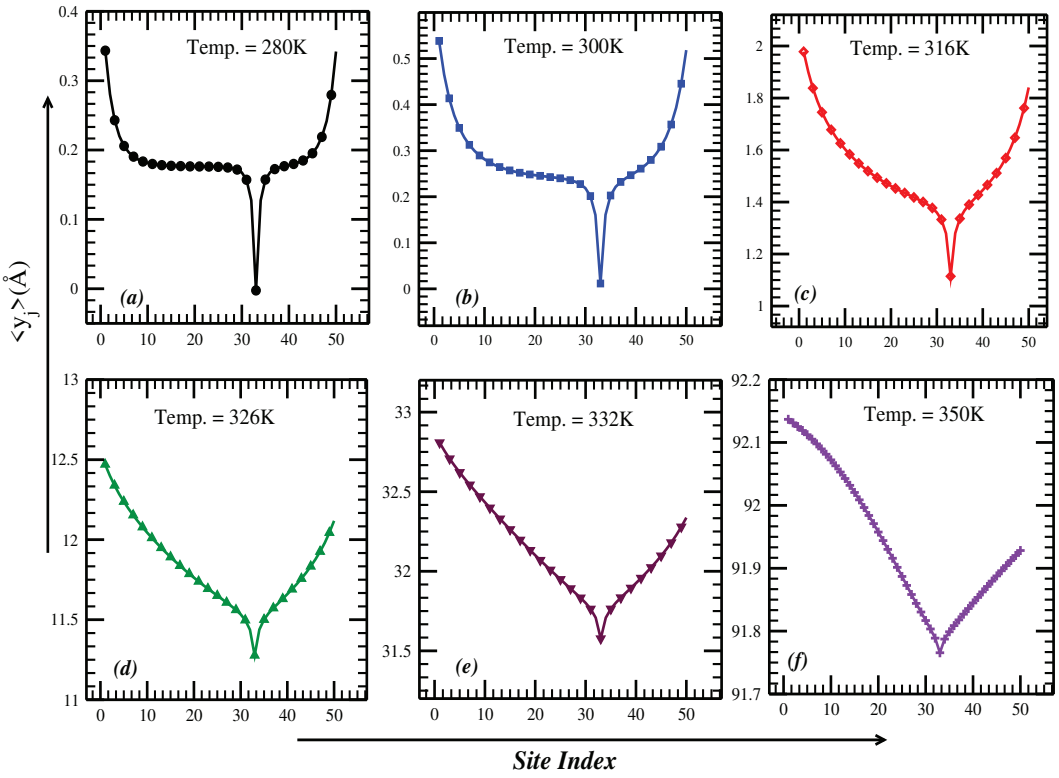

Figure 4.4: The variation in the $\langle y_j \rangle$ in the presence of single nanoparticle that is located on 33$^{\text{rd}}$ site.

average displacements of different base pairs, denoted as $\langle y_j \rangle$, and the displacement of the restricted site, $\langle y_{33} \rangle$. We calculate the difference, $\Delta\langle y_j \rangle = \langle y_j \rangle - \langle y_{33} \rangle$, where $j = 1, 2, 3....$ for four distinct locations in the DNA chain, which consists of 50 base pairs. The **four** defined locations are as follows: (i) one of the ends of the DNA chain (1$^{\text{st}}$ base pair), at this location, the effect of the nanoparticle is expected to be minimal. (ii) away from the restricted site (21$^{\text{st}}$ base pair), this position allows us to observe the saturation region, where the effect of the restricted site remains constant up to some temperature range. (iii) In the vicinity of the nanoparticle (35$^{\text{th}}$ base pair), this base pair is situated close to the nanoparticle, and its effect is most significant. (iv) approximately on the other end of the chain (48$^{\text{th}}$ base pair), this location experiences an entropic contribution from the end and an enthalpic contribution from the restricted site. For each case, we analyze $\Delta\langle y_j \rangle$ as a function of temperature. Point to note that, for case-(i) we monitor the change in the $\langle y_1 \rangle$ temperature. In case-(ii), we observe the change in $\langle y_{21} \rangle$ with the temperature. In both these cases, we calculate $\Delta\langle y_j \rangle$ and present the results in Fig. 4.5. The interesting feature of this plot is the variation in the value of $\Delta\langle y_j \rangle$.

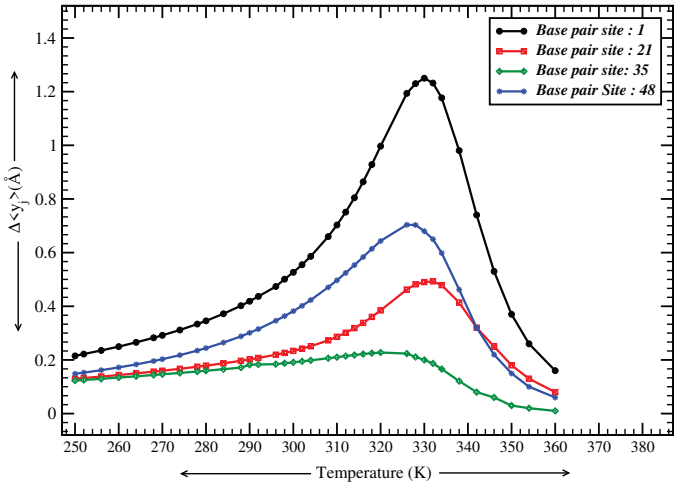

Figure 4.5: The figure shows the variation in Δy_i versus temperature for four different locations on chain length.

An important point to note is that for the second case, the peak height is less than the previous one, which indicates the slow variation in $\Delta\langle y_j\rangle$ compared to case-a. Next, we focus on a location near the restricted site, the 35^{th} base pair. Here, as the temperature increases, the peak height in the plot decreases. This finding suggests that this location is under the influence of the 33^{rd} site, given its proximity. Lastly, we explore the variation in $\langle y_{48}\rangle$ (end location) with temperature. At this location, near the end, the base pair experiences an entropic contribution from the end and an enthalpic contribution from the restricted site. Due to the asymmetric positioning of the two ends with respect to the nanoparticle, there is a difference in the peak height between cases (a) and (b) in Fig. 4.5. To better illustrate the opening process, we present a schematic diagram in Fig. 4.6. This diagram provides a visual representation of how the presence of the nanoparticle influences the opening behavior of individual base pairs in the DNA chain and the correlation between the restricted site and different base pair locations. Initially, DNA exists in its double-stranded structure (Fig. 4.6a), while a nanoparticle is positioned at the 33^{rd} location of the chain. As we progressively raise the system's temperature, the displacement of the first base pair increases from its equilibrium position. Simultaneously, the nanoparticle remains completely confined, resulting in zero displacements (Fig. 4.6b). As the temperature continues to rise, $\Delta\langle y_1\rangle$ experiences a sharp increase and eventually reaches its maximum value. This maximum point corresponds to the melting temperature (T_m) of the system. Since the nanoparticle is asymmetrically positioned in the chain, more than half of the

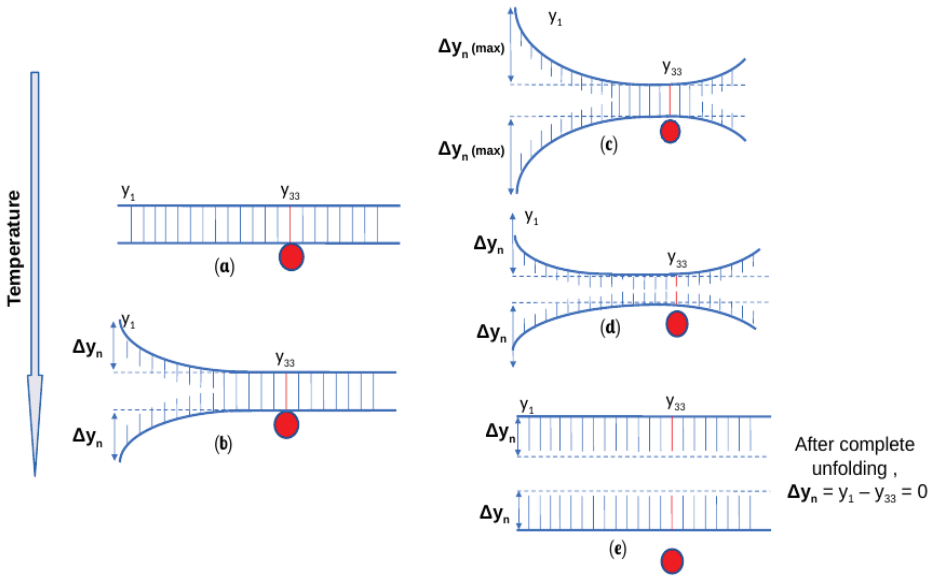

Figure 4.6: Mechanism of opening of DNA chain with respect to first base pair for the case-(i). The sub-figures (a)-(f) show the breaking of the pair.

chain is in an open state when $\Delta\langle y_1\rangle$ reaches its maximum value. With further temperature increase, the DNA chain starts to open from the right section. The opening process continues until the base pair attached to the nanoparticle opens. Consequently, as $\langle y_{33}\rangle$ increases, there is a corresponding decrease in the value of $\Delta\langle y_1\rangle$ until $\langle y_1\rangle = \langle y_{33}\rangle$. At this point, $\Delta\langle y_1\rangle$ becomes zero, and intriguingly, this coincides with the melting temperature of the chain. A similar pattern is observed for $\Delta\langle y_j\rangle$ for the rest of the three cases (b, c, d) considered. The height of the peaks varies for these cases, indicating different degrees of correlation with the restricted site. The plot reveals that when we are far away from the restricted site, there is a sharp peak in $\Delta\langle y_j\rangle$, whereas the peak height decreases as we move closer to the nanoparticle's restricted site. This observation suggests a strong correlation between the restricted site and the neighboring sites, influencing the opening behavior of the DNA chain at different locations.

4.6 Summary

The thermal stability of DNA-linked AuNPs is a crucial parameter for their practical applications. Understanding the effect of molecular solvents on the thermal stability of DNA duplexes on AuNP surfaces is critical for developing new applications for these hybrid nanomaterials. In this study, we have investigated the

behavior of DNA-linked AuNPs in the presence of different molecular solvents. In the first part of our study, we focused on a DNA-linked gold nanoparticle with 15 base pairs and analyzed the influence of solvent molecules on its thermal stability. By making suitable modifications to the PBD model, we calculated the melting temperature (T_m) of the DNA-AuNP system. The results demonstrated the significant role that solvents play in determining the thermal stability of DNA structures.

In the subsequent part of the investigation, we explored the effects of AuNP attachment at different locations in short homogeneous DNA chains. By systematically calculating the melting temperature for each case, we observed that T_m is highly sensitive to the location of the AuNP along the chain. Particularly, when the AuNP was placed in the middle section, the melting temperature remained higher and almost constant for several adjacent base pairs. For instance, in a 12 base pairs chain, the constant region lasted for approximately ~ 4 base pairs. Similar patterns were observed in longer chains of 18 and 24 base pairs, with the plateau regions extending to approximately ~ 6 and ~ 8 base pairs, respectively. We determined that the ratio of base pairs in the plateau region to the total number of base pairs was approximately $\sim 1/3$. We then explored how the presence of AuNPs influences the melting profile of the DNA chain. To do so, we strategically chose a specific site (33rd) in the chain, where we attached the AuNP, and then carefully monitored the $\langle y_j \rangle$ at different temperatures. Our findings revealed a fascinating pattern of DNA unwinding, characterized by a "necklace pattern" and a "bird-like pattern." Notably, as the temperature increased, the suppression of the restricted site diminished, leading to a rapid and sharp opening of both the left and right sections adjacent to the restricted site. We also calculated the change in $\langle y_j \rangle$ ($\Delta\langle y_j \rangle$) at different temperatures around the 33rd site. The peak value of $\Delta\langle y_j \rangle$ precisely corresponds to the melting temperature of the DNA chain. This method we developed proved highly effective for determining the melting temperature of short DNA chains. Therefore, it is crucial to consider various factors when preparing DNA-AuNP systems in the presence of solvents. Careful selection of solvents, thoughtful DNA sequence design, and precise reaction conditions are essential to ensure the stability and functionality of the resulting system. Hence, our study plays a pivotal role of solvent molecules in influencing the stability of DNA-linked AuNP systems. This research helps us understand how DNA and gold nanoparticles interact in a detailed way. These insights open up exciting possibilities for using these hybrid nanomaterials in various fields like nanobiotechnology

and bionanotechnology.

Chapter 5

Effect of partial confinement on the stability of DNA

5.1 Introduction

The analysis of DNA molecules within a confined shell or chamber has received considerable attention in scientific research. By confining DNA within a small space like a nano-scale container or channel, researchers aim to study specific properties and behaviors of DNA under these conditions. Different techniques are employed to manipulate DNA, including complexation with polycations [231], charged copolymers, cationic lipids, or liposomes. DNA can also be confined within gels [232] or polymeric nanocapsules (micelles) [81, 233, 234]. In a study conducted by Ding *et al.*, they found that the confinement of lipid-raft proteins resulted in the attraction between framework nucleic acids (FNAs) and the cytoplasmic membrane [235]. One common experimental method employed to study DNA confinement is single-molecule fluorescence microscopy. This technique enables real-time visualization and tracking of individual DNA molecules, providing valuable insights into their behavior and structural changes. Computational simulations and theoretical models play a crucial role in understanding the behavior of confined DNA by simulating interactions between DNA and the surrounding shell. Such analysis has yielded important findings, including conformational changes that alter the shape and flexibility of DNA. The degree of confinement, container size and shape, and DNA-shell interactions all influence these changes [31, 95, 236]. Studying DNA packing in eukaryotic chromosomes and viral capsids in confined spaces highlights the significance of investigating DNA in confined geometries. Understanding the structural properties of DNA within a confined shell has various applications, such

as enhancing the design and optimization of DNA-based nanodevices and drug delivery systems. It also provides insights into DNA behavior within cellular environments, where DNA is naturally confined within the cell nucleus or other subcellular compartments.

In this study, we investigate the influence of confinement on the thermal stability and structural properties of double-stranded DNA. The primary focus is to understand how different confinement geometries affect the behavior of DNA molecules. Specifically, we confine a B-DNA molecule within a cylindrical structure. This B-DNA molecule is 12 base pairs in length and it is a crystal structure of a B-form DNA dodecamer with the sequence (5'-(*CP*GP*CP*GP*AP*AP*TP*TP*CP*-GP*CP*G)-3'), which is often used as a model to study DNA and its interactions due to its well-defined structure. To achieve this, we employ a statistical model known as the PBD model. Furthermore, we examine how confinement impacts DNA molecules of various lengths. These DNA molecules are confined within cylindrical shells, either partially or completely. By altering the sizes of the cylindrical shells, we observe how the cylinder's dimensions influence the fine details of the base pair opening in the DNA.

5.2 Theoretical Approach

To investigate the thermodynamic properties of DNA within a confined shell, we utilize the Peyrard-Bishop-Dauxois (PBD) model (Chapter 2) [26]. This model enables researchers to explore the effects of the cylindrical environment on the structural and dynamical properties of the DNA molecule. By incorporating appropriate boundary conditions and potential energy terms that account for the confinement, the model offers valuable insights into how the cylindrical shell influences the stability, melting behavior, and opening dynamics of the confined DNA [237]. Moreover, the model reveals that in the open state, DNA bases exhibit a greater degree of freedom compared to when they are confined. This framework provides a deeper understanding of the differential behavior of DNA in these states.

Initially, we calculate the effect of confinement on DNA by completely confining the double-stranded DNA chain within a cylindrical geometry. This approach enables us to analyze the behavior of DNA under strong confinement conditions. Further, we consider DNA molecules of varying lengths to explore how confinement influences DNA behavior at different scales. By systematically varying the length of the DNA chain, we can investigate the interplay between confinement,

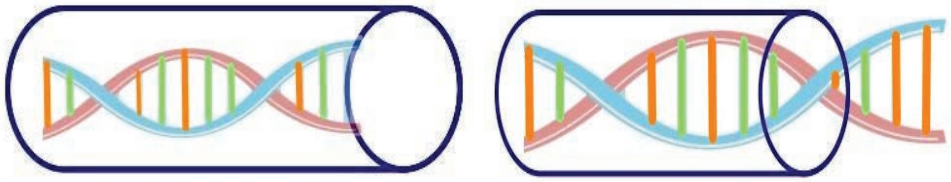

Figure 5.1: The schematic representation of the DNA molecule is confined in a cylindrical shell. The r is the distance of the confined wall from the DNA strand. The radius of the cylinder is $R_c = r$ + DNA radius (10 Å). The DNA is confined in the shell either completely or partially.

chain length, and the thermodynamic properties of DNA.

5.3 Melting of 1-BNA

To study the thermodynamics of DNA in cylindrical confinement, we supposed that the movement of base pairs will be restricted, and it affects the overall movement of the molecule. We restrict the configuration space of the system, as shown in Fig. 5.1. Using the modified scheme in Chapter 2, we calculate the partition function and hence evaluate all the thermodynamical properties of DNA confined in a cylindrical shell. In this calculation, we keep, the lower limit of integration -5 Å while the upper limit of integration for each base pair is r Å, the radius of the cylinder. To investigate the thermodynamics of DNA within cylindrical confinement, we assumed that the movement of base pairs would be limited, thereby impacting the overall movement of the molecule. We calculate the thermodynamic properties of DNA confined in a cylindrical shell and determine the partition function.

In the initial phase of the study, we examined a DNA molecule of 12 base pairs confined within a cylinder and calculated its melting temperature. Our focus is to establish a correlation between the chain size and the radius of the cylinder with the melting temperature. For the 12 base pairs chain confined in a cylinder with a radius of 20 Å, we found the melting temperature to be 338.4 K. Next, we systematically increased the radius of the cylinder, reaching up to 190 Å, and determined the melting temperature for the molecule. For the 12 base pairs chain confined in a cylinder with a radius of 190 Å, the T_m was found to be 289.5 K. To investigate the impact of chain length on the melting temperature, we doubled the chain length and extended it up to 192 base pairs. For all the chain lengths, we observed a consistent pattern. The melting temperature exhibited a decrease,

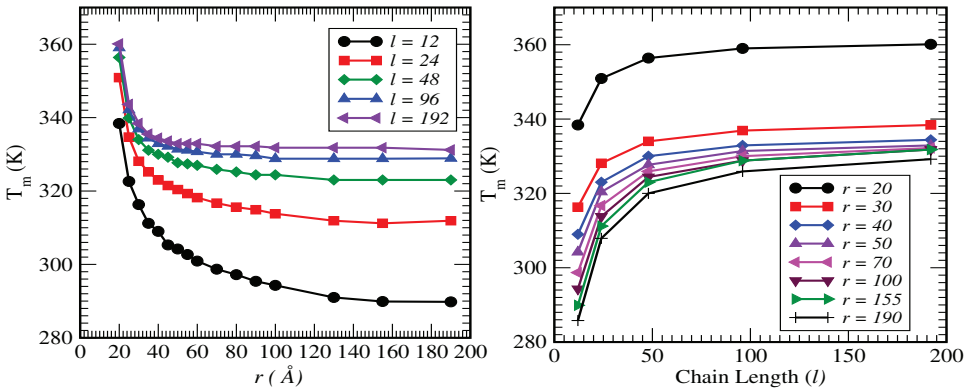

Figure 5.2: The plot shows the change in the melting temperature of the DNA chain of different lengths. (a) The variation in the melting temperature with the increasing cylinder radius from 20 Å to 190 Å for different chains ($l = 12$ to $l = 192$). (b) The change in the melting temperature with the increasing chain length from $l = 12$ to $l = 192$ for different cylinder radii (20 Å to 190 Å).

which eventually reached a saturation point. To understand this pattern better,

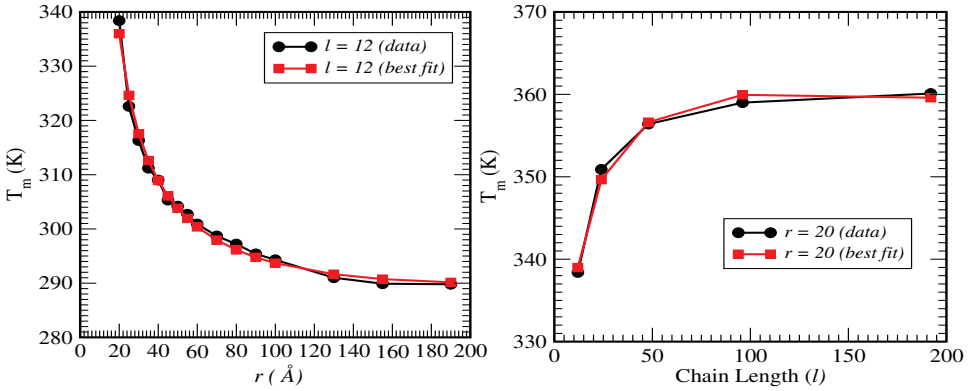

Figure 5.3: (a) The variation in melting temperature with the radius of the cylindrical shell for the 12-bp chain ($5' - GGGGAAAAGGGG - 3'$). The best fit parameters are: $T_m^0 = 431.08$ K, $\lambda_1 = -52.57$, & $\lambda_2 = 4.89$. (b) The variation in the melting temperature with the chain length for the DNA confined in a cylinder shell of radius 10 Å. The best fit parameters are: $T_m^0 = 270.61$ K, $\lambda_1 = 37.01$, & $\lambda_2 = -3.82$.

we used a non-linear curve-fitting program to fit the obtained results. The best-fit equation that captured the pattern of decay in T_m with increasing cylinder size (radius) is identified.

$$T_m = T_m^0 + \lambda_1 \ln(x) + \lambda_2 \ln^2(x), \tag{5.1}$$

where x is either the number of base pairs (l) in a given chain (for fixed cylinder width) or the radius (r) of the cylindrical shell (of fixed DNA chain). The parameters, $T_m^0,\ \lambda_1,\ \&\ \lambda_2$ are fitting parameters. We have observed that the decay in the melting temperature (T_m) with the radius of the cylinder follows a logarithmic trend. Specifically, for a chain of 24 base pairs, the melting temperature saturates at $311.9K$. For a chain of 48 base pairs, it saturates at $323.5K$, and for a chain of 192 base pairs, it saturates at $330.9K$. To further investigate the stability of a molecule confined in a cylinder, we kept the radius of the cylinder fixed and varied the length of the DNA molecule. We found that as the chain length increased, the melting temperature also increased and eventually reached a saturation point. For example, when we considered a DNA molecule of 12 base pairs confined in a cylindrical shell with radii ranging from 20 Å to 190 Å, we obtained the best-fit parameters as follows: $T_m^0 = 431.08$ K, $\lambda_1 = -52.57$, and $\lambda_2 = 4.89$. Notably, in this case, λ_1 is negative. On the other hand, when we confined DNA molecules of different lengths in a cylinder with a radius of 20 Å, we obtained the following best-fit values: $T_m^0 = 270.61$ K, $\lambda_1 = 37.01$, and $\lambda_2 = -3.82$. Here, the value of λ_1 is positive. The third term in Eq. (5.1) is the correction term. Although we have determined the best-fit values for other confined radii as well, we are not presenting those results here to avoid overcrowding the plots. However, we provide the best-fit plots for both cases in Figure 5.3. In another part of our study, we aim to explore the behavior of DNA molecules during the encapsulation process, which is a subject of significant research interest. Our focus is on examining the stability of double-stranded DNA molecules with varying lengths within a confined shell, employing a statistical model. Specifically, we investigate the behavior of DNA molecules when they are partially or fully confined within a cylindrical shell. By varying the sizes of the cylinders, we analyze how the microscopic aspects of base pair opening are influenced. In Fig. 5.1, we show the effect of partial confinement.

5.4 Effect of partial confinement of DNA in cylindrical shell

In this study, we consider the first 12 base pairs of the phage-λ DNA chain and repeat the sequence to form other sequences for our studies. The sequence of the chain is $-GGGGAAAAGGGG-$. Each chain is confined in a cylinder of lengths 20, 50, and 150 bp. Here we consider the length of the cylinder in terms of base pairs. We calculate free energy per base pair by evaluating the partition function

and hence the specific heat as a function of temperature. Through the peak in the specific heat, we identify the melting temperature T_m of the chain at different diameters of the cylinder as shown in Fig. 5.4.

In our study, we aimed to investigate the effect of confinement on the melting tem-

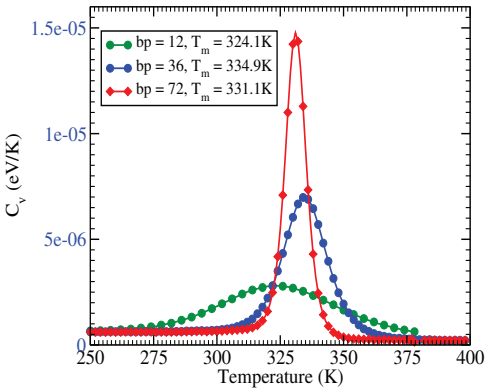

Figure 5.4: The change in specific heat with the temperature of the system. The plot is for DNA molecules of lengths 12, 36 & 72 base pairs confined in a cylinder of length 50 base pairs and radius of 10 Å.

perature of DNA. Our previous research [129, 238] has demonstrated the influence of confinement on DNA's melting temperature, and we sought to further explore this phenomenon in the context of partially confined DNA molecules, which closely resembles DNA translocation through cells. To begin, we considered cylindrical confinement with a fixed length of $l = 20$ and a radial distance of $r = 10$ Å. It's important to note that in this case, the cylinder's radius R_c is equal to r plus the DNA radius ($R_c = r +$ DNA radius). We investigated how the melting temperature of the system changed as the radial distance increased. The results are presented in Figure 5.5, where it can be observed that the melting temperature of the DNA molecule decreases with increasing radial distance (r). This decrease is attributed to the limited available volume for the DNA molecule, which affects its stability. However, an intriguing and noteworthy difference emerges at $r = 10$ Å for DNA molecules longer than 20 base pairs. We found that the melting temperature (T_m) is nearly the same for 36- and 42-base pair chains, while it decreases for chains consisting of 72, 96, and 192 base pairs. This unexpected behavior is distinct from the expected stability trend. We also observed a similar pattern when examining cylinders of different lengths, as depicted in Figure 5.5. Nevertheless, when the DNA molecules were confined within a cylinder of length 150 base pairs, the previously observed pattern disappeared (Figure 5.5). The behavior change

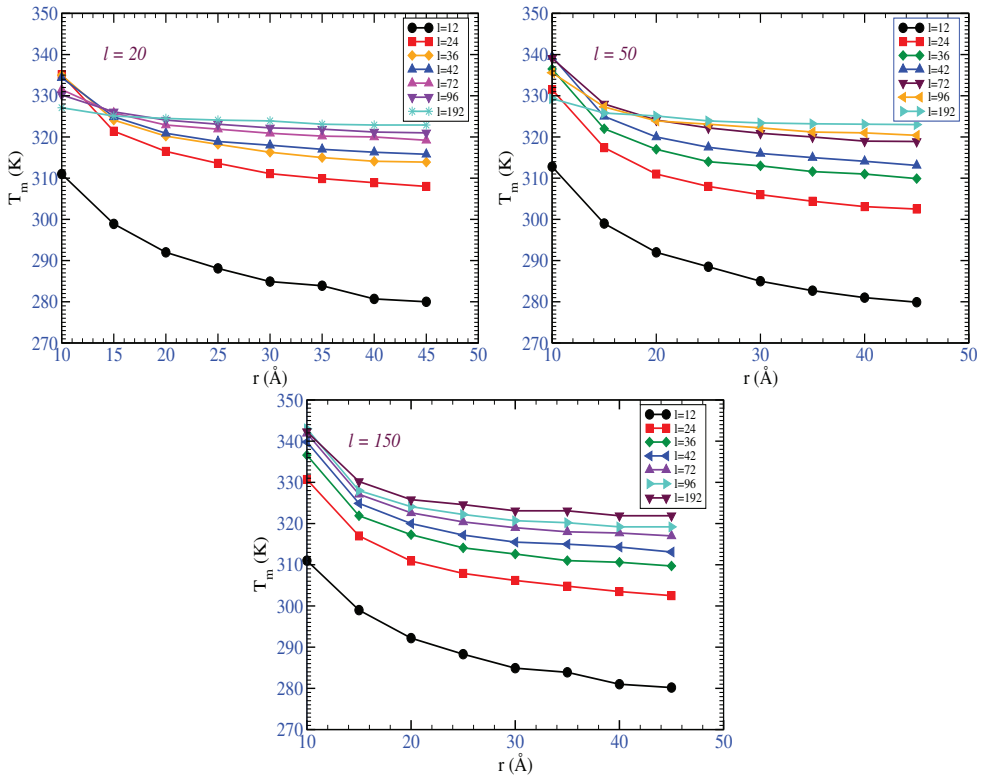

Figure 5.5: The melting temperature of the DNA molecules that are confined in a cylinder of different lengths. We consider lengths as 20, 50, and 150 base pairs. The plots show the changes in the T_m with the increasing radius of the cylinder for the chains 12-192 base pairs.

can be attributed to the length of the confinement. In this case, the entropy of the system is suppressed due to the large size of the cylinder, resulting in the loss of the previously observed trends. We plotted the changes in the melting temperature (T_m) as a function of different chain lengths for three distinct cylinder lengths. By varying the size of the DNA molecules from 12 to 192 base pairs, we calculated the corresponding melting temperature for each chain length. We observed that as the chain length increases, the stability of the system, represented by the melting temperature, also increases up to a certain limit. However, beyond this limit, the melting temperature started to decrease. This behavior indicates that when the size of the DNA molecule exceeds this critical length, different sections of the chain exhibit distinct behaviors. One section, which remains confined, experiences reduced entropy due to its constrained movement. Conversely, another section of the chain, which is relatively unconfined, possesses greater entropy and contributes to driving the system from a zipped state to an unzipped state.

In the next part of the study, we specifically examined the effect of a cylinder radius of $r = 10$ Å on the melting temperature (Figure 5.6). Interestingly, we observed an increase in the melting temperature up to the length of the cylinder itself. However, beyond this point, the melting temperature began to decrease. It's important to note that this pattern is not universal and depends on the specific cylinder radius. For larger cylinder radii, we observed an initial increase in T_m, which then saturated to a certain value. For a cylinder of length $l = 150$ bp, even for the $r = 10$ Å, there is no point of inflection.

To get a deeper understanding, we calculated the average separation and it is

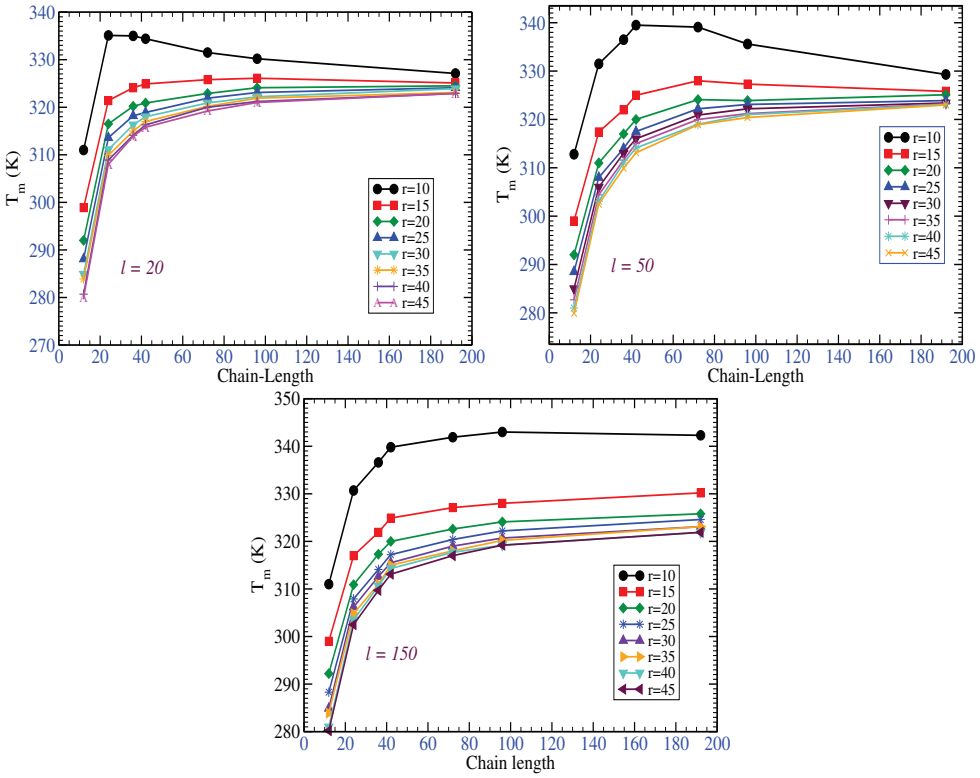

Figure 5.6: The melting temperature of the DNA molecules that are confined in a cylinder of different lengths. We consider lengths as 20, 50, and 150 base pairs. The plots show the changes in the T_m with the increasing chain length for different radii of the cylinder.

denoted as $\langle y_i \rangle$. The $\langle y_j \rangle$, of the j^{th} pair of the chain is given by:

$$\langle y_j \rangle = \frac{1}{Z} \int \prod_{i=1}^{N} y_j \exp(-\beta H) dy_i, \tag{5.2}$$

We consider DNA chains of lengths 12, 36, and 72 base pairs, and each chain is confined within two different types of cylinders: one with a length of 20 base pairs and a radius of 10 Å, and the other with the same length but a different radial distance of $r = 40$ Å. The results of these calculations are depicted in Figures 5.7. By examining these figures, we can observe several intriguing features related to

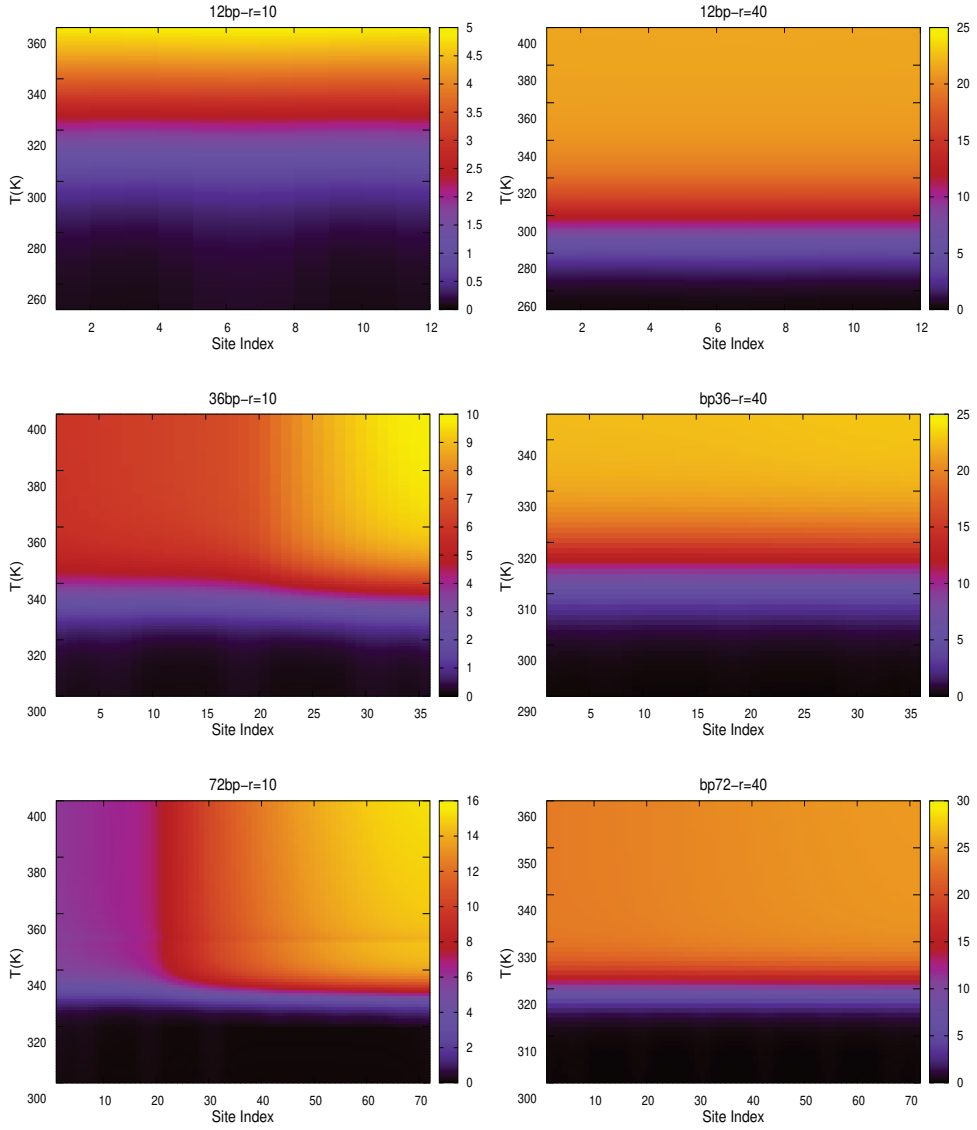

Figure 5.7: The density plots showing the change in the average separation, $\langle y_j \rangle$ for DNA of 12 base pairs confined in a cylinder of length 20 base pairs and radii r=10 and r=40 Å, for DNA of 36 base pairs confined in a cylinder of length 20 base pairs and radial distance, r=10 and r=40 Å, for DNA of 72 base pairs confined in a cylinder of length 20 base pairs and radial distance r=10 and r=40 Å.

the opening of the DNA molecules. In the case of completely confined chains, the

opening tends to be relatively uniform throughout the chain. However, for the chain consisting of 36 base pairs and confined with a radius of 10 Å, the chain predominantly opens from the free end, as indicated by the yellow color. On the other hand, when the radial distance is increased to $r = 40$Å, the opening becomes more homogeneous. In this scenario, the DNA molecule has more space to move, weakening the effect of confinement. A similar pattern is observed for the chain of 72 base pairs. When confined within a radial distance of 10 Å, the maximum distance over which the base pairs can move is limited to 10 Å, resulting in a heterogeneous opening pattern. However, when the radius is larger, this heterogeneity disappears, and the opening becomes more homogeneous.

5.5 Summary

We have considered heterogeneous DNA molecules of different lengths (12-192 bps) and investigated the correlation between the melting temperature (T_m) of a system and the size of heterogeneous DNA molecules. We focused on cylinders of infinite length and varied the cylinder's radius. By employing a non-linear curve fitting equation, we determined that T_m exhibits a logarithmic relationship with both the chain length and the cylinder radius. Specifically, as the system size increases, the melting temperature increases, while it decreases with an increasing cylinder radius. Our primary research question revolved around exploring the correlation between the decrease in melting temperature and the decrease in the cylinder radius. These calculations demonstrated that the molecule is more stable when placed inside a cylinder, confirming our earlier observations in the first part of the study and our previous works [129, 238]. The reason for the stability is as follows: the decrease in the cylinder's radius, the confining wall becomes closer, which suppresses the molecule's entropy, and hence the molecule is more stable.
We then examined the stability of a phage-λ DNA molecule that is partially confined within a cylindrical shell. During the translocation process, the DNA molecule is partially inside the cell, leading to different segments of the DNA experiencing various forces from neighboring molecules. Our focus in this work was to gain insights into the stability of a DNA molecule that is only partially confined in a cylinder. We considered DNA molecules of different lengths and confined them within cylinders of varying radii and lengths. By exploring the influence of the cylinder's radius and length, we aimed to understand the opening behavior of heterogeneous DNA molecules confined in the cylinder. To examine the behavior,

we calculated the average displacement $\langle y_j \rangle$ and observed that the DNA confined in a cylinder experiences uniform suppression of system entropy. However, the opening of the partially confined DNA molecule proved to be particularly intriguing. In our future work, we plan to investigate the effect of applying a force to the DNA molecule confined within a cylindrical shell.

Chapter 6

Effect of molecular crowders on DNA

6.1 Introduction

Living cells contain a diverse array of biomolecules, such as nucleic acids, proteins, lipids, and metabolites, which collectively occupy a significant portion (20-40%) of the cellular space [97, 133, 148, 211]. This crowded intracellular environment, known as molecular crowding, has attracted considerable attention in biophysics, medicine, and pharmaceutical sciences [209, 210]. The interaction between DNA and these crowding agents has become a focal point of research, with implications for molecular transport, reaction rates, and chemical equilibrium [212, 213]. Recent studies have been focused on how crowders impact DNA condensation, cell surface dynamics, and the overall organization of the cellular interior [149, 239, 240]. Notably, molecular crowders play a vital role in phase separation within the cytoplasm and the compactness of DNA into the nucleoid of bacterial cells [139, 221, 222, 241]. Recently, Takanashi has shown how molecular crowders modify the DNA and RNA polymerase reactions [242, 243]. Therefore, DNA-crowder complex systems have explored the remarkable diversity, complexity, and intriguing nature of the conformations that nucleic acids can assume.

In this study, we utilized atomistic molecular dynamic simulation techniques to calculate the structural stability of DNA in a crowded environment. Specifically, we focused on a 12-base pair sequence of DNA, which is surrounded by two different crowders. To investigate the influence of crowders on dsDNA, we systematically increased the concentration of crowders in the vicinity of the DNA molecule. This allowed us to thoroughly analyze the interactions occurring within

the DNA-crowder complex system. Therefore, the study of DNA-crowder interactions contributes to a better understanding of the stability and behavior of DNA under biologically relevant conditions.

6.2 Molecular dynamics simulation methods

The molecular dynamics studies were carried out with the AMBER22 software package to perform simulations on a system of interest. We have taken twelve base pair sequences of 1-BNA (C,G,C,G,A,A,T,T,C,G,C,G) and arranged two different crowders aspartame [244] and PEG-200 [245] in the surrounding of DNA. We know that all the biomolecules are randomly distributed *in vivo*, thus we considered different distributions of crowders, including their placement above or below one another, at the ends of the DNA, and near each other. Fig. 6.1 displays snapshots

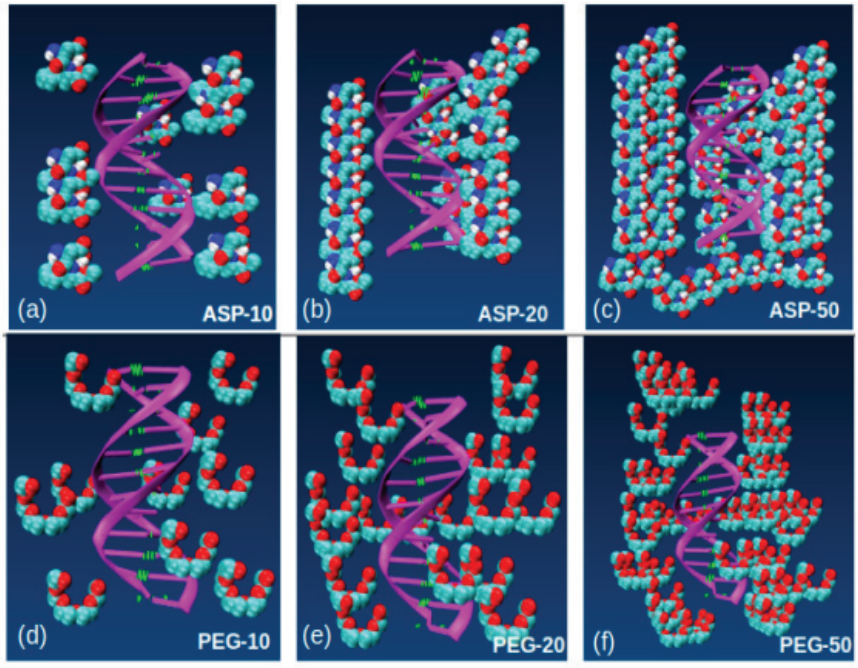

Figure 6.1: In Fig. 6.1(a-c) DNA is surrounded by the aspartame crowders while in Fig. 6.1(d-f) DNA is surrounded by the PEG200 crowders in the vicinity of DNA.

of the initial system, where we have investigated the influence of crowders on a 12-base pair DNA chain. The crowders are randomly distributed in the system to mimic the heterogeneous environment present *in vivo*, considering the coexistence of other biomolecules. To examine the impact of crowders on the DNA structure, we highlighted the variation of hydrogen bonds between the DNA bases because

these bonds play a crucial role in maintaining the stability and structure of the DNA molecule. Also, we employed the Visual Molecular Dynamics (VMD) tool by which we could manipulate the coordinates of individual crowder molecules and create a system in which the DNA is surrounded by two different types of crowders [246]. In Fig. 6.1(a-c) a DNA molecule is surrounded by ten, twenty, and fifty aspartame molecules, respectively. Conversely, in Fig., 6.1(d-f) DNA is surrounded by ten, twenty, and fifty Polyethylene glycol-200 molecules respectively.

To perform the simulation we use BSC1 DNA and general amber force field (gaff) force field parameters for nucleic acid simulation. In addition, to generate the force field of crowders, we also use the "Antechamber package" suite to prepare the topology and coordinate files. Since we know that there is no direct force field available for the aspartame molecules. To neutralize the negative charges on the DNA, 22 Naˆ+ counterions were added to the system. Also, we surround the system with solvent molecules modeled using the TIP3P water model, while keeping a minimum distance of 12.0 Å between the system and the edges of the simulation box. Here 5492 residues (likely water molecules) have been added to the system and 55.366 Å × 55.536 Å × 73.748 Å is the size of the simulation box, including both solute and solvent molecules when considering the van der Waals interactions. It represents the dimensions of the box used for the simulation. After defining the complete simulation system we obtain the topology and co-ordinate file of individual systems.

In our simulation, we start by minimizing the energy of the system in two stages. First, we keep the DNA structure fixed while adjusting the positions of water molecules and ions to find the lowest energy state. After that, we minimize the entire system, including the DNA. For the heating-up phase, we conduct a molecular dynamics simulation over 50,000 steps, with a time step of 0.001 picoseconds. We begin at a low temperature of 10K and gradually increase it to 300K. Here we also apply periodic boundary conditions and a non-bonded cutoff of 9.0Å. To keep specific parts of our system stable, we use positional restraints with a force constant of 20.0. In addition, our simulation uses the SHAKE algorithm to keep bond lengths constant, does not consider polarizability, and utilizes a random seed for the thermostat that controls the temperature. To achieve a stable state that accurately reflects the desired temperature, pressure, and structural conditions in molecular dynamics simulations, we perform an equilibration phase after the heating. This equilibration is carried out over a period of 2 nanoseconds. After the equilibration phase, a 500-nanosecond production run is performed in

the simulation which provides a substantial period for observing and analyzing the system's behavior. To maintain structural integrity, we apply the SHAKE algorithm to bonds involving hydrogen atoms, with a very high tolerance level. The simulation employs Langevin dynamics to maintain a temperature of 300 K, using a collision frequency of 2.0 for the Langevin thermostat. For all the different DNA-Crowding systems we repeat all the steps of minimization, heating, and equilibration and perform the molecular dynamics for 500ns.

6.3 Analysis on DNA-Crowding system

6.3.1 Snapshots of individual molecular dynamics system

In the interesting study conducted by Kashanian *et al* [244], the researchers explored the interaction between aspartame and DNA. They found that aspartame tends to bind to the grooves of DNA. To explore the groove-binding properties

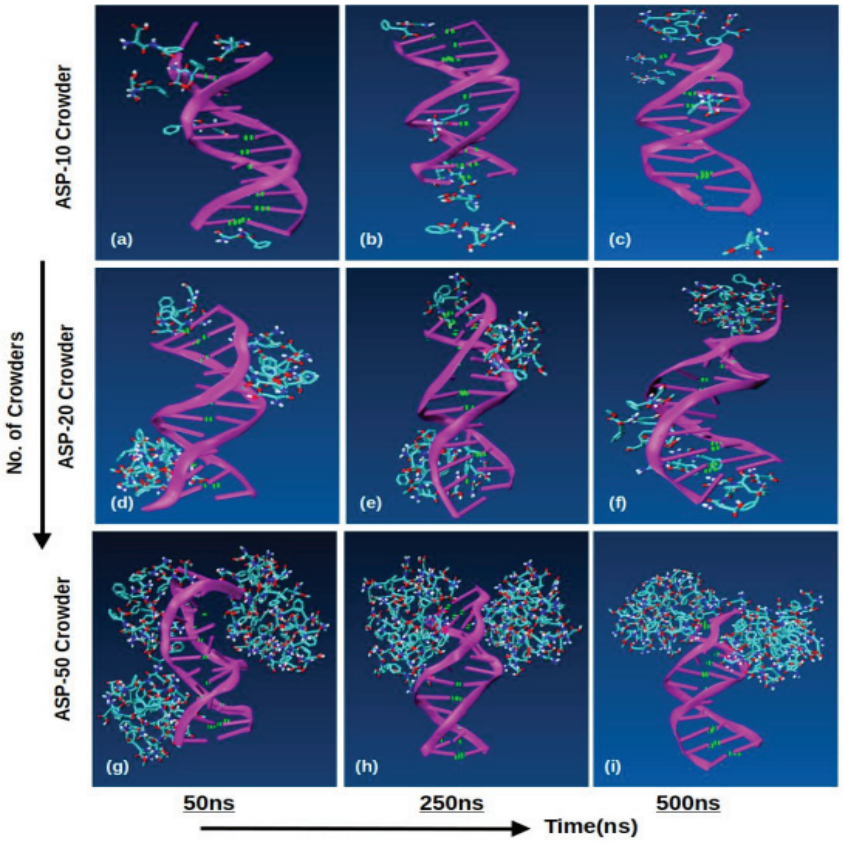

Figure 6.2: Figures 6.2(a-i) show the snapshots of DNA in the presence of aspartame crowders for 500 ns.

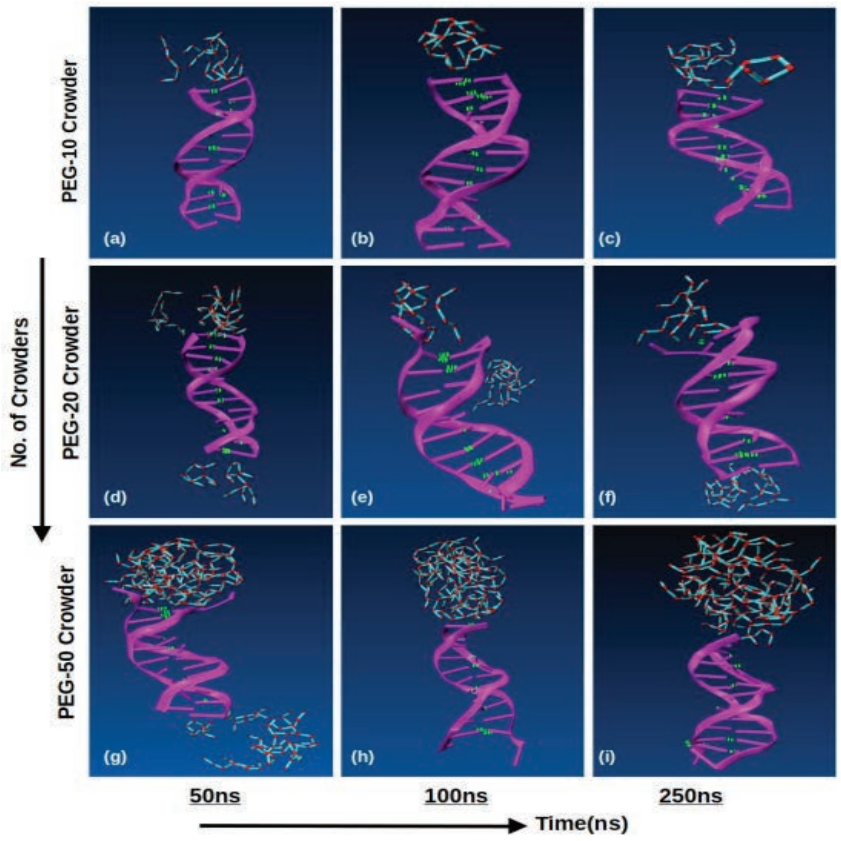

Figure 6.3: Figures 6.3(a'-i') show the snapshots of DNA in the presence of PEG-200 crowders for 500 ns.

of aspartame, we designed various systems where DNA molecules were immersed in a solution containing both aspartame and polyethylene glycol (PEG-200) as crowders. The snapshots of these systems provided interesting insights into the dynamics of the interaction (see Fig. 6.2 and Fig. 6.3). In Fig. 6.2(a), it was observed that ten aspartame molecules encircled the DNA. However, during the simulation, only six or seven of these molecules influenced the structure of DNA, while the remaining molecules drifted away and did not participate in the interaction. The snapshots at different time points (Fig. 6.2(a-c)) showed the evolution of the system with ten crowders over 50ns, 250ns, and 500ns, respectively. Our study also investigated the impact of increasing the number of crowders from ten to twenty. The results revealed that as more crowders were introduced, they began to form clusters and accumulated within the grooves of the DNA. Over time, these clusters of crowders moved from the grooves to the ends of the DNA. Fig. 6.2(g-i) clearly illustrates the snapshots of the system with fifty crowders, showing the formation of massive clusters that spread from the grooves to the entire length

of the DNA. As a consequence of this accumulation of crowder clusters, the DNA strand underwent deformation, leading to the opening of hydrogen bonds. This extended behavior of aspartame along the entire length of the DNA highlighted the significant influence on DNA dynamics and structure. In the case of PEG-200 crowders, the study revealed that only a small number of crowders interacted with the DNA, while a significant portion of the molecules drifted away from the DNA. During the simulation of ten crowders, it was observed that approximately five to six PEG-200 molecules moved away from the DNA and not a single molecule appeared to interact directly with the DNA chain. This indicates a lack of strong interaction between these molecules and the DNA chain. In Fig. 6.3(a'-c'), four or five crowders accumulate at the ends of DNA while in the case of twenty crowders, three bunches of crowders present at the ends of DNA (see Fig. 6.3(d'-f')). As the number of crowders increased further, the bunches of PEG-200 molecules settled even more prominently at the ends of the DNA chain. For instance, when fifty crowders surrounded the DNA, two large bunches of molecules were observed specifically at the chain ends (see Fig. 6.3(g'-i')). In contrast, not a single PEG-200 molecule settled into the grooves of the DNA. These findings strongly suggest that the presence of crowders, whether at the grooves or the ends of the DNA, significantly disrupts the hydrogen bonds within the DNA chain. This disruption of hydrogen bonds may have important implications for the overall stability and conformation of the DNA molecule.

6.3.2 Calculation of root mean square deviation

The crowding study we conducted focused on the effect of crowders, specifically ten, twenty, and fifty crowders, on the root-mean-square deviation (RMSD) of DNA. It measures the average distance between the atoms of a simulated structure and a reference structure. In this study, we compare our findings with the DNA in the absence of crowders. The results showed that the RMSD values of the DNA changed based on the presence and number of crowders in the system. Here we calculate, the RMSd of the DNA backbone atoms (P, O3', O5' C3', C4' and C5') and show the variation plots with respect to time for two distinct crowders in Fig. 6.4(a-b). In this study, we examined the impact of crowder number, crowder-DNA interactions, crowder positioning, and crowder saturation on the variation in RMSD of DNA. When DNA was simulated without crowders, we obtained a baseline RMSD representing the DNA's native stability and dynamics under normal conditions. Introducing ten aspartame crowders led to a decrease in DNA's

RMSD compared to the baseline.

This suggests that a small number of crowders stabilized the DNA, possibly

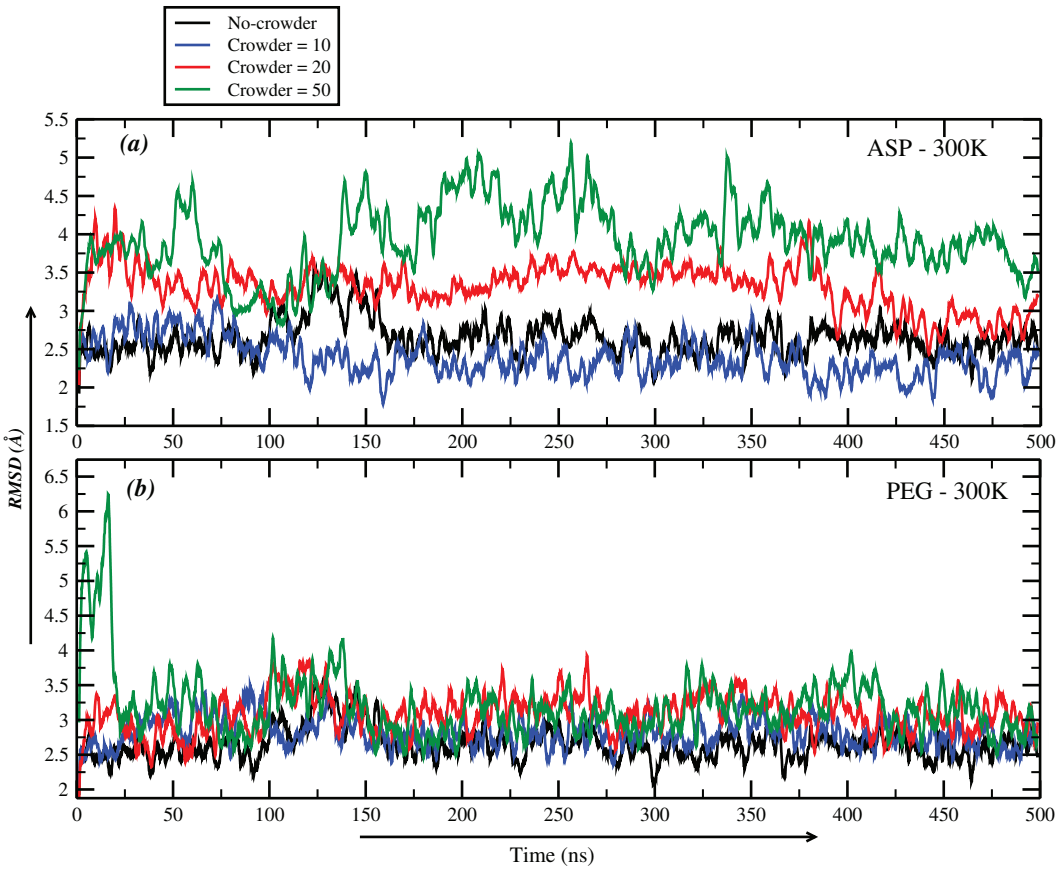

Figure 6.4: The figure shows the root mean square deviation for all the possible distributions of aspartame and PEG crowders.

through crowder-DNA interactions, supporting the DNA's structure and limiting its mobility. The decreased RMSD indicates that the DNA structure was more compact and closer to its initial conformation. As the number of crowders increased to twenty, the DNA's RMSD increased. This higher RMSD suggests that more crowders caused increased perturbations, destabilizing the DNA structure. The crowders might have crowded around the DNA changing its natural conformation and increasing its flexibility. With the further increase in number of crowders (fifty) in the system, the RMSD of the DNA increased even further. This significant increase in RMSD indicates that the presence of a large number of crowders had a substantial impact on the stability and conformation of the DNA.

On the other hand, when we introduced ten PEG-200 crowders (Fig. 6.4b), the RMSD of the DNA remained almost equal to the baseline (no crowders). This suggests that the presence of ten crowders had a minimal influence on the DNA's

stability and conformation. As we increased the PEG-200 crowder concentration to twenty, the DNA's RMSD slightly increased. This indicates that a higher crowder concentration started to exert some influence on the DNA dynamics, leading to a slight increase in RMSD. We can also say that the crowding effect may have started to affect the mobility and conformational flexibility of the DNA. Finally, with fifty PEG-200 crowders, the DNA's RMSD significantly increased up to 20ns of simulation. After this initial increase, the RMSD stabilized at a level similar to that with ten PEG-200 crowders. This suggests that the crowding effect of PEG-200 reached a saturation point beyond fifty crowders, resulting in a limited additional impact on the DNA dynamics. This observation suggests that different crowders, such as aspartame and PEG-200, exhibit distinct effects on DNA dynamics which influences its stability and conformation in crowded environments. Therefore, understanding the behavior of these two molecules in complex cellular conditions has implications for various biological and pharmaceutical applications.

6.3.3 Radial Distribution of crowders and ions

The radial distribution function (RDF) is a valuable tool for understanding the spatial organization and solvation properties of molecules in a system. It describes the probability of finding a particle (crowder or ion) at a given distance from a reference particle (DNA). In this study, the RDF analysis is performed to investigate how crowders (aspartame and PEG200) interact with the DNA molecule and how ions are distributed around the DNA in the presence of different numbers of crowders (10, 20, and 50). The cutoff distance used for the RDF calculation is 25.0 Å which means that interactions between particles beyond this distance are not considered. In Fig. 6.5(a), RDF for crowders (aspartame molecules) shows that there is an increased probability of finding crowders closer to the DNA molecule within a distance of 0-7.5 Å. At 7.5 Å, we obtain a maximum value of RDF 0.52 for crowders. This indicates that crowders tend to accumulate around the DNA. However, beyond 7 Å, the probability of finding crowders decreases. This suggests that at larger distances, crowders are more evenly distributed throughout the system and are less likely to be found near the DNA molecule. Similarly, for ions, the value of RDF increases up to a distance of 6.8 Å, where it reaches its maximum value of 0.38. This indicates a higher probability of finding ions closer to the DNA within this range. Beyond 6.8 Å, the RDF value for ions starts to decrease which indicates a reduced probability of finding ions at larger distances from the DNA.

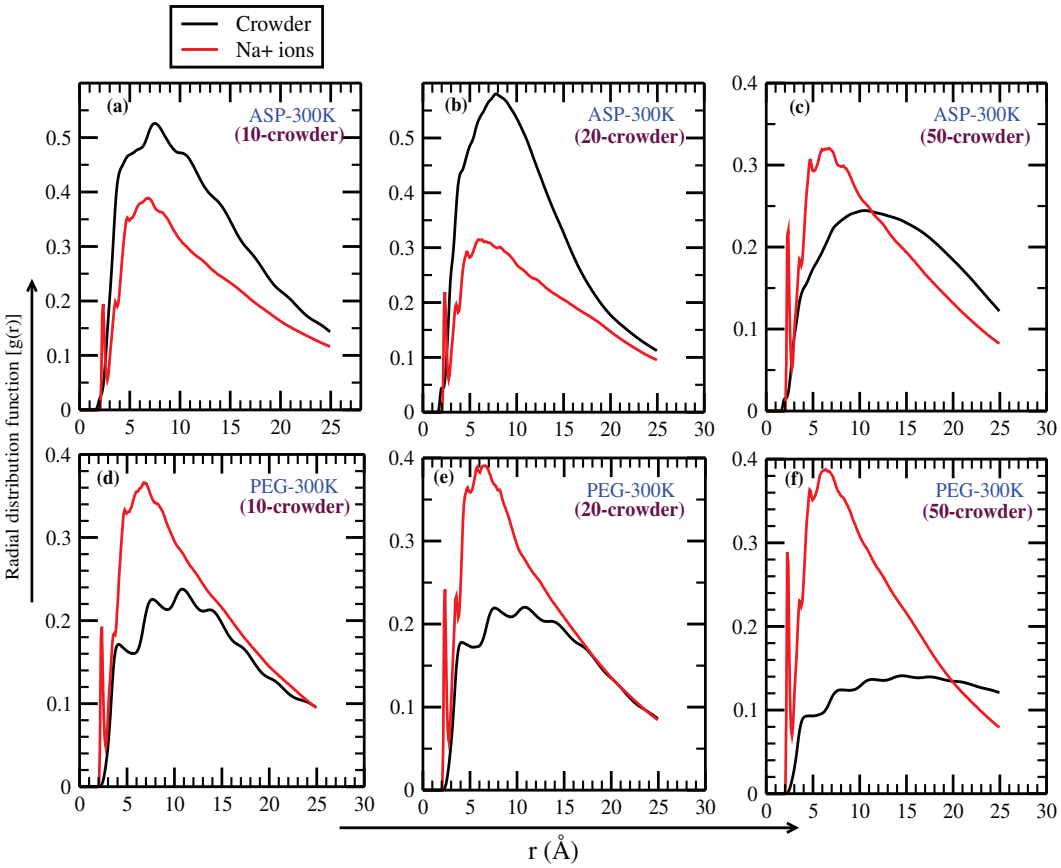

Figure 6.5: The radial distribution of crowders and Na+ ions in the vicinity of DNA.

In Fig. 6.5(b), we can see that the maximum RDF value increases up to 0.58 for crowders while it is 0.31 for the presence of ions. As we increase the number of crowders up to fifty, the maximum value obtained at 0.24 for crowders distribution is less as compared to previous cases. Here, all these crowders occupy more space within the system which leads to an increase in the excluded volume. In the system, crowders act as obstacles and restrict the movement of other molecules, including themselves. Consequently, the crowders become more evenly distributed throughout the system, resulting in a reduced probability of finding them near any particular reference species (DNA). On the other hand, the RDF for ions shows the same value as we obtained in 20 crowders.

In comparison to the above outcomings, the RDF for PEG200 crowders always remains lower compared to the RDF for ions. This suggests that PEG200 crowders have a lower probability of being found near the reference species (DNA). We observe that for all three cases (10, 20, and 50 PEG200 crowders), the RDF shows multiple peaks and troughs with an overall decreasing trend as the distance from

the reference structure increases. Here, the highest peak for 10 and 20 PEG200 crowders is obtained at 10.8 Å while for 50 PEG200 crowders, maximum variation is obtained at 15.3 Å. In addition to this, the RDF of ions for 10-PEG200 crowders increases up to 0.36 while for 20 and 50 crowders it attains maximum value at 0.39. Interesting to note that, in the variation of ions RDF, we also obtained a little peak in all three cases at 2.4 Å. The height of this peak increases as we move towards the higher crowded system. In the case of 10 crowders, the height of the peak increases up to 0.19, for 20 crowders it increases by 0.24, and for the last case (50 crowders) height increases up to 0.29.
This suggests that ions tend to accumulate at this distance from the reference species due to specific interactions. This study confirms that a lower RDF value for PEG200 crowders as compared to ions indicates that PEG200 crowders have a lower affinity for the reference species (DNA) and they are accumulated at the ends of the DNA(Please see the snapshots of simulation). The RDF for ions shows a peak at 2.5 Å, which suggests that ions tend to accumulate at this distance from the reference species, likely due to specific interactions

6.3.4 Water Shell Analysis in DNA-Crowder Environment

The water shell analysis is a valuable tool to investigate the solvation properties and behavior of water molecules around DNA and crowders. It helps researchers understand the role of solvent (water) in biomolecular systems and provides a deeper understanding of the system's stability, dynamics, and molecular interactions. In this study, we set the lower and upper limits of the distance range for the water shell analysis. We considered water molecules between 3.4 Å to 5.0/5.5/6.0 Å from the solute. The lower limit (3.4) Å in the water shell analysis ensures that we focus on the water molecules that can interact with DNA through hydrogen bonding. This is important for studying the stability and behavior of DNA in a realistic biological environment. In fig. 6.6(a-c), we observe that water shell occupancy decreases as the number of aspartame crowders increases around the DNA system which suggests that the presence of crowders has a significant effect on the solvation properties of water molecules. As the number of aspartame crowders increases from 10 to 50, they occupy more space in the vicinity of the DNA molecule. This crowding effect can restrict the available space for water molecules and reduce their ability to access the immediate environment around DNA. In other words, we can say that water molecules are pushed away from the crowder-DNA interface and unable to penetrate the crowded region around DNA.

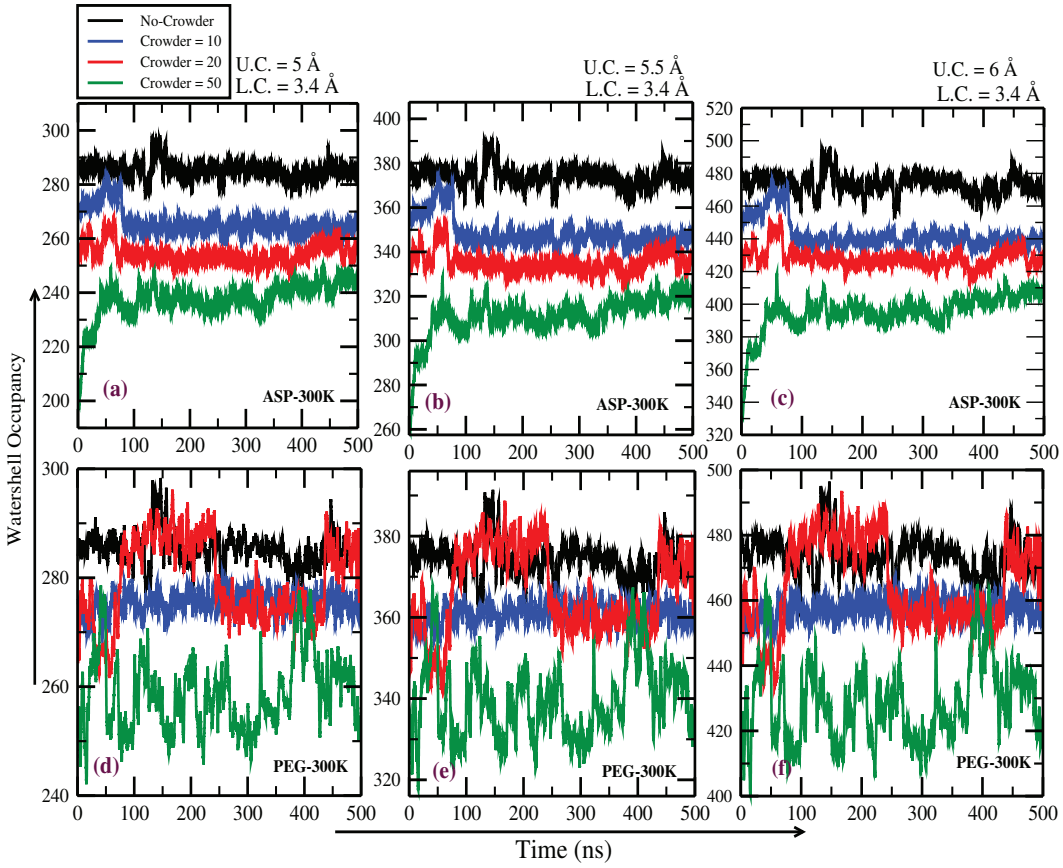

Figure 6.6: The figure shows the watershell occupancy with respect to simulation time for aspartame and PEG200 crowders.

In all these cases, we obtain maximum occupancy of water molecules when no other molecule or crowder is present in the surrounding DNA. Point to note that in all Fig. 6.6(a-c), water shell occupancy increases as we extend the upper limit of the water shell analysis from 5 Å to 6 AA. This study suggests that, as we extend the upper limit from 5 Å to 6 Å, we include more water molecules that are constantly moving and exchanging positions due to their natural thermal motion. This extension helps us capture water molecules that may briefly move closer or farther away from the DNA-crowder system during the simulation. By observing this broader range of water molecules, we gain a better understanding of how they interact with the DNA-crowder system and contribute to its behavior.

In the case of PEG200 crowders, we also observe a decrease in water shell occupancy as the number of PEG200 crowders increases. Similar to the above case, as the number of PEG200 crowders increases, they take up more space around the DNA and create a crowded environment. This crowding effect restricts the

available space for water molecules to solvate the DNA molecule effectively. In comparison, PEG molecules have less tendency to interact with the DNA chain, and all molecules are settled at the ends of the chain. This may be a reason for the large watershell variation in the case of PEG200 as compared to aspartame molecules. Hence, these fluctuations reflect the dynamic and complex nature of water-PEG interactions and their influence on the solvation behavior of water molecules around DNA in a crowded environment.

6.4 Summary

In the first part of the study, we showed captivating snapshots of the simulation and shed light on the potential impact of this interaction. This comparison study revealed that aspartame has a higher affinity for interacting with DNA and settling into its grooves, while PEG200 prefers to accumulate at the ends of the DNA. The accumulation of crowders, regardless of their type, leads to the disruption of hydrogen bonds in the DNA chain. As we increased the number of crowders, the clusters became more prominent and spread from the grooves to the entire length of the DNA. Therefore, our findings highlight the significance of crowder-induced clustering and its implications for DNA stability. In the second part, the RMSD analysis indicates that when a small number of crowders were introduced (ten crowders), they appeared to stabilize the DNA structure but as the number of crowders increased to twenty and fifty, the RMSD of the DNA also increased. This suggests that more crowders caused higher perturbations, leading to the destabilization of the DNA structure. In contrast to aspartame crowders, the presence of ten PEG-200 crowders had minimal influence on the DNA's stability and conformation. As the concentration of PEG-200 crowders increased to twenty, there was a slight increase in RMSD which indicates a mild effect on DNA dynamics and conformational flexibility. Hence this study reveals that different crowders, such as aspartame and PEG-200, exhibit distinct effects on DNA dynamics, stability, and conformation in crowded environments. In the third part of the study, RDF analysis reveals that crowders accumulate around the DNA molecule, especially within a distance of 7.5 Å. As the number of crowders increases, they act as obstacles and restrict the movement of molecules which leads to a reduced probability of finding crowders near the DNA molecule. Also, compared to ions, PEG200 crowders show lower RDF values and indicate a lower affinity for the DNA molecule. Besides this, the DNA-crowding system has a significant effect on the occupancy of water

molecules in the vicinity of the DNA. As the number of crowders increases, they occupy more space and reduce the probability of finding the water molecules in the surrounding DNA. Overall with this study, we gain a better understanding of DNA dynamics and its interactions, contributing to the advancement of nanotechnology and biophysics research.

Conclusions and Future Scope

The behavior of double-stranded DNA (dsDNA) under various environmental conditions is a subject of significant interest. Its complexity poses an interesting challenge that attracts researchers, as exploring its mysteries can lead to valuable insights across several fields of study. This molecule is very important for living things, and both experiments and theories have shown its significance in biology. It helps us understand how cells work, how genes are expressed and regulated, and how genetic information is passed from parents to offspring. Therefore, DNA plays an active role in diverse areas, including drug development, biotechnology, genetic engineering, nanotechnology, and many more. In our current research, we use a statistical model and molecular dynamics simulation tool to study the confinement of DNA in different conditions. Our findings can be summarized as follows:

- In **Chapter-3**, We have studied the effect of solvent on the melting profile of homogeneous and heterogeneous DNA molecules in force and thermal ensembles providing valuable insights into the complex behavior of DNA and its potential applications. In this part of the study, we examined the unzipping of homogeneous DNA chains of varying lengths in the presence of solvent molecules under a constant force. We observed that the location of solvent molecules influenced the critical force required to unzip the chain. When the solvent was placed at the end of the chain, a slightly higher force was needed to unzip the chain, indicating a reduction in end entropy. Conversely, when the solvent was at the center of the chain, more force was required to unzip it due to reduced entropy away from the solvent location. Additionally, we noticed that when DNA melts, it behaves differently depending on whether force or temperature is involved. When force is applied, the melting process is mostly driven by a change in energy (enthalpy), whereas the temperature change is more about the disorder (entropy). We also looked at how the position of solvent molecules affects the melting of short, different DNA molecules. Although there was a slight difference in the temperature

at which the DNA starts to melt for different solvent setups, what caught our attention was that when the solvents were in the middle part of the DNA chain, the unwinding process started at a completely different point compared to when the solvents were elsewhere. Our findings contribute to a better understanding of how solvent molecules impact the stability and behavior of DNA molecules during melting and unzipping. This knowledge can serve as a valuable guideline for predicting DNA thermodynamic quantities and designing DNA nanostructures in practical applications.

- In **Chapter-4**, We emphasize the importance of DNA linked gold nanoparticles and its thermal stability in the presence of various molecular solvents, with potential applications in bionanotechnology and nanotechnology. Through this research, we analyze the melting profile of a 15-base pair DNA-linked AuNP chain under the influence of different solvents. The results highlight the significant impact of solvents on the thermal stability of DNA which plays the crucial role of solvent selection in the design and application of DNA-AuNP systems. Subsequently, we examined how the position of AuNPs affects the melting temperature (T_m) of short, homogeneous DNA chains. It was observed that the position of the AuNPs plays a vital role in determining T_m. Also, a plateau region in T_m was observed for certain positions, which signifies increased stability in those regions. Additionally, we explore the influence of AuNPs on the melting profile of the DNA chain by analyzing the unwinding pattern at different temperatures. Surprisingly, we discover unique necklaces and bird-like patterns, showing the dynamic behavior of DNA in the presence of AuNPs. Overall, this analysis significantly contributes to our understanding of how solvent molecules and AuNPs influence the stability of DNA-linked AuNP systems. The findings from this study have important implications for the design and application of DNA-AuNP systems in various fields, including bionanotechnology and nanotechnology.

- In **Chapter-5**, We examined the impact of confinement on the thermal stability of double-stranded DNA. Using the PBD model, we found a correlation between the change in the melting temperature and the change in the cylinder radius. We also investigated the correlation between heterogeneous DNA molecules' melting temperature (T_m) and their sizes when confined within cylinders of varying radii. We found that T_m follows a logarithmic relationship with chain length and cylinder radius. The confined DNA molecules

exhibited increased stability as the cylinder radius decreased due to suppressed entropy. This research provides valuable knowledge into the behavior of molecules confined within a shell, which is relevant to gene therapy and understanding cellular crowding. In the second part of the study, we have calculated the stability of partially confined phage-λ DNA molecules within cylindrical shells of varying radii and lengths. The DNA experienced uniform suppression of system entropy, while the opening behavior of partially confined DNA proved intriguing. Hence, our findings highlight the importance of considering confinement effects, particularly in nano-scale or confined spaces. Such insights are crucial for designing and optimizing DNA-based nanodevices and drug delivery systems, where DNA interactions within confined geometries play a pivotal role.

- In **Chapter-6**, Our study focuses on the role of molecular crowders on the structural transition in DNA. Cellular environments plays a crucial role in shaping the behavior and functions of biomolecules, including DNA. The atomistic simulation techniques gave us valuable insights into the complex interplay between DNA and crowders under different crowding conditions. Our investigation focused on a 12-base pair sequence of DNA surrounded by crowders at varying concentrations. By increasing the crowder concentration near the DNA, we evaluated the interactions within the DNA-crowder complex system. The analysis was performed at 300K. In addition, we calculated various parameters like root mean squared deviation, the radial distribution function of crowders and ions, number of water molecules in the surrounding DNA-crowding system. These findings contribute to a better understanding of how crowding conditions affect the physical properties and biological functions of DNA. The knowledge gained from this study can have broader implications for various biological processes and cellular functions, providing a foundation for future investigations into DNA dynamics in crowded environments. Therefore our atomistic simulation approach offers a valuable tool for studying complex biomolecular interactions and provides a framework for further research.

Future Scope

Even though scientists have made sincere efforts in the past to understand processes like the breaking of base pairs, DNA movements, and the formation of complex structures in DNA but we still don't fully understand how these pro-

cesses happen inside living organisms. The translocation of DNA confined in a cylindrical nanotube is a topic of my further research. In this study, we calculate the amount of force for the translocation of individual base pair. I have obtained some interesting results and found more outcomes of this study. In addition, with the help of the statistical model, we attempt to understand the role of crowders on the stability of the DNA molecule and obtained the melting profile of short and long DNA chains in the presence of crowders. For future works, the calculation of how the time scale of the presence of a crowder at a particular location along the chain will provide more interesting results. In addition, the atomistic molecular dynamics simulations [247, 248] of the different DNA hairpins when it is subjected to an unzipping force are also improving our understanding of the interactions and the force response of nucleic acids. In the future work of force-induced unzipping in the presence of solvents, we intend to explore how the time scale of solvent presence at specific locations along the DNA chain affects the melting behavior. Understanding these dynamics will further enrich our understanding of DNA-solvent interactions and their implications in various biological and nanotechnological contexts. In the present study of DNA-aspartame complex system we explored into the complex details of how aspartame interacts with DNA and exhibit a remarkable tendency to cluster together and settle within the grooves of the DNA structure. According to recent research conducted by the World Health Organization (WHO), there is growing evidence suggesting a potential link between the presence of aspartame molecules in the human body and an increased risk of developing cancer. Therefore this discovery has raised concerns due to the well-known fact that certain molecules have the ability to cause DNA mutations, which can lead to the formation of cancer. Through advanced simulations, we further explore the presence of these crowders and their accumulation in the minor and major groves of the DNA at different temperature scale. Hence our future findings will give us important information about how aspartame might play a role in causing cancer. To compare our findings with day to day activity of humans, we imagine an example of regular 300ml diet coke. It harmless beverage contains large number of around 10^{20} aspartame molecules. If a very large number of aspartame molecules were to interact with the DNA in our bodies, their combined effect could be incredibly significant which can produce several disorders in the human body.

Appendix A

This chapter explains the importance of biomolecules, the genetics of organisms, and the main building block of life. We know that these biomolecules play important roles throughout our lives, from medicine to agriculture, from biotechnology to forensics, and cellular evolution. Here we explore the structural parameters and binding of DNA in the nucleus of the cell. We have discussed the different conformations of double-stranded DNA and their stability. Additionally, we also describe some important techniques and various applications of DNA as a template.

Nucleic acid structural elements

Cells contain two distinct varieties of nucleic acids: deoxyribonucleic acid (DNA) and ribonucleic acid (RNA). These two biopolymers have many similarities, but there are also some minor differences between them. They are divided into primary, secondary, tertiary, and quaternary structures that play important roles in many biological functions. These biopolymers consist of long, linear macromolecules that contain the genetic information for all cellular functions. Generally, DNA exists as a double helix in eukaryotes and procaryote, but sometimes a single-stranded form of DNA also exist in bacteria. Similarly, RNA is usually found in single-stranded form in the nucleus and then it enters into the cytoplasm to bind with proteins. These two nucleic acids are considered an acidic substance and it was first discovered by Friedrich Meischer in 1868, and he named them "Nuclein". Later in 1953, Watson and Crick demonstrated the simple and well-known structure of DNA double helix [249]. These two important molecules support all life and are responsible for storing genetic information. The basic difference between the two biopolymers are:

1. DNA and RNA are long chains of nucleotides. DNA transmits genetic information to make new cells while RNA transfers genetic code from the nucleus to the ribosomes to make proteins.

2. DNA is more stable in alkaline conditions while RNA is much more reactive and unstable in alkaline conditions.

3. DNA is easily damaged by UV rays, while RNA is much more resistant to UV damage.

4. DNA is a self-replicating molecule and RNA is made from DNA.

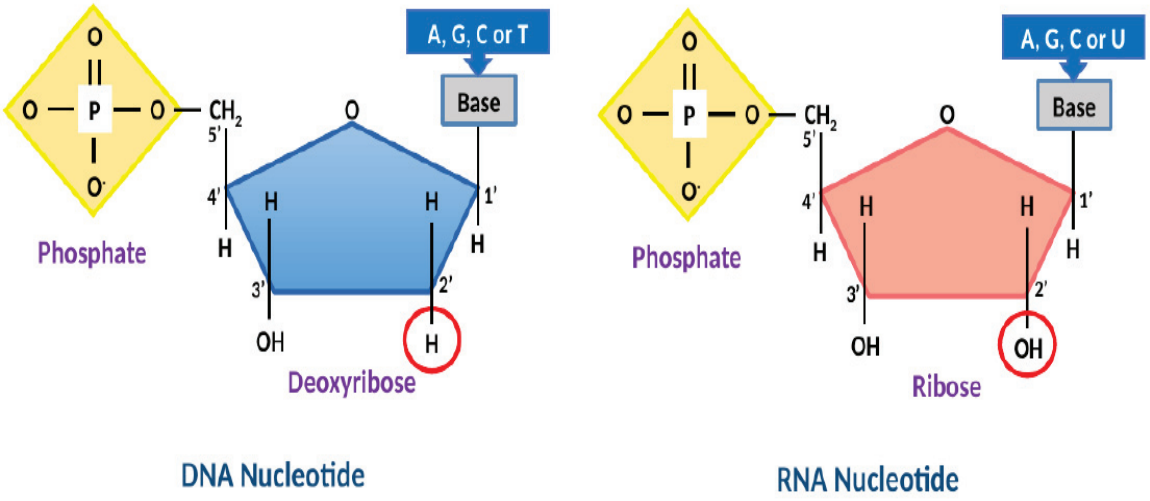

Figure 6.7: The monomer of DNA and RNA strand; the nucleotide. The phosphate and carbonic bases are covalently bonded with the sugar.

In the above structure, the base and sugar form a nucleoside structure *i.e.*, adenine and ribose combine to form adenosine and adenine and deoxyribose sugar form Deoxyadenosine [250]. In addition to the nucleoside, phosphate groups are attached to both the biopolymers, so the addition of bases, sugars, and phosphate(s) groups leads to the nucleotides. In nucleotides, a phosphate group and a carbonic base are covalently attached to the sugar. On the level of bases, they are categorized under Purines and Pyrimidines. Purine is an aromatic heterocyclic organic compound containing fused pyrimidine and imidazole rings, while pyrimidine is an aromatic heterocyclic compound containing only carbon and hydrogen. Adenine (A) and Guanine (G) are purine nucleotides while cytosine (C), thymine (T), and uracil (U) are pyrimidine nucleotides. These bases in two strands are paired through hydrogen bonds (H-bonds) which form base pairs (bps). In DNA, adenine forms two hydrogen bonds with thymine and guanine forms three hydrogen bonds with cytosine from opposite strands. This hydrogen bond consists of hydrogen atoms

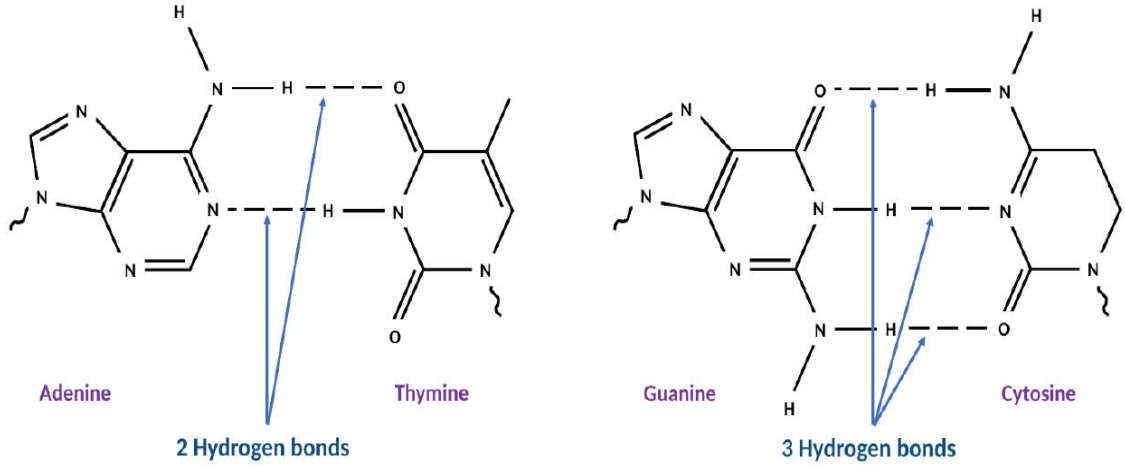

Figure 6.8: Formation of the double and triple bond between the nitrogenous bases.

between two electronegative atoms ($OorN$) with one part being a covalent bond and another one being an ionic bond. According to Chargaff's rule, the ratios between AT and GC remain constant and equal. The continuous addition of nucleotides creates a single-stranded structure with a free phosphate group at the $5'$-end of the chain and a free OH group at the $3'$-end of the chain. This nucleic acid sequence is expressed from $5'$ to $3'$ end that determines the covalent structure of the entire molecule. Also, when these two single-stranded DNAs are linked by hydrogen bonds, the secondary structure of DNA is formed. The bonding between the bases is known as "base pairs" and the stability of the bonds is different. This base pairing between two polynucleotides makes the double helix of DNA. In the Double helix formation, the two strands are connected in opposite directions. DNA has both hydrophobic and hydrophilic groups, the aromatic bases form the hydrophobic part while the phosphate backbone is a hydrophilic one. Due to the hydrophobic nature of bases both the strands come together and remove water from the core. To protect the core, the negatively charged phosphate groups are pushed out and each base pair gets the rotation of 35 °with the adjacent base pair. This continuous pairing of bases with rotation makes the double-helix structure. This helical structure is stabilized in the molecule due to the presence of the H-bond and base pair stacking. The studies of the backbone of the DNA helix provide information on two grooves of different widths. These two grooves are of two types: major and minor grooves. In their formation, when two antiparallel strands run closest to each other, there will be the formation of minor grooves while major grooves are generated when strands move furthest apart.

Structural variants of DNA

Depending on the helix sense and orientation of the atoms, DNA takes several different conformations. The primary base sequence is categorized as A-, B-, C-, D-, and Z-DNA [251, 252]. Among all these A-, and B-DNA both have right-handed structures. B-DNA has a wider major groove and narrow minor gloves, while A-DNA has a more compressed structure with wider and deeper minor grooves. The C-, D-DNA have high helical twist $(38.6 - 40.0)$ and are obtained with Li and Na ions under low hydration conditions. Similarly, Z-DNA adopts a left-handed geometry and it has 12 bp per cycle where sugar phosphates form a zigzag shape pattern. In a more complex manner, DNA also adopts other conformations such

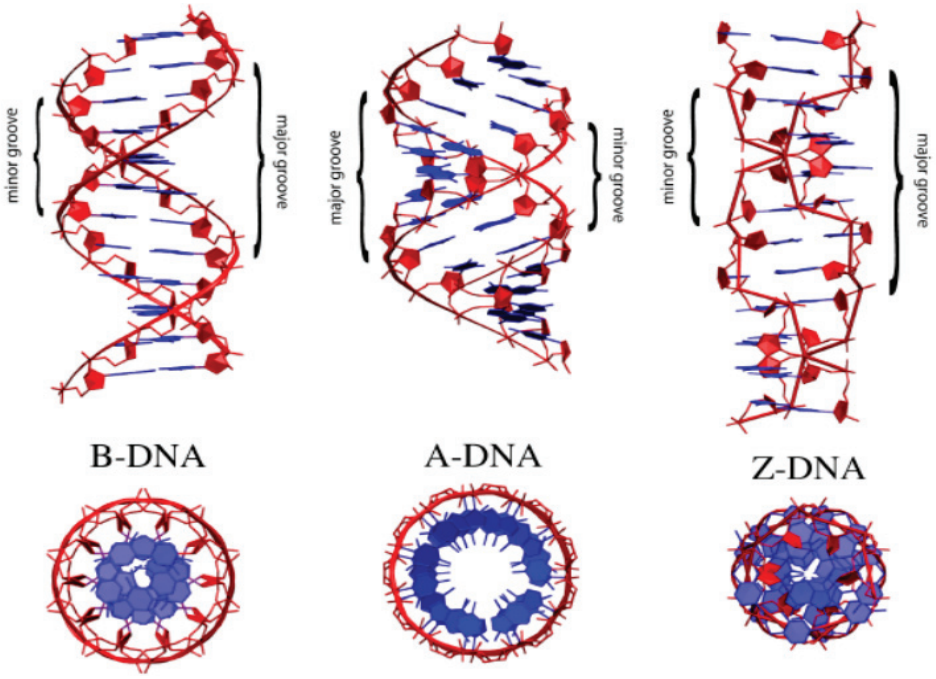

Figure 6.9: Three different structures of DNA Image taken from Garcia*et al.*, Journal of the Mexican Chemical Society, 57, 3, 2013.

as tetraplex (G-quadruplex and motifs), hairpin structure, triplex $(H - DNA)$, and cruciform. To obtain this complex structure, the DNA helix must fold many times or form mismatched base pairs (Hoogsteen base pairs). In the formation of hairpins or cruciform structures, the self-complementary sections of single-stranded DNA participate and these structures have been considered for controlling gene expression. Hence DNA can form more and more complicated structures in which atoms are arranged in the three-dimensional space with the formation of loops, pseudoknots, stems, and junctions. The pictorial representation of all the different

structures is as follows:

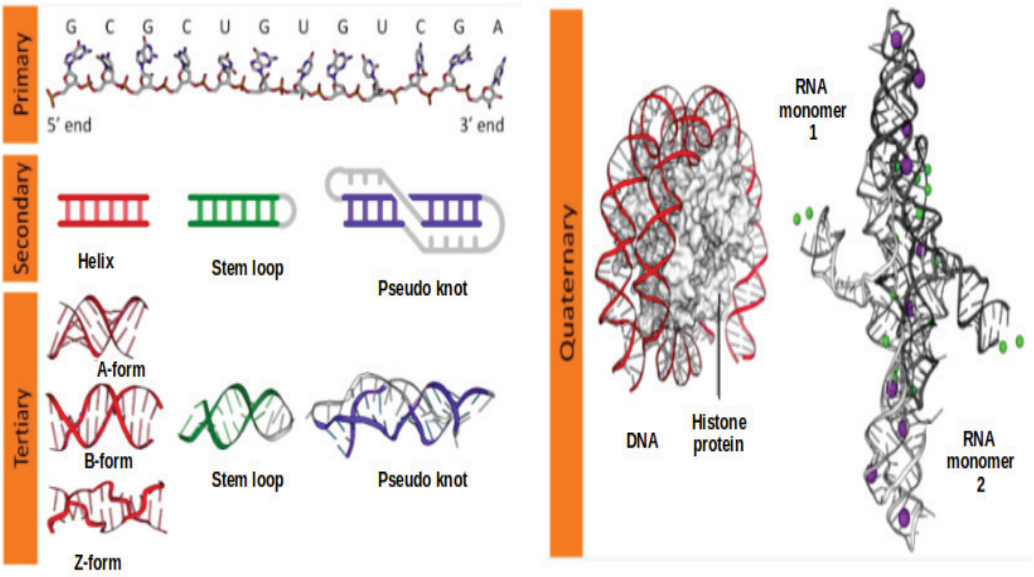

Figure 6.10: Different conformations (primary, secondary, tertiary, and quarternary) of Nucleic acid. (Image taken from Wikipedia)

Packaging of double helix DNA (dsDNA) and importance of instruction book of life

In B-DNA, the spacing between successive bases measures 0.34 nanometers. If the total number of base pairs in DNA is 6.6×10^9, then the length of the DNA double helix comes out to be approximately 2.2 m. This length of DNA is much greater than the size of the nucleus (10^{-6}) m. This calculation poses an interesting question in the field of research How is such a long biopolymer packed into the cell? In prokaryotic cells such as *E. Coli* does not have a defined shape of the nucleus, so DNA(negatively charged molecule) binds to a protein (positively charged species) in a certain region. This region is called the nucleoid and connects the DNA in large loops and junctions. In comparison, eukaryotic cells are much more complex and contain a set of positively charged proteins. These proteins are called histones and it is made up of amino acid residues of lysine and arginine. Histones are organized in such a way that a unit of eight molecules forms the histone octamer structure. Due to the negative nature of DNA helixes, they wrapped around the positively charged histone octamer. This complete structure is called the nucleosome and contains 200 bp of DNA. Nucleosomes carry the repeating unit of structures inside the nucleus which is known as chromatin. This thread-like structure can be viewed

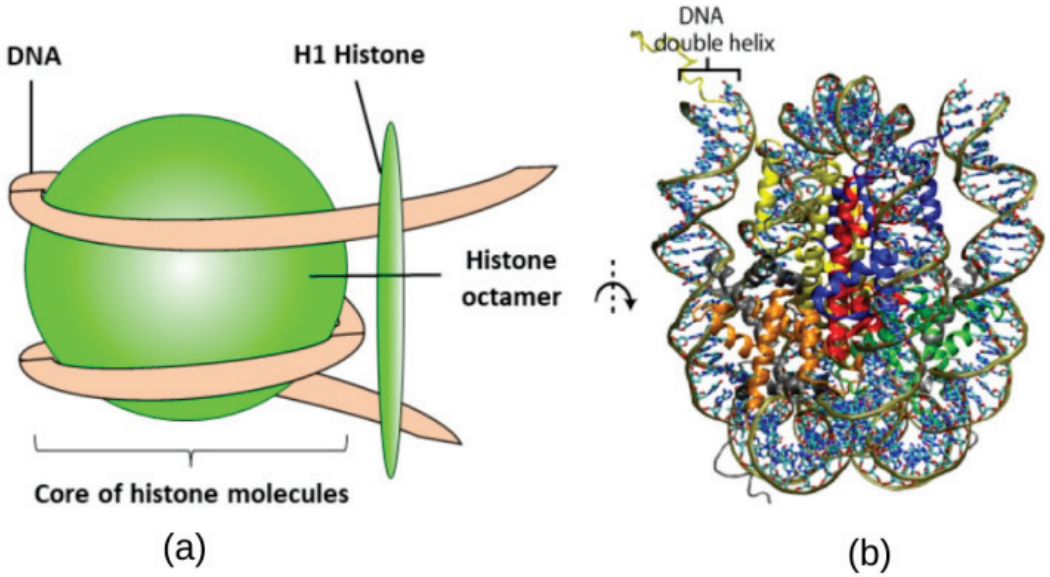

Figure 6.11: (a) Structure of Nucleosome (b) The organization of DNA on Histone protein Image taken from ASBMB Today (Click Here)

under an electron microscope.

Cells are complex and dense due to the presence of many components. Inside the cell nucleus are present nucleolus and chromatin. The nucleus is surrounded by the nuclear membrane, whereas the nucleolus has no clear boundaries. In chromatin, DNA is tightly packed and contains genetic information. It is also a universal blueprint for life on Earth. This molecule is sometimes found in the cytoplasm(cpDNA) of the cell and in the nucleus. In humans, the nucleus of a cell carries 3×10^9 base pairs. These huge number of base pairs are divided into 23 pairs of chromosomes. In the nucleus, DNA is wrapped with a lot of twisting and

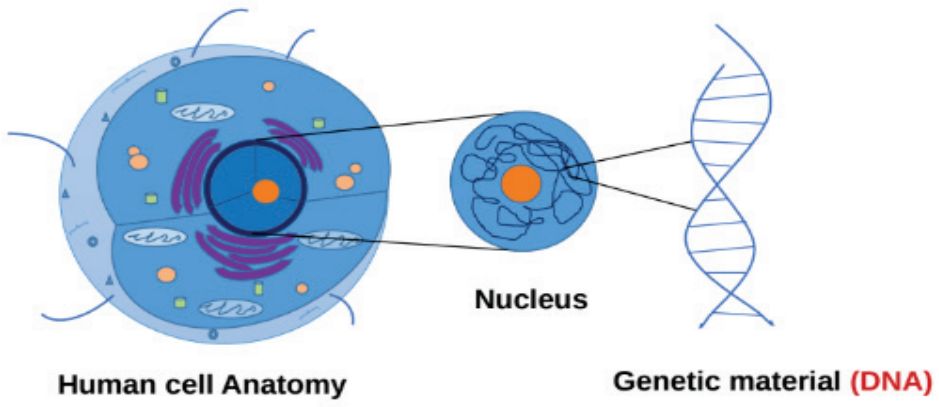

Figure 6.12: The magnification in the structure of a cell.

winding and contains the genetic codes. These codes can be expressed as either DNA codons or RNA codons and they provide direct evidence for the common origin of life on earth. The presence of the molecule in the cell determines many functions, such as how people look and how their bodies work different functions. DNA also participates in the central dogma of molecular biology. During this process, many events such as replication, mutation, transcription, and translation occur in the cell, and genetic information flows from DNA to protein synthesis All the processes in which DNA participates are explained as:

DNA Replication

DNA replication is the mechanism by which an exact duplicate of the original DNA molecule is synthesized [55, 253]. During this process, DNA splits into two parts and produces two single-stranded DNA. These two separated DNAs are identical, hence this process is semiconservative. In 1958, Meelson and Stahl experimented and explained the concept behind the replication process [254]. During replication, two separate strands are further joined by a strand, and daughter DNAs are generated with the parent's DNA. In this daughter DNA, one parental helix and one newly synthesized helix are present. *In vivo*, four different enzymes play a role in DNA replication These important enzymes are Helicase, DNA polymerase, RNA primase, and DNA ligase [255]. Generally, DNA occurs as a double helix in which

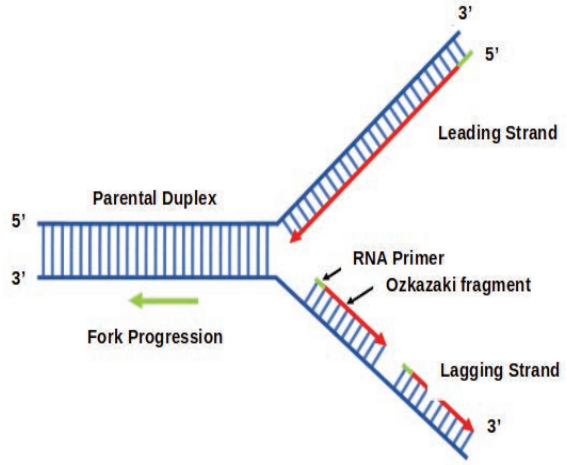

Figure 6.13: The replication process of double helix DNA.

both strands have antiparallel polarity. Both the strands of DNA are linked with H- bonds. Of all four bases, adenine forms a double bond with thymine, while

guanine forms a triple bond with cytosine. The replication process begins in the AT-rich region, which is less stable than GC. This region is called the replication center. At first, the helicase enzyme finds the replication site and attaches to the strand. At the point of contact, it breaks the H-bond between two strands and the DNA chain unravels. When the bond between the bases breaks, a Y- Y-shaped pattern is formed and it is also called the Y-curve [256]. Helicase can not unwind the DNA helix in one go, so there are two types of base pairs present, some are in the strand of DNA (bonded bps) and some are present in the Y-curve of DNA. After that, DNA polymerase binds to the 3′ end of the DNA to maintain the polarity of the strand. When forming a new strand, the RNA primase gives the location to DNA polymerase and it starts the formation of a new single strand. This newly synthesized strand from 5′ to 3′ is also known as the leading strand. Further, another strand of parent DNA runs in the 3' to 5' end so to maintain the polarity of DNA, primer attaches at different segments of the parental strand. Once the primer is attached, DNA polymerase begins the formation of a complementary strand with segments of correct polarity. These pieces are called Okazaki pieces and the strand is known as the Lagging strand [257]. At the end of the replication, DNA polymerase removes RNA primer and connects DNA ligase. This DNA ligase acts as an adhesive agent and forms the phosphodiester the bond between the segments of the DNA chain.

DNA transcription

The process of transcription encompasses the transfer of genetic information from a DNA strand to RNA. To express it in another manner, the formation of RNA from DNA is known as transcription [258]. In 1957, Frances Crick proposed the central dogma of biology. Which states that DNA produces RNA by the transcription method while RNA produces proteins by the translation method. In this process, one strand of DNA participates in the formation of RNA and this strand is known as the antisense strand. The genetic code of DNA is usually involved in the initiation process and DNA-dependent RNA polymerase binds to it. This bounded polymerase breaks the hydrogen bonds between the two complementary strands [4, 259]. These RNA polymerase enzymes are divided into three types: RNA Polymerase– 1, 2, 3. All these types of polymerase produce different types of RNA (mRNA, tRNA, rRNA). During the elongation phase of the transcription process, the enzyme begins to form a complementary strand with RNA nucleotides. At the same time, RNA polymerase binds to the nearest mRNA nucleotides with a

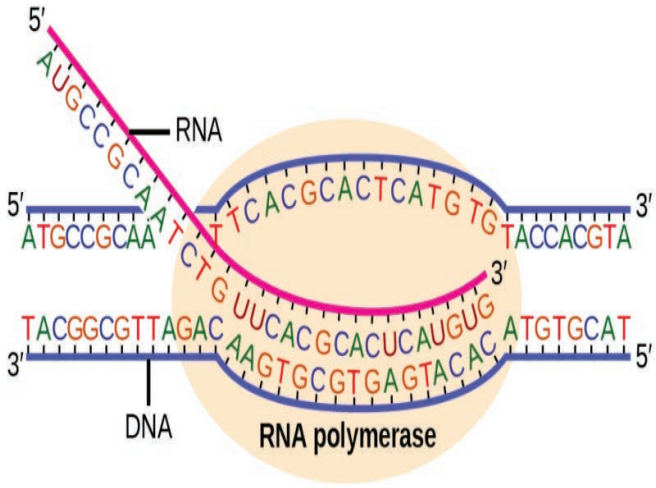

Figure 6.14: The transcription process of dsDNA.

phosphodiester bond. At the terminator, RNA polymerase removes itself and a pre-mature RNA (hnRNA) separates. Later hnRNA is then converted into mRNA by splicing, capping, and tailing functions. This mature RNA (mRNA) comes out to the nucleus and participates in the translation process of molecular biology [197, 260].

DNA Mutation

Mutation is a process that occurs in the DNA sequence. Sometimes DNA changes the A, T, G, or C sequence while copying the genetic information or due to other factors such as ultraviolet radiation, sunlight, and cigarette smoke. Mutation can also affect normal gene function, leading to severe diseases like cancer. The process

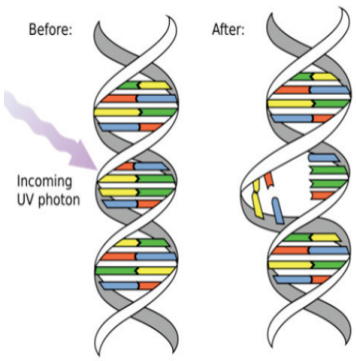

Figure 6.15: The pictorial representation of DNA mutation. Image taken from Internet (Click Here)

of mutation sometimes affects human brain cells. Sickle cell anemia, *for example*, is a disease caused by the mutation found to protect the African population from Malaria. Many mutations occur in the human body such as point genetic mutation, chromosomal mutation, and copy number mutations [261].

Application of DNA

DNA is the genetic material that contains the information for the evolution and proper functioning of the cell. This biopolymer is used in multiple directions such as nanotechnology, biological science, medicine, and chemical sciences. Across various DNA application domains, some interesting and latest applications are as follows :

DNA Fingerprinting

This technique, also known as DNA profiling was developed in 1985 [262, 263]. This technique facilitates the comparison of DNA samples from multiple individuals and enables the examination of similarities and variations. It is used for solving criminal investigations, forensic reasons, and confirmation of paternity testing. It also recognizes that people are interconnected. Globally, two people on Earth share 99.9% of the same DNA, so this technique detects the remaining 0.1% of differences. Hence this advanced technology exhibits remarkable sensitivity which requires merely a few skin cells, hair roots, or a small quantity of blood and saliva for accurate testing [264]. In addition to all this, the fingerprinting technique is also used to identify the disorderliness in genes.

DNA Nanomaterials

DNA nanotechnology can be used to design and manufacture artificial nucleic acid structures that use DNA as a non-biological material [265]. It was first developed by Seeman in 1980 and operates on a scale of $100nm$ range. This nanotechnology facilitates the creation of two- and three-dimensional crystal lattices, nanotubes, and DNA computers. Among them, DNA computers are used to discover new methods in medical devices. In present days, these computers are performing logical and arithmetic operations by using the molecular properties of DNA in which silicon chips are replaced with biochips. DNA nanomaterials are designed in different shapes and sizes. Some three-dimensional (3D) nanostructures are stable

and are used as drug carriers to deliver numerous antitumor medicines [266]. With the superior accuracy of the Watson-Crick base combination, DNA materials have the potential for nanofabrication. These nanostructures are complex materials with wide applications in immunology, biosensors, and disease diagnosis.

Agriculture

In addition to molecular biology, DNA technology has shown significant potential in improving the efficiency of agriculture and fertilization [267]. This technology improves the quality and outputs of breeding products. For plants, this genetic material is very useful in the identification and extraction of useful genes to replicate in successive generations of plants. In agriculture, transgenic technology is the latest and widely used to control insect pests and various diseases in plants. Nitrogen fixation efficiency improves plant growth by cloning disease genes and reintroducing them into plant cells [268]. Nowadays, due to the crisis of soaring population and food shortage, agricultural production has become an important tool in the construction of the domestic economy. Therefore, using DNA technology to improve food production and agriculture quality is an important choice for scientists [269].

DNA Encapsulation

This process is an important tool for gene storage. In addition, this technique facilitates DNA protection and gene delivery [270]. In this method, DNA macromolecules and oligomers are placed into the polyelectrolyte capsules, and their properties are studied in a micro-confined area. Storing DNA in a small space helps maintain its integrity without electrical power and can remain stable for long periods without data loss [124]. Usually, encapsulation is done in four steps. In the first step, DNA is compressed with polyvalent cations; sequentially then DNA is captured into C_aCO_3 beads where the DNA is condensates. In the third step, polyelectrolyte multilayers are assembled on the bead structure and finally, the bead dissolves in which DNA folds and releases. In future developments, the characterization of this encapsulated process will give promising results for the construction of 'artificial cells' to deeply understand the behavior of genes [271].

Digonisis of genetic Diseases

Genetic diseases are diagnosed through the utilization of DNA testing. Today, these tests provide information about genetic mutations and the presence or absence of a gene material[272]. Because not all genetic diseases produce a defect in a particular site, it is very difficult to identify the defect in a certain region. One of the new methods, PCR, is used to prevent sickle cell anemia [273]. This polymerase chain reaction is a widely used method that produces millions to billions copy of DNA samples that researchers then use to amplify the specific region on the DNA strand.

Gene Therapy

This research technology helps to modify human genes or treat diseases. This treatment works through several mechanisms. It replaces defective genes with a healthy copy of the genes [274]. Sometimes this treatment also inactivates a disease-causing gene and modifies the gene in the body for the proper functioning of cells. Recently different types of gene therapy products include; Plasmid DNA, Viral vectors, Bacterial vectors, and human gene editing therapy. Gene therapy is also an effective tool in the treatment of heart attacks, diabetes, cancer, AIDS, and many other diseases [275].

DNA Sequencing

This process helps to determine the sequence of nucleotides or how nucleotide bases are arranged in a DNA helix [276]. DNA sequencing information plays an important role in many fields such as diagnostics, virology, forensic testing, and molecular biology. In this way, comparison between healthy and unhealthy DNA sequences gives information about various diseases [277]. There are two types of DNA sequencing:

- Sanger Method: This is a traditional approach for the sequencing of complete chromosomes or long DNA strands. The process involves amplifying the stimulated sample to read 100 to 1000 base pairs of DNA. Moreover, this kind of pattern is overlapped with a computed analysis system [278].
- Next-Generation Sequencing (NGS) method: This technology has led to the rapid development of DNA sequencing. It is the fastest and newest way to match the sequencing of thousands of base pairs [279].

The other sequencing method to study the information encoded in DNA is the translocation of DNA through nanopores. It is a direct, fast, and inexpensive technology. A simple form of nanopore sequencing exploits the fact that individual nucleotides of DNA pass through the nanopore, adding an ionic current. This electronic recording of the current set up the DNA sequence. The Mycobacterium smegmatis porin A (MspA) was the first nanopore sequenced by DNA [116].

DNA amplification: Polymerase Chain Reaction

This procedure involves the repeating replication to amplify the small amounts of DNA and this sufficient amount of DNA helps to identify the contagious cell [280]. This laboratory technique quickly magnifies billions to trillions copy of DNA segments, which examines them in greater detail. In this methodology, specific pieces of DNA called primers select a specific region of DNA. This region of DNA was amplified multiple times for the study. With the aid of this strategy, difficult organisms can be detected with high precision and sensitivity [281]. Therefore PCR gives remarkable results for the diagnosis of Pneumonia, chronic disease, Persistent illness, and many more. With some modification, PCR technology has some more advanced methods such as Randomly amplified polymorphic DNA (RAPD), Reverse Transcriptase (RT-PCR), Nucleic acid sequence-based amplification (NASBA), and Ligase chain reaction (LCR) [282]. Among all these PCR methods, one of the most important and widely used methods in the detection of Coronavirus is the RT-PCR method. This is a molecular test that analyzes samples from upper respiratory infections where scientists have elevated small amounts of RNA (the genetic material of SARS-CoV-2) to deoxyribonucleic acid (DNA). This process is repeated until SARS-CoV-2 is detected. It is an accurate and reliable temperature test for the diagnosis of COVID-19.

Numerical Integral Quadrature Method: Gauss Quadrature

Gauss Quadrature is a numerical integration method that approximates the definite integral of a function. It is especially efficient for functions that are approximately polynomial in behavior. The method is based on the principle of using weighted sums of the function values at specific points (nodes) within the domain of integration. The general form of the integral approximation in Gauss Quadrature

is:

$$\int_a^b f(x)\,dx \approx \sum_{i=1}^{n} w_i f(x_i) \tag{6.1}$$

where,

- $\int_a^b f(x)\,dx$ is the definite integral of $f(x)$ from a to b.
- n is the number of nodes or points.
- x_i are the nodes or specific points in the interval $[a, b]$.
- w_i are the weights assigned to each $f(x_i)$.

The nodes x_i and weights w_i are determined based on the polynomial degree of accuracy we desire. For a Gauss Quadrature of order n, the integral will be exact for polynomials of degree $2n - 1$ or less. Gauss-Legendre quadrature is naturally defined for the interval [-1,1]. To apply it to any other interval, like [-5, 200], we used a linear transformation to map the interval [-1,1] to [-5,200]. This transformation adjusts both the locations of the grid points and their weights.

References

[1] B. Alberts et al., Molecular Biology of the Cell, Third Edition (Garland Science, 1994).

[2] L. Stryer, Biochemistry, 4 ed. (W.H. Freeman and Company, 1995).

[3] P. Nelson, Biological Physics (Updated Edition) (Macmillan, 2003).

[4] C. R. Calladine, H. Drew, B. Luisi, and A. Travers, Understanding DNA, Third Edition: The Molecule and How it Works (Academic Press, 2004).

[5] J. Gibbs and E. DiMarzio, The Journal of Chemical Physics **30**, 271 (1959).

[6] C. Kittel, American Journal of Physics **37**, 917 (1969).

[7] R. M. Wartell and A. S. Benight, Physics Reports **126**, 67 (1985).

[8] Physics Reports **486**, 1 (2010).

[9] A. Singh, A. Maity, and N. Singh, Entropy **24**, 1587 (2022).

[10] R. Merkel, Physics Reports **346**, 343 (2001).

[11] J. D. Watson and F. H. Crick, Nature **171**, 737 (1953).

[12] B. H. Zimm and J. K. Bragg, The Journal of Chemical Physics **31**, 526 (1959).

[13] B. H. Zimm, The Journal of Chemical Physics **33**, 1349 (1960).

[14] F. Ritort, Journal of Physics: Condensed Matter **18**, R531 (2006).

[15] K. Tóth, V. Sauermann, and J. Langowski, Biochemistry **37**, 8173 (1998).

[16] S. Laib and S. Seeger, Journal of fluorescence **14**, 187 (2004).

[17] C. A. Gelfand, G. E. Plum, S. Mielewczyk, D. P. Remeta, and K. J. Breslauer, Proceedings of the National Academy of Sciences **96**, 6113 (1999).

[18] J. Choi and T. Majima, Chemical Society Reviews **40**, 5893 (2011).

[19] J. G. Duguid, V. A. Bloomfield, J. M. Benevides, and G. Thomas, Biophysical journal **71**, 3350 (1996).

[20] A. Wildes et al., Physical Review Letters **106**, 048101 (2011).

[21] R. Owen, L. Hill, and S. Lapage, Biopolymers: Original Research on Biomolecules **7**, 503 (1969).

[22] E. Stellwagen, J. M. Muse, and N. C. Stellwagen, Biochemistry **50**, 3084 (2011).

[23] D. Poland and H. A. Scheraga, The Journal of chemical physics **45**, 1464 (1966).

[24] D. Poland and H. A. Scheraga, Theory of Helix-Coil Transitions in Biopolymers; Statistical Mechanical Theory of Order-Disorder Transitions in Biological Macromolecules (Academic Press, 1970).

[25] M. Peyrard and A. R. Bishop, Phys. Rev. Lett. **62**, 2755 (1989).

[26] T. Dauxois, M. Peyrard, and A. R. Bishop, Phys. Rev. E **47**, R44 (1993).

[27] M. L. Deng and W. Q. Zhu, Physical Review E **77**, 021918 (2008).

[28] S. Buyukdagli and M. Joyeux, Phys. Rev. E **76**, 021917 (2007).

[29] A. Krueger, E. Protozanova, and M. D. Frank-Kamenetskii, Biophysical Journal **90**, 3091 (2006).
[30] Y. Liu et al., The Journal of Physical Chemistry B **114**, 9905 (2010).
[31] A. Maity, A. Singh, and N. Singh, European Biophysics Journal **46**, 33 (2017).
[32] A. Singh and N. Singh, Physica A **419**, 328 (2015).
[33] A. Singh and N. Singh, Physica A **392**, 2052 (2013).
[34] M. Santosh and P. K. Maiti, Journal of Physics: Condensed Matter **21**, 034113 (2008).
[35] R. Kapri and S. M. Bhattacharjee, Journal of Physics: Condensed Matter **18**, S215 (2006).
[36] S. Amnuanpol, Journal of biological physics **42**, 69 (2016).
[37] I. Heller, T. P. Hoekstra, G. A. King, E. J. Peterman, and G. J. Wuite, Chemical reviews **114**, 3087 (2014).
[38] A. Neuman, Keir C.and Nagy, Nat Meth **5**, 491 (2008).
[39] U. Bockelmann, P. Thomen, B. Essevaz-Roulet, V. Viasnoff, and F. Heslot, Biophysical journal **82**, 1537 (2002).
[40] E. Evans, K. Ritchie, and R. Merkel, Biophysical Journal **68**, 2580 (1995).
[41] G. Binnig, C. F. Quate, and C. Gerber, Phys. Rev. Lett. **56**, 930 (1986).
[42] R. Simmons, J. Finer, S. Chu, and J. Spudich, Biophysical Journal **70**, 1813 (1996).
[43] F. Amblard, B. Yurke, A. Pargellis, and S. Leibler, Review of Scientific Instruments **67**, 818 (1996).
[44] T. R. Strick et al., Reports on Progress in Physics **66**, 1 (2003).
[45] S. B. Smith, L. Finzi, and C. Bustamante, Science **258**, 1122 (1992).
[46] S. B. Smith, Y. Cui, and C. Bustamante, Science **271**, 795 (1996).
[47] P. Cluzel et al., Science **271**, 792 (1996).
[48] I. Tinoco Jr and C. Bustamante, Biophysical chemistry **101**, 513 (2002).
[49] S. R. Tee and Z. Wang, ACS omega **3**, 292 (2018).
[50] M. Mosayebi, A. A. Louis, J. P. Doye, and T. E. Ouldridge, ACS nano **9**, 11993 (2015).
[51] A. Upadhyaya, S. Nath, and S. Kumar, The Journal of Chemical Physics **148** (2018).
[52] P. L. Privalov and C. Crane-Robinson, Progress in Biophysics and Molecular Biology **135**, 30 (2018).
[53] C. Danilowicz et al., Journal of Physics: Condensed Matter **22**, 414106 (2010).
[54] S. Kumar and D. Giri, Physical Review E **72**, 052901 (2005).
[55] S. M. Bhattacharjee, Journal of Physics A: Mathematical and General **33**, L423 (2000).
[56] D. K. Lubensky and D. R. Nelson, Phys. Rev. Lett. **85**, 1572 (2000).
[57] S. Cocco, R. Monasson, and J. F. Marko, Phys. Rev. E **65**, 041907 (2002).
[58] N. Singh and Y. Singh, The European Physical Journal E **19**, 233 (2006).
[59] A. Upadhyaya and S. Kumar, Physical Review E **103**, 062411 (2021).
[60] R. Everaers, N. B. Becker, and A. Rosa, The journal of chemical physics **154**, 024903 (2021).
[61] R. K. Mishra, G. Mishra, M. Li, and S. Kumar, Physical Review E **84**, 032903 (2011).
[62] A. J. Guttmann, J. L. Jacobsen, I. Jensen, and S. Kumar, Journal of mathematical chemistry **45**, 223 (2009).
[63] K. Liebl and M. Zacharias, The Journal of Physical Chemistry B **121**, 11019 (2017).
[64] M. Zoli, Physica A: Statistical Mechanics and its Applications **492**, 903 (2018).
[65] N. Singh and Y. Singh, The European Physical Journal E **17**, 7 (2005).

[66] S. Rudra, K. Chauhan, A. R. Singh, and S. Kumar, Physical Review E **107**, 054501 (2023).

[67] J. E. Mark et al.Physical properties of polymers handbook Vol. 1076 (Springer, 2007).

[68] N. Dawass, P. Krüger, S. K. Schnell, J.-M. Simon, and T. J. Vlugt, Fluid Phase Equilibria **486**, 21 (2019).

[69] S. Ausaf Ali et al., Current Protein and Peptide Science **15**, 456 (2014).

[70] D. Mohanta, D. Giri, and S. Kumar, Soft Matter (2023).

[71] A. Arcella et al., The Journal of Physical Chemistry B **118**, 8540 (2014).

[72] D. Majumdar, Journal of Statistical Physics **190**, 14 (2023).

[73] A. B. Menhaj, B. D. Smith, and J. Liu, Chemical Science **3**, 3216 (2012).

[74] J. Katz, R. Dougherty, and L. Boucher, Infrared and nuclear magnetic resonance spectroscopy of chlorophyll, in The chlorophylls, pp. 185–251, Elsevier, 1966.

[75] Ö. Irmak, E. O. Orhan, K. Görgün, and B. C. Yaman, PLoS One **13**, e0202081 (2018).

[76] X. Huang and M. A. El-Sayed, Journal of advanced research **1**, 13 (2010).

[77] L. A. Dykman and N. G. Khlebtsov, Acta Naturae **3**, 34 (2011).

[78] E. A. Gorbunova, A. V. Epanchintseva, D. V. Pyshnyi, and I. A. Pyshnaya, Applied Sciences **13**, 7324 (2023).

[79] R. Sakthi Devi, A. Girigoswami, M. Siddharth, and K. Girigoswami, Applied Biochemistry and Biotechnology **194**, 4187 (2022).

[80] X.-F. Zhang, Z.-G. Liu, W. Shen, and S. Gurunathan, International journal of molecular sciences **17**, 1534 (2016).

[81] C. A. Mirkin, R. L. Letsinger, R. C. Mucic, and J. J. Storhoff, Nature **382**, 607 (1996).

[82] X. Ma, X. Li, G. Luo, and J. Jiao, Frontiers in Chemistry **10**, 1095488 (2022).

[83] A. G. Kanaras, Z. Wang, A. D. Bates, R. Cosstick, and M. Brust, Angewandte Chemie **115**, 201 (2003).

[84] A. O. Maslova and I. M. Hsing, Nanoscale Advances **1**, 430 (2019).

[85] B. Liu and J. Liu, Matter **1**, 825 (2019).

[86] D. Miyoshi and N. Sugimoto, Biochimie **90**, 1040 (2008).

[87] C. J. Whitfield et al., Chemical Reviews **121**, 11030 (2021).

[88] A. Zaki, N. Dave, and J. Liu, Journal of the American Chemical Society **134**, 35 (2012).

[89] S. Dutta, DNA functionalized gold and silver nanoparticles, in Gold and Silver Nanoparticles, pp. 411–434, Elsevier, 2023.

[90] R. Wu, H. Peng, J.-J. Zhu, L.-P. Jiang, and J. Liu, Frontiers in chemistry **8**, 121 (2020).

[91] C. Kokkinos, Nanomaterials **9**, 1361 (2019).

[92] W. Xu et al., Angewandte Chemie International Edition **60**, 6890 (2021).

[93] Y. Zhang et al., Advanced Materials **30**, 1703658 (2018).

[94] M. P. Busson et al., Nano letters **11**, 5060 (2011).

[95] S. Kumar, S. Kumar, D. Giri, and S. Nath, Europhysics Letters **118**, 28001 (2017).

[96] R. Kumar, A. Chaudhuri, and R. Kapri, arXiv preprint arXiv:2102.08067 (2021).

[97] B. Akabayov, S. R. Akabayov, S. Lee, G. Wagner, and C. C. Richardson, Nature communications **4**, 1 (2013).

[98] S. E. Henrickson, M. Misakian, B. Robertson, and J. J. Kasianowicz, Phys. Rev. Lett. **85**, 3057 (2000).

[99] S. E. Henrickson, E. A. DiMarzio, Q. Wang, V. M. Stanford, and J. J. Kasianowicz, The Journal of Chemical Physics **132**, 135101 (2010).
[100] S. Nakano, D. Yamaguchi, and N. Sugimoto, Molecular Biology Reports (2018).
[101] H. Kumar, Y. Lansac, M. A. Glaser, and P. K. Maiti, Soft Matter **7**, 5898 (2011).
[102] S. Mogurampelly and P. K. Maiti, The Journal of Chemical Physics **138**, 034901 (2013).
[103] M. Wanunu, Physics of Life Reviews **9**, 125 (2012).
[104] A. Singer, S. Rapireddy, D. H. Ly, and A. Meller, Nano Lett **12 (3)**, 1722 (2012).
[105] B. A. Nicholas, C. Kaikai, G. Sandip, R. Maria, and U. F. Keyser, Nature Communications **8**, 380 (2017).
[106] D. T. C. Q. Liu Zewen, Wang Yifan, Journal of Nanomaterials **13**, 1 (2016).
[107] M. M. Marshall, J. Yang, and A. R. Hall, Scanning **34**, 101 (2012).
[108] B. M. Venkatesan, A. B. Shah, J. Zuo, and R. Bashir, Advanced Functional Materials **20**, 1266 (2010).
[109] H. W. C. Postma, Nano Letters **10**, 420 (2010).
[110] K. K. Saha, M. Drndić, and B. K. Nikolić, Nano Letters **12**, 50 (2012).
[111] W. Reisner, J. N. Pedersen, and R. H. Austin, Reports on Progress in Physics **75**, 106601 (2012).
[112] R. B. Inman, Journal of Molecular Biology **18**, 464 (1966).
[113] Y. Lin et al., Chem. Commun. **53**, 3539 (2017).
[114] S. Kumar and S. Kumar, Physica A: Statistical Mechanics and its Applications **499**, 216 (2018).
[115] M. Akeson, D. Branton, J. J. Kasianowicz, E. Brandin, and D. W. Deamer, Biophysical journal **77**, 3227 (1999).
[116] I. M. Derrington et al., Proceedings of the National Academy of Sciences **107**, 16060 (2010).
[117] B. Lin, J. Hui, and H. Mao, Biosensors **11**, 214 (2021).
[118] S. L. Singh et al., International Journal of Molecular Sciences **24**, 6153 (2023).
[119] Y. Xing, A. Rottensteiner, J. Ciccone, and S. Howorka, Angewandte Chemie International Edition , e202303103 (2023).
[120] Z. Yuan, Y. Liu, M. Dai, X. Yi, and C. Wang, Nanoscale research letters **15**, 1 (2020).
[121] F. Yao et al., Analytical chemistry **92**, 3827 (2020).
[122] R. Peters, A. Brünger, and K. Schulten, Proceedings of the National Academy of Sciences **78**, 962 (1981).
[123] D. Zhao et al., Frontiers of Chemical Science and Engineering **15**, 922 (2021).
[124] A. N. Zelikin et al., ACS nano **1**, 63 (2007).
[125] J. Z. Chen, Physical Review Letters **121**, 037801 (2018).
[126] D. Mohanta, D. Giri, and S. Kumar, Journal of Statistical Mechanics: Theory and Experiment **2019**, 043501 (2019).
[127] W. Reisner et al., **2004**, W8 (2004).
[128] P. Cifra, Z. Benková, and T. Bleha, Physical Chemistry Chemical Physics **12**, 8934 (2010).
[129] A. Maity, A. Singh, and N. Singh, EPL (Europhysics Letters) **127**, 28001 (2019).
[130] A. Maity and N. Singh, European Biophysics Journal **49**, 561 (2020).
[131] D. Ibraheem, A. Elaissari, and H. Fessi, International journal of pharmaceutics **459**, 70 (2014).

[132] K. Chauhan and S. Kumar, Physical Review E **103**, 042501 (2021).
[133] S. Nakano, D. Miyoshi, and N. Sugimoto, Chemical reviews **114**, 2733 (2014).
[134] J.-M. Yuan et al., Protein Science **17**, 2156 (2008).
[135] C. H. Spink, N. Garbett, and J. B. Chaires, Biophysical Chemistry **126**, 176 (2007).
[136] D. Miyoshi, S. Matsumura, S. Nakano, and N. Sugimoto, Journal of the American Chemical Society **126**, 165 (2004).
[137] Y. Sasaki, D. Miyoshi, and N. Sugimoto, Biotechnology Journal: Healthcare Nutrition Technology **1**, 440 (2006).
[138] K. S. Harve, R. Lareu, R. Rajagopalan, and M. Raghunath, Nucleic Acids Research **38**, 172 (2010).
[139] I. Khimji, J. Shin, and J. Liu, Chem. Commun. **49**, 1306 (2013).
[140] S. Ghosh et al., Proceedings of the National Academy of Sciences **117**, 14194 (2020), https://www.pnas.org/content/117/25/14194.full.pdf.
[141] T. Fujimoto, S. Nakano, N. Sugimoto, and D. Miyoshi, The Journal of Physical Chemistry B **117**, 963 (2013).
[142] R. Moriyama, Y. Iwasaki, and D. Miyoshi, The Journal of Physical Chemistry B **119**, 11969 (2015).
[143] G. P. Goodrich, M. R. Helfrich, J. J. Overberg, and C. D. Keating, Langmuir **20**, 10246 (2004).
[144] A. R. Singh, D. Giri, and S. Kumar, Physical Review E **79**, 051801 (2009).
[145] C. A. Brackley, M. E. Cates, and D. Marenduzzo, Phys. Rev. Lett. **111**, 108101 (2013).
[146] S. Qin and H. X. Zhou, Phys. Rev. E **81**, 031919 (2010).
[147] S. Qin and H.-X. Zhou, Biophysical Journal **97**, 12 (2009).
[148] J. Kim, C. Jeon, H. Jeong, Y. Jung, and B.-Y. Ha, Soft Matter **11**, 1877 (2015).
[149] M. P. Taylor, C. Vinci, and R. Suzuki, The Journal of Chemical Physics **153**, 174901 (2020), https://doi.org/10.1063/5.0025640.
[150] T. Dauxois and M. Peyrard, Physical Review E **51**, 4027 (1995).
[151] N. Theodorakopoulos, T. Dauxois, and M. Peyrard, Physical Review Letters **85**, 6 (2000).
[152] M. D. Frank-Kamenetskii and S. Prakash, Physics of Life Reviews **11**, 153 (2014).
[153] A. Bergues-Pupo, J. Bergues, and F. Falo, Physica A **396**, 99 (2014).
[154] Z. Rapti et al., Physical Review E **73**, 051902 (2006).
[155] N. K. Voulgarakis, A. Redondo, A. R. Bishop, and K. Rasmussen, Physical review letters **96**, 248101 (2006).
[156] M. Peyrard, Nonlinearity **17**, R1 (2004).
[157] S. Meyer et al., Biophysical journal **105**, 1904 (2013).
[158] A. Maity, N. Mathur, P. Imhof, and N. Singh, Physica A: Statistical Mechanics and its Applications **609**, 128382 (2023).
[159] M. Peyrard, S. Cuesta-Lopez, and G. James, Journal of biological physics **35**, 73 (2009).
[160] Z. Rapti, K. Ø. Rasmussen, and A. R. Bishop, Journal of Nonlinear Mathematical Physics **18**, 381 (2011).
[161] T. van Erp, S. Cuesta-López, and M. Peyrard, The European Physical Journal E **20**, 421 (2006).
[162] A. Campa and A. Giansanti, Phys. Rev. E **58**, 3585 (1998).
[163] M. Barbi, S. Lepri, M. Peyrard, and N. Theodorakopoulos, Phys. Rev. E **68**, 061909

(2003).
[164] A. Djine, G. R. Deffo, and S. B. Yamgoué, Chaos, Solitons and Fractals **170**, 113334 (2023).
[165] B. Alberts et al., Principles of Biochemistry, 4th ed. WH Freeman (2004).
[166] B. S. Alexandrov et al., Nucleic Acids Research **37**, 2405 (2009).
[167] M. Zoli, The European Physical Journal E **34**, 1 (2011).
[168] T. Dauxois, M. Peyrard, and A. R. Bishop, Phys. Rev. E **47**, 684 (1993).
[169] Y.-l. Zhang, W.-M. Zheng, J.-X. Liu, and Y. Z. Chen, Phys. Rev. E **56**, 7100 (1997).
[170] J. Elschner, ZAMM - Journal of Applied Mathematics and Mechanics / Zeitschrift für Angewandte Mathematik und Mechanik **73**, 376 (1993).
[171] S. Srivastava and N. Singh, The Journal of Chemical Physics **134**, 115102 (2011).
[172] A. Singh and N. Singh, Physica A **392**, 2052 (2013).
[173] W. H. Press, B. P. Flannery, S. A. Teukolsky, and W. T. Vetterling, Numerical Recipes in C: The Art of Scientific Computing, Second Edition (Cambridge University Press, 1992).
[174] M. Barbi, S. Cocco, and M. Peyrard, Physics Letters A **253**, 358 (1999).
[175] N. Singh and Y. Singh, Phys. Rev. E **64**, 042901 (2001).
[176] A. Campa and A. Giansanti, Journal of Biological Physics **24**, 14 (1999).
[177] M. P. Allen et al., Computational soft matter: from synthetic polymers to proteins **23**, 1 (2004).
[178] H. Kumar and P. K. Maiti, Computational statistical physics: Lecture notes, guwahati serc school , 161 (2011).
[179] R. Schneider, A. R. Sharma, and A. Rai, Introduction to Molecular Dynamics (Springer Berlin Heidelberg, Berlin, Heidelberg, 2008).
[180] K.-Y. Wong and B. M. Pettitt, Biophysical journal **95**, 5618 (2008).
[181] Y. He, Y. Shang, Y. Liu, S. Zhao, and H. Liu, SpringerPlus **4**, 1 (2015).
[182] J. Wereszczynski and J. A. McCammon, Quarterly reviews of biophysics **45**, 1 (2012).
[183] G. Ciccotti, C. Dellago, M. Ferrario, E. Hernández, and M. Tuckerman, The European Physical Journal B **95**, 3 (2022).
[184] M. J. Abraham et al., SoftwareX **1**, 19 (2015).
[185] D. A. Case et al., Journal of computational chemistry **26**, 1668 (2005).
[186] B. R. Brooks et al., Journal of computational chemistry **30**, 1545 (2009).
[187] J. C. Phillips et al., Journal of computational chemistry **26**, 1781 (2005).
[188] A. P. Thompson et al., Computer Physics Communications **271**, 108171 (2022).
[189] E. Fadrná, K. Hladečková, and J. Koča, Journal of Biomolecular Structure and Dynamics **23**, 151 (2005).
[190] V. H. Man, X. He, J. Gao, and J. Wang, Journal of chemical theory and computation **17**, 6458 (2021).
[191] H. Zhang, Y. Jiang, Z. Cui, and C. Yin, Journal of Chemical Information and Modeling **58**, 1669 (2018).
[192] S. A. Hollingsworth and R. O. Dror, Neuron **99**, 1129 (2018).
[193] M. S. Badar, S. Shamsi, J. Ahmed, and M. A. Alam, Molecular dynamics simulations: concept, methods, and applications, in Transdisciplinarity, pp. 131–151, Springer, 2022.
[194] H. Zou, Y. Feng, L. Qiu, and X. Zhang, International Journal of Heat and Mass Transfer **183**, 122216 (2022).

[195] N. Piasentin, G. Lian, and Q. Cai, ACS omega **6**, 35363 (2021).

[196] C. R. Cantor and P. R. Schimmel, Biophysical Chemistry, Part 2: Techniques for the Study of Biological Structure and Function, 1 ed. (W. H. Freeman and Company, 1980).

[197] R. R. Sinden, DNA structure and function (Gulf Professional Publishing, 1994).

[198] G. Gaeta, Journal of Biological Physics **24**, 81 (1999).

[199] A. M. Poveda, M. Le Clech, and P. Pasero, Transcription **1**, 99 (2010).

[200] D. delToro and D. E. Smith, Applied physics letters **104** (2014).

[201] S. Kumar, Statistical mechanics of force-induced transitions of biopolymers, in Handbook of Computational Chemistry, pp. 397–419, Springer, 2017.

[202] G. Lee, L. Chrisey, and R. Colton, Science **266**, 771 (1994).

[203] R. K. Mishra, T. Modi, D. Giri, and S. Kumar, The Journal of Chemical Physics **142**, 174910 (2015).

[204] R. Kapri and S. M. Bhattacharjee, Physical review letters **98**, 098101 (2007).

[205] D. Poland and H. A. Scheraga, J.Chem.Phys **45**, 1456–1463 (1966).

[206] A. Singh and N. Singh, Phys. Rev. E **94**, 032410 (2016).

[207] R. C. DeMille, T. E. I. Cheatham, and V. Molinero, The Journal of Physical Chemistry B **115**, 132 (2011), https://doi.org/10.1021/jp107028n, PMID: 21155552.

[208] G. Kalosakas and S. Ares, The Journal of Chemical Physics **130**, 235104 (2009).

[209] M. Löwe, M. Kalacheva, A. J. Boersma, and A. Kedrov, The FEBS Journal **287**, 5039 (2020).

[210] S. L. Speer, C. J. Stewart, L. Sapir, D. Harries, and G. J. Pielak, Annual Review of Biophysics **51**, 267 (2022).

[211] G. Rivas and A. P. Minton, Biophysical reviews **10**, 241 (2018).

[212] G. Nettesheim et al., Nature Physics **16**, 1144 (2020).

[213] T. P. Silverstein and K. Slade, Journal of Chemical Education **96**, 2476 (2019).

[214] P. Dey and Bhattacherjee, Soft Matter **15**, 1960 (2019).

[215] S. Y. Park, J. S. Lee, D. Georganopoulou, C. A. Mirkin, and G. C. Schatz.

[216] R. Jin, G. Wu, Z. Li, C. A. Mirkin, and G. C. Schatz, Journal of the American Chemical Society **125**, 1643 (2003), https://doi.org/10.1021/ja021096v, PMID: 12568626.

[217] J. M. Gibbs et al., J. Am. Chem. Soc. **127**, 1170 (2005).

[218] T. R. Prytkova, I. Eryazici, B. Stepp, S. B. Nguyen, and G. C. Schatz.

[219] B. R. Stepp, J. M. Gibbs-Davis, D. L. F. Koh, and S. T. Nguyen, J. Am. Chem. Soc. **130**, 9628 (2008).

[220] S. Y. Park and D. Stroud, Phys. Rev. B **67**, 212202 (2003).

[221] S. B. Zimmerman and L. D. Murphy, FEBS letters **390**, 245 (1996).

[222] S. Hormeno, B. Ibarra, J. M. Valpuesta, J. L. Carrascosa, and J. Ricardo Arias-Gonzalez, Biopolymers **97**.

[223] A. K. R. Lytton-Jean et al., Advanced Materials **21**, 706 (2009).

[224] E. Grueso, R. M. Giráldez-Pérez, P. Perez-Tejeda, E. Roldán, and R. Prado-Gotor, Phys. Chem. Chem. Phys. **21**, 11019 (2019).

[225] C. Lu et al., TrAC Trends in Analytical Chemistry , 116533 (2022).

[226] O. Lee, T. R. Prytkova, and G. C. Schatz, The Journal of Physical Chemistry Letters **1**, 1781 (2010), https://doi.org/10.1021/jz100435a, PMID: 20606716.

[227] H. Wang, R. Yang, L. Yang, and W. Tan, ACS nano **3**, 2451 (2009).

[228] K. Saha, S. S. Agasti, C. Kim, X. Li, and V. M. Rotello, Chemical Reviews **112**, 2739 (2012), https://doi.org/10.1021/cr2001178, PMID: 22295941.

[229] H. Karimata, S. Nakano, T. Ohmichi, J. Kawakami, and N. Sugimoto, **48**, 107 (2004).

[230] D. Mohanta, D. Giri, and S. Kumar, Physica A: Statistical Mechanics and its Applications **562**, 125379 (2021).

[231] D. Jour Putnam, Nature Materials **5**, 1476 (2006).

[232] A. des Rieux, A. Shikanov, and L. D. Shea, Journal of Controlled Release **136**, 148 (2009).

[233] E. Haladjova, S. Rangelov, C. B. Tsvetanov, and S. Pispas, Soft Matter **8**, 2884 (2012).

[234] E. Auyeung, R. J. Macfarlane, C. H. J. Choi, J. I. Cutler, and C. A. Mirkin, Advanced Materials **24**, 5181 (2012).

[235] H. Ding et al., ACS Central Science **4**, 1344 (2018).

[236] B. Akabayov, S. Akabayov, S. Lee, G. Wagner, and C. Richardson, Nature Communications **4** (2013).

[237] M. D. Frank-Kamenetskii and S. Prakash, Physics of life reviews **11**, 153 (2014).

[238] A. Maity and N. Singh, European Biophysics Journal **49**, 561 (2020).

[239] F. Hong, J. S. Schreck, and P. Šulc, Nucleic Acids Research **48**, 10726 (2020), https://academic.oup.com/nar/article-pdf/48/19/10726/34133785/gkaa854.pdf.

[240] Y. Jung and B.-Y. Ha, The Journal of Chemical Physics **155**, 054902 (2021), https://doi.org/10.1063/5.0056446.

[241] S. Ghosh et al., Nucleic acids research **47**, 3284 (2019).

[242] S. Takahashi, P. Herdwijn, and N. Sugimoto.

[243] S. Takahashi, H. Okura, P. Chilka, S. Ghosh, and N. Sugimoto, RSC Adv. **10**, 33052 (2020).

[244] S. Kashanian, M. M. Khodaei, and F. Kheirdoosh, Journal of Photochemistry and Photobiology B: Biology **120**, 104 (2013).

[245] S.-i. Nakano, H. Karimata, T. Ohmichi, J. Kawakami, and N. Sugimoto, Journal of the American Chemical Society **126**, 14330 (2004).

[246] W. Humphrey, A. Dalke, and K. Schulten, Journal of molecular graphics **14**, 33 (1996).

[247] P. M. Vallone et al., Biopolymers: Original Research on Biomolecules **50**, 425 (1999).

[248] D. A. Case et al., (2008).

[249] E. Lamm, O. Harman, and S. J. Veigl, Genetics **215**, 291 (2020).

[250] F. Pu, J. Ren, and X. Qu, Chemical Society Reviews **47**, 1285 (2018).

[251] J. C. García-Ramos, R. Galindo-Murillo, F. Cortés-Guzmán, and L. Ruiz-Azuara, Journal of the Mexican Chemical Society **57**, 245 (2013).

[252] J. Maji and S. M. Bhattacharjee, Europhysics Letters **92**, 58004 (2011).

[253] N. Chaffey, Alberts, b., johnson, a., lewis, j., raff, m., roberts, k. and walter, p. molecular biology of the cell. 4th edn., 2003.

[254] E. J. Yoxen, Science **205**, 1119 (1979).

[255] A. Kornberg and T. A. BakerDNA replication Vol. 3 (Wh Freeman New York, 1992).

[256] R. P. Anand, S. T. Lovett, and J. E. Haber, Cold Spring Harbor perspectives in biology **5**, a010397 (2013).

[257] V. O. Chagin, J. H. Stear, and M. C. Cardoso, Cold Spring Harbor perspectives in biology **2**, a000737 (2010).

[258] D. S. Latchman, The international journal of biochemistry and cell biology **29**, 1305 (1997).

[259] C. R. Cantor and P. R. Schimmel, Biophysical Chemistry: Part III: The Behavior of Biological Macromolecules (Their Biophysical Chemistry), First edition ed. (W. H. Freeman, 1980).

[260] V. A. Bloomfield et al., Nucleic Acids: Structures, Properties, and Functions, 1st ed. (University Science Books, 2000).

[261] R. W. Taylor and D. M. Turnbull, Nature Reviews Genetics **6**, 389 (2005).

[262] L. T. Kirby, DNA fingerprinting: an introduction (Oxford University Press, 1993).

[263] M. Lynch, DNA fingerprinting: approaches and applications , 113 (1991).

[264] L. YatTung, Bioinformatics for DNA Sequencing Data Analysis (, 2023).

[265] W. Ma et al., Signal transduction and targeted therapy **6**, 351 (2021).

[266] N. C. Seeman, Annual review of biochemistry **79**, 65 (2010).

[267] J. Fang, X. Zhu, C. Wang, and L. Shangguan, Current Genomics **17**, 379 (2016).

[268] K. Guo, J. Yang, N. Yu, L. Luo, and E. Wang, Plant Communications , 100499 (2022).

[269] S. Khan et al., International journal of genomics **2016** (2016).

[270] A. Zinchenko, E. Inagaki, and S. Murata, ACS omega **4**, 458 (2019).

[271] P. Fillion, A. Desjardins, K. Sayasith, and J. Lagacé, Biochimica et Biophysica Acta (BBA)-Biomembranes **1515**, 44 (2001).

[272] S. C. Kogan, M. Doherty, and J. Gitschier, New England Journal of Medicine **317**, 985 (1987).

[273] R. S. Wappner, Pediatric annals **22**, 282 (1993).

[274] C. E. Dunbar et al., Science **359**, eaan4672 (2018).

[275] I. M. Verma and N. Somia, Nature **389**, 239 (1997).

[276] J. Shendure et al., Nature **550**, 345 (2017).

[277] L. T. França, E. Carrilho, and T. B. Kist, Quarterly reviews of biophysics **35**, 169 (2002).

[278] A. E. Men, P. Wilson, K. Siemering, and S. Forrest, Next Generation Genome Sequencing: Towards Personalized Medicine , 1 (2008).

[279] W. R. McCombie, J. D. McPherson, and E. R. Mardis, Cold Spring Harbor perspectives in medicine **9**, a036798 (2019).

[280] L. Garibyan and N. Avashia, The Journal of investigative dermatology **133**, e6 (2013).

[281] J. M. Bartlett and D. Stirling, PCR protocols , 3 (2003).

[282] P. T. Monis and S. Giglio, Infection, Genetics and Evolution **6**, 2 (2006).

List of Publications and Presentations

International Journals:

- *"DNA Molecule Confined in a Cylindrical Shell: Effect of Partial Confinement"* **Neha Mathur**, Arghya Maity and Navin Singh, Advances in Computational Modeling and Simulation, Springer **31-40**, 2022.
- *"Structural analysis of DNA molecule in a confined shell"*
  Arghya Maity, **Neha Mathur** and Navin Singh, Physica A, **609** 128382 (2023).
- *"Melting of dsDNA attached with AuNPs"*
  Neha Mathur and Navin Singh, The European Physical Journal E, (2023)
- *"Force-induced unzipping of DNA in the presence of solvent molecules"*
  Neha Mathur, Amar Singh and Navin Singh, Biophysical Chemistry, 2024 (Accepted).
- *"Comparative Study on DNA Dynamics in the presence of different crowders"*. **Neha Mathur**, Anurag Upadhyay and Navin Singh, (Communicated).

Presentations:

- *"DNA Unzipping in presence of Molecular Crowders "*
  Neha Mathur and Navin Singh, Indian National Young Academy of Sciences (INYAS),
  December 13, 2021.
- *"Augmenting Writing Skills for Articulating Research "* **Neha Mathur** and Navin Singh, Popular Science Writing under AWSAR Programme
  October, 14 2021, Department of Science and Technology (DST) and Vigyan Prasar (VP)

List of conferences/schools attended/participated:

- *"DNA Bubble Formation: From Physics to Biological Functions"*,
  February, 14-20 2020, IIT, **Banaras Hindu University, INDIA.**

- *"Application of next-generation sequencing for the analysis of RNA sequencing and metagenome data"*,
  June 08-09, 2020, **BITS Pilani, Pilani, INDIA**.

- *"Banglore School on Statistical Physics – XI"*,
  June 29- July 10, 2020, **Ramanujan Lecture Hall, ICTS, Bengaluru**(Online).

- *"The DNA molecule: A physicist's perspective"*,
  July 13, 2020, IIT, **ISM, Dhanbad**(Online).

- *"New Horizons in Physics – IPA 50, Kinetics Phase Transition"*,
  October 10, 2020, **JNU, New Delhi**(Online).

- *"Statistical Biological Physics: From single molecule to cell"*(Online)
  December 7-18, 2020, **ICTS, Bengaluru**

- *"Banglore School on Statistical Physics – XII"*,
  June 28-09 July 2021, **Ramanujan Lecture Hall, ICTS, Bengaluru**(Online).

- *"Recent Advances in Photonics"*,
  November 25-29, 2021, **All India Council for Technical Education" (AICTE) Training and Learning (ATAL) Academy, Vasant Vihar, New Delhi**(Online).

- A workshop on *"Teaching-Learning Workshop for Next Generation Academicians"*,
  November 27, 2021, **BITS Pilani, Pilani, INDIA**.

- *"Lectures on thin film and Application"*,
  February 12, 2022, **BITS Pilani, Pilani, INDIA**.

- *"Workshop on recent trends on nanostructured thin film and application"*,
  February 19, 2022, **BITS Pilani, Pilani, INDIA**.

- *"StatPHYS XI, IISER Kolkata"*,
  March 21-25, 2022, **Mohanpur, West Bengal, INDIA**(Online).

- *"Non-Markovian Dynamics Far from Equilibrium"*,
  July 11-22, **Trieste, Italy**(Online).

- *"Computational Methods for Physics and Materials Science (CMPMS-2022)"*,
  December 29- January 3, 2023, **JUIP, Solan, Himachal Pradesh, India**(Online).

Brief Biography of the Supervisor

Prof. Navin Singh is a highly accomplished physicist with a focus on Biophysics and Soft Condensed Matter Physics. He completed his Ph.D. from the Department of Physics at Banaras Hindu University in 2004. After his Ph.D., Prof. Singh gained international research experience by joining the theory group at the Max Planck Institute for Polymer Research in Mainz, Germany. There, he worked on breaking dynamics of rubber. He joined the Department of Physics at BITS Pilani, Pilani Campus, in December 2006. Since then, he has been actively involved in teaching undergraduate courses in various physics subjects, including Statistical Mechanics, Computational Physics, and Solid State Physics which demonstrates his commitment to education and mentoring students. He has made significant contributions to the fields of Biophysics and Soft Condensed Matter Physics, by publishing quality research papers in well-known international journals. His contributions are widely recognized and cited by other researchers. Prof. Singh has guided both doctoral and undergraduate thesis students in the areas of Biophysics and Statistical Mechanics. He has received grants from reputable organizations like the University Grants Commission (UGC) and the Science and Engineering Research Board (SERB) to support his research endeavors and further contributed to his academic and research achievements. He is also active in giving technical and popular-level talks at conferences and workshops relevant to his field.

In addition to his research and teaching roles, Prof. Navin Singh has taken on various administrative responsibilities. Currently, he serves as the Associate Dean of the Student Welfare Division (SWD), demonstrating his commitment to the overall growth and development of students.

Brief Biography of the Co-Supervisor

Prof. Shibasish Chowdhury obtained a master's degree in physical chemistry from Calcutta University. Then, he shifted to biophysics and obtained a Ph.D. degree from the Molecular Biophysics Unit (MBU) at the Indian Institute of Science, Bangalore on "Computer modeling studies on G-rich unusual DNA structure". Subsequently, entered into the protein folding field and worked as a postdoctoral research fellow in the Department of Chemistry and Biochemistry, University of Delaware, the USA. Currently, Prof. Chowdhury is working as a Professor in the Department of Biological Sciences, Birla Institute of Technology and Science, Pilani. His group is involved in decoding inherent molecular signals within miRNA, which plays a crucial role in the specificity of target binding and gene silencing. All the experimentally validated human miRNA within the miRBase database were analyzed through different machine-learning techniques. The sequence and structural features within miRNA were identified which may lead to target specificity. Different in-silico techniques are utilized to understand the evolution process of various DNA repair protein families. He is involved in analyzing the molecular basis of different biological processes like drug resistance, molecular recognition, and evolution. He has received several research grants from various government funding authorities.

Brief Biography of the Student

I completed my Bachelor of Science degree in 2013 from Jai Narayan Vyas University in Jodhpur, Rajasthan. After that, I pursued my Master's in Physics from Lachoo Memorial College of Science and Technology in Jodhpur. During my postgraduate studies, I specialized in Condensed Matter Physics and under the mentorship of Dr. Mahipal Deora, I completed my final year project. I received the prestigious GARGI Prize from the Rajasthan government during my academic years. Additionally, I actively participated in various general knowledge competitions, winning multiple prizes throughout my school and college days. In 2018, I successfully qualified for the Graduate Aptitude Test of Engineering (GATE) and the PhD entrance exam of BITS Pilani. I joined the Physics Department of Birla Institute of Technology and Science (BITS) Pilani Campus under the mentorship of Prof. Navin Singh. My research journey focused on the theoretical study of DNA melting in cellular-like environments. Over time, I developed my skills in Molecular Dynamics Simulation tools such as GROMACS and AMBER. This expertise has allowed me to pivot into more advanced research areas. I have participated in numerous academic conferences and workshops that have broadened my understanding of the field. As a result of my research efforts, I have published several papers in international journals and contributed a book chapter. Some more are under preparation.

In the future, I plan to work on the problems of translocation of DNA through the nanopores. Another problem that I would like to pursue my studies is the effect of molecular crowders on structural transition in DNA and RNA molecules.